UNIVERSITY OF CALIFORNIA, IRVINE

Microglial contributions to Adult-Onset Leukoencephalopathy with Axonal Spheroids and Pigmented Glia Pathology

DISSERTATION

submitted in partial satisfaction of the requirements

for the degree of

DOCTOR OF PHILOSOPHY

in Biological Sciences

by

Miguel Angel Arreola

Dissertation Committee:

Professor Kim Green, Chair

Professor Jorge Busciglio

Professor Karina Cramer

2022

Dedication

Dedicated to the people. Like, ya know, just in general.

“And this I believe: that the free, exploring mind of the individual human is the most valuable thing in the world. And this I would fight for: the freedom of the mind to take any direction it wishes, undirected. And this I must fight against: any idea, religion, or government which limits or destroys the individual. This is what I am and what I am about.”

- John Steinbeck, *East of Eden*

Table of Contents

List of Figures

List of Abbreviations

AC	Axonal Coat
AD	Alzheimer's Disease
ALS	Amyotrophic Lateral Sclerosis
ALSP	Adult Onset Leukoencephalopathy with Axonal Spheroids and Pigmented Glia
Aβ	Amyloid beta
CC	Corpus Callosum
chABC	Chondroitinase ABC enzyme
CR3	Complement receptor 3
CSF1R	Colony Stimulating Factor Receptor 1
CSF1Ri	Low dose CSF1R inhibition
CSPG	Chondroitinase sulfate proteoglycan
CSPG5	Neuroglycan C
DACS	Dandelion clock-like structure
DAM	Disease associated microglia
DAMP	Disease Associated Molecular Patterns
DEG	Differentially expressed gene
ECM	Extracellular Matrix
GWLA	Genome wide linkage analysis
HD	Huntington's Disease
HDLS	Hereditary Diffuse Leukoencephalopathy with Spheroids
iCSF1R$^{+/-}$	Inducible CSF1R$^{+/-}$
IL-10	Interleukin 10
IL-6	Interleukin 6
ITAM	Immunoreceptor tyrosine based activation motif
MBP	Myelin Basic Protein
MMP	Matrix Metalloproteinase
NHD	Nasu-Hakola Disease
NO	Nitric oxide
NPC	Neural precursor cell
OPC	Oligodendrocyte Precursor cell
PD	Parkinson's Disease
PNN	Perineuronal Nets
PV	Parvalbumin
PVM	Perivascular macrophage
ROS	Reactive Oxygen Species
TGFβ	Transforming growth factor beta
WFA	Wisteria floribunda lectin
WGCNA	Weighted gene coexpression network analysis

Acknowledgements

I am forever grateful for the teachings and support of my mentor, Dr. Kim Green. His patience with me for the past couple years as I stumbled my way through graduate school, signed up for the wrong lab, or forgot some deadline is nothing short of saintly. You're a G.

I would like to thank my committee members Dr. Karina Cramer and Dr. Jorge Busciglio for providing helpful suggestions and critique throughout the years.

Special thanks to Dr. Lindsay Hohsfield, Dr. Allison Najafi, Dr. Elizabeth (Spangenberg) Dominguez, Dr. Joshua Crapser, Edna Hingco Esq., Dr. Laura Fernandez Garcia-Agudo, and Sung jin Kim (Steve, my best friend) who took me under their wing and made me feel like a part of a family. Your unwavering support and constant laughter at my mediocre attempts at humor made lab feel like home. I am so lucky and blessed to have found some of my closest friends with you all. My only regret is not having sabotaged your experiments so that I could have spent that much more time with you all.

I would also like to thank Kristine Tran and Jacqueline Bravo for their technical assistance over the years.

And finally, I would like to thank my family who has stuck beside me and continuously made me laugh despite how difficult things may have gotten or how grumpy I may have been. Everything I have done and will do is for you.

This work was supported by the NIH under the following awards: R01NS083801 (NINDS), R01AG056768 (NIA), and U54 AG054349 [NIA Model Organism Development and Evaluation for Late-onset Alzheimer's Disease (MODEL-AD)] to K.N.G.; 1F31NS111882-01A1 (NINDS) to M.A.A.; F31NS108611 (NINDS) to J.D.C.

Vita

Miguel Angel Arreola

Education

University of California, Irvine, B.S. Neurobiology and Behavior 2011-2015

University of California, Irvine, Ph.D. Biological Sciences 2017-2022
Investigated microglial dyshomeostasis and the effects of this immune cell population on the central nervous system in various neurodegenerative conditions.

Publications

Arreola MA, Soni N, Crapser JD, … Green KN, Microglial dyshomeostasis drives perineuronal net and synaptic loss in a CSF1R +/- mouse model of ALSP, which can be rescued via CSF1R inhibitors (2021)

Crapser JD[#], **Arreola MA[#],** Tsourmas KI, Green KN, Microglia as hackers of the matrix: sculpting synapses and the extracellular space (2021)

Henningfield CM, **Arreola MA**, Soni N, Spangenberg EE, Green KN. Microglia-specific ApoE knock-out does not alter Alzheimer's disease plaque pathogenesis or gene expression (2022)

Fernández-Mendívil C, **Arreola MA,** … Lopez MG. Aging and Progression of Beta-Amyloid Pathology in Alzheimer's Disease Correlates with Microglial Heme-Oxygenase-1 Overexpression. (2020)

Crapser JD, Spangenberg EE, Barahona RA, **Arreola MA**, Hohsfield LA, Green KN. Microglia facilitate loss of perineuronal nets in the Alzheimer's disease brain. (2020)

Awards

2019 – 2022	Ruth L. Kirschstein National Research Service Award Individual Predoctoral Fellowship to Promote Diversity in Health-Related Research
2017-2019	University of California, Irvine, Provost Ph.D Fellowship

Abstract of the Dissertation

Microglial contributions to Adult Onset Leukoencephalopathy with Axonal Spheroids and Pigmented Glia Pathology

By

Miguel Angel Arreola

Doctor of Philosophy in Biological Sciences

University of California, Irvine 2022

Professor Kim Green

Adult-Onset Leukoencephalopathy with Axonal Spheroids and Pigmented Glia (ALSP) is a rare autosomal dominant neurodegenerative white matter disease. Pathologically, this disease is characterized by the presence of cerebral white matter lesions, which induce early thinning of the corpus collosum followed by cortical atrophy in affected regions. Genome-wide linkage analyses (GWLAs) have discovered a genetic origin of disease with the identification of multiple mutations that affect CSF1R in families with ALSP. In the adult brain, CSF1R is primarily expressed by microglia. However, the cellular biology underlying detrimental ALSP phenotypes induced by mutations in *Csf1r* (e.g. cellular source(s) of pathology) remains elusive. Moreover, the expression of CSF1R in neurons during development has been noted in mice, and thus it is critical to delineate microglial versus non-microglial, as well as the developmental versus non-developmental contributions to disease onset. As recent studies into myeloid biology have clarified that microglia are not merely sentinel cells, but rather active participants in the maintenance of the central nervous system at large, it is important to understand the extent to which dysfunctional microglia may be able to affect central nervous system health. Moreover, microgliosis is common to many neurogenerative diseases and central nervous system

injuries; however, it remains unclear whether microglia play a causative role in neurodegeneration or a reactive role by responding to the presence of pathology/injury.

Given these outstanding gaps in our knowledge of microglia cell biology, the primary goal of my thesis was to identify the role of microglial CSF1R haploinsufficiency in mediating pathogenesis. Using an inducible $Cx3cr1^{CreERT2/+}$-$Csf1r^{+/fl}$ system, we found that postdevelopmental, microglia-specific Csf1r haploinsufficiency resulted in reduced expression of the homeostatic microglial markers P2RY12 and TMEM119. This was associated with loss of presynaptic surrogates and perineuronal nets. Similar phenotypes were observed in constitutive global Csf1r haploinsufficient mice and could be reversed/prevented by elimination of microglia in adulthood. As microglial elimination is unlikely to be clinically feasible for extended durations, we treated adult $CSF1R^{+/-}$ mice with a microglia-modulating dose of the CSF1R inhibitor PLX5622, which prevented microglial dyshomeostasis along with synaptic- and PNN-related deficits. Intriguingly, treatment of wild-type microglia with the microglia-modulating dose of PLX5622 similarly reduced expression of canonical microglia homeostatic marker expression. However, aside from reductions in presynaptic markers, behavioral and ECM outputs were unchanged. These data thus highlight microglial dyshomeostasis as a driver of pathogenesis and show that CSF1R inhibition can mitigate these phenotypes.

As proper diagnosis for ALSP tends to occur once pathology has set in, we further aimed to verify whether CSF1R inhibitor treatment could be used during late stage disease timepoints as a viable treatment paradigm. To do so we extended the time of observation to 14 months at which point mice were given CSF1R inhibitor for the next two months. Here we observed losses to cognitive functions as assessed by Novel Object and Novel

Place tasks in CSF1R$^{+/-}$ mice, however, treatment with CSF1R inhibitor had marginal affects on the recovery of performance. However, deviations from microglial homeostasis, with respect to lowered P2RY12, and heightened CD68 and Lamp1 expression, were still attenuated with CSF1R inhibitor treatment. Importantly, corpus callosum damage was attenuated with CSF1R inhibitor treatment. This was seen with increased MBP and SMI-31 immunostaining as well as decreased levels of Nf-L, a marker for axonal damage. Unexpectedly, wild-type mice that were treated with CSF1R inhibitor treatment showed striking parallels to CSF1R$^{+/-}$ mice when comparing levels of corpus callosum damage, a feature that was absent when comparing younger cohorts, suggesting an environmental influence of aging that compounds the effect of CSF1R inhibitor treatment. Given that many CSF1R inhibitors are currently going towards phase 3 clinical trials, it is highly relevant and crucial to determine the consequences of altered CSF1R signaling on CNS homeostasis. Collectively the results from the studies throughout this thesis highlight the extent to which microglia dyshomeostasis can affect central nervous system health and provide crucial insight into the impact of globally altering CSF1R signaling on disrupting central nervous system homeostasis.

Chapter One:

Microglia as sculptors of the Central Nervous System

Adult-Onset Leukoencephalopathy with Axonal Spheroids and Pigmented Glia

Adult Onset Leukoencephalopathy with Axonal Spheroids and Pigmented Glia (ALSP), also reported as hereditary diffuse leukoencephalopathy with spheroids (HDLS), is a rare autosomal dominant neurodegenerative white matter disease. Pathologically, this disease is characterized by the presence of patchy cerebral white matter lesions, which predominantly affect frontal and parietal white matter - including early thinning of the corpus collosum - and by subsequent cortical atrophy in the affected regions(*1-4*). Clinically, patients with this disease present variable manifestations, including motor impairments, dementia, seizures, and depression(*5, 6*). The mean age of onset is around 42 years with average occurrence of morbidity a decade after onset(*7, 8*). It is predicted that ALSP accounts for 10-15% of the leukodystrophies reported; however, because it shares many pathological hallmarks with other neurodegenerative diseases, it is believed that ALSP diagnoses are generally underreported(*9*) and may be more prevalent than traditionally believed.

CSF1R: the genetic cause of ALSP

Mutations in genes expressed uniquely in microglia are known to cause progressive leukodystrophies and neurodegenerative disorders, termed microgliopathies (*10-14*). Dysregulation of microglial homeostasis is considered the basis for these neurodegenerative and neuroinflammatory diseases. While historically the diagnosis of ALSP was contingent on histopathological characterization from brain biopsies or

autopsies, using genome-wide linkage analyses, researchers identified mutations affecting the tyrosine kinase domain of CSF1R in families with ALSP, providing a genetic origin for disease onset. Importantly, in the adult brain, CSF1R is primarily expressed by microglia, and the mutations discovered in the genome-wide linkage analyses have been shown to effectively eliminate the kinase activity of this receptor (*5, 6, 15*). *In vitro* models of such mutations found in human patients diagnosed with ALSP demonstrate that autophosphorylation of the tyrosine residues in the kinase domain is impaired in cells with mutated CSF1R receptors(*2, 6*). Additionally, CSF1R haploinsufficiency was found in an ALSP patient(*2*), leading to the subsequent development of $CSF1R^{+/-}$ mice as a model of ALSP. This mouse model develops behavioral and histopathological deficits similar to those found in ALSP patients(*16*), highlighting the validity of using these mice to investigate ALSP disease mechanisms. Together, these data suggest that a partial loss of CSF1R function and subsequent microglial dyshomeostasis could be an underlying cause for ALSP development.

Linking microglial activation to ALSP

In addition to mutations in genes associated with microglial function, recent phenotypic evidence indicates that microglia could play an important role in the development of ALSP. During early pathogenesis, microglial densities increase, characterized by swelling of microglial bodies and increased number of $CD68^+$, $CD163^+$, and $CD204^+$ microglia. With the progression of the disease in ALSP patients and under advanced pathology, microglia then substantially decrease in number. Generally, microglial alterations in protein expression and number in ALSP patients is reminiscent of microglial changes observed in a multitude of other neurodegenerative disorders such as Alzheimer's

Disease (AD)(*17, 18*), Parkinson's Disease (PD)(*19*), and amyotrophic lateral sclerosis (ALS)(*20-22*), although the exact timeline in which expression of these markers change is unique to each disease. The activation of microglia occurring concurrently with disease progression then, indicates microglial involvement to some degree. Conflicting results were found in a zebrafish model of ALSP, however, where fewer microglia were observed without affecting the microglial homeostatic signature, implying no obvious changes to inflammatory states in the microglia population. Rather, in response to increased phagocytic demand, microglia were unable to proliferate and had a delayed response to damage, alluding to a disease mechanism of reduced functional microglia and fewer available microglia as drivers of disease onset. Despite these conflicting reports, in all these investigational ALSP studies microglia are undoubtedly affected. Given the microglial gene-specific etiology of the disease and the reported changes to microglia, further study of ALSP could reveal how primary microglial dysregulation can lead to overall CNS dysregulation.

Nasu-Hakola Disease (NHD)

Nasu-Hakola disease (NHD) is another rare neurodegenerative disorder. NHD is caused by loss of function mutations in the microglial/myeloid cell-associated genes TREM2 or DAP12 (*23, 24*). NHD is characterized by the formation of multifocal bone cysts and, like ALSP, disease pathology includes early-onset dementia, degeneration of white matter, swelling of axons, and neuronal loss (*23, 25-27*). Upon the discovery that TREM2 mutations are involved in NHD pathogenesis, studies sought to clarify the role of TREM2 in CNS homeostasis. From these studies, TREM2/DAP12 signaling was found to mediate phagocytosis of multiple microbial and endogenous ligands, thereby facilitating the

clearance of debris after insult or injury(*24, 28, 29*). Deficiencies in TREM2 revealed a deficit in microglial phagocytic activity when incubated with *E. Coli(30, 31)* apoptotic Neuro2A cells(*29*), or amyloid beta (Aβ)(*31, 32*). Further analysis of TREM2/DAP12 signaling revealed its role in the suppression of inflammatory processes and the induction of transcriptional profiles indicative of enhanced myeloid cell proliferation and reduced death(*24, 33-36*). While the details of the disease require further investigation, it is possible that dysfunctions in phagocytic capacity and immune regulatory processes are key to disease pathogenesis. Interestingly, signaling through TREM2/DAP12 shares significant crosstalk with CSF1R signaling. For example, Src tyrosine kinase, one of the main effectors of CSF1R signaling, phosphorylates the immunoreceptor tyrosine-based activation motif (ITAM) of DAP12, highlighting overlapping pathways possibly involved in the development of ALSP and NHD that could explain the similar pathology found in both diseases(*37-40*). Thus, insights obtained from NHD studies may help clarify aspects of ALSP pathogenesis.

Microglial Homeostasis

Microglia are the brain resident myeloid cells that regulate CNS homeostasis. The continual extension and retraction of their ramified processes allow microglia to modulate brain activity, including the regulation of synaptic activity, restructuring of synapses, and clearance of cellular debris(*41-44*). Upon detection of an insult in the brain, microglia proliferate and migrate to the disrupted site. At the site of injury, microglia secrete chemokines, cytokines, and reactive oxygen species (ROS) to direct the immune response, ultimately resulting in the phagocytosis of pathogens and damaged cells(*45,*

46). To promote resolution of the insult, microglia secrete anti-inflammatory cytokines, such as transforming growth factor beta (TGFβ) and interleukin (IL)-10, resulting in tissue repair(*47-49*).

Phagocytosis

One of the more comprehensively studied functions of microglia in the brain is their role in clearance (via phagocytosis); this process is important for protecting the brain from invading pathogens and for removing cellular debris. Effective microglial clearance also regulates and prevents the accumulation of neurotoxic species(*50-52*). High levels of these toxic species could lead to neuronal damage that may eventually culminate in neurodegenerative phenotypes. In addition to the clearance of cellular debris, microglia are also reported to phagocytose neurons and synapses, allowing for the refinement of neuronal populations during development or adult neurogenesis(*53, 54*). Proper degradation of internalized components by microglia is thus essential for normal CNS function. Dysregulated or abnormal degradation of material can result in the intracellular accumulation of toxic molecules, including ROS (*55*). Several targets and receptors are responsible for dictating differential microglial responses. For example, Fc receptor signaling promotes an inflammatory response and clearance, whereas SIRPα blocks microglial phagocytosis(*56, 57*). Importantly, recent studies indicate that defective microglial phagocytosis is implicated in a multitude of different neurodegenerative disorders where impaired phagocytosis leads to the accumulation of toxic debris that inhibit the return of the CNS and microglia to a homeostatic state(*58, 59*).

Microglia remodel the Extracellular Matrix

The Extracellular Matrix (ECM) is a highly complex and dynamic molecular meshwork with roles in plasticity, biophysical protection, and cell signaling(*60*). The ECM and interstitial environment critically regulate neuroinflammation and the immune response. Structural components of the ECM and products of its degradation may serve as damage-associated molecular patterns (DAMPs) that induce or suppress microglial reactivity by signaling through pattern recognition receptors (e.g., Toll-like receptors). For instance, culturing microglia on a CSPG substrate in vitro induces microglial activation, proliferation, and the expression of IGF-1, MMP-2, and MMP-9, whereas pharmacological inhibition of CSPG production with xyloside following spinal cord injury differentially alters inflammation and cytokine production depending on the timing of treatment(*61*). Alternatively, disaccharides generated from the degradation of CSPGs with the bacterial enzyme chondroitinase ABC (ChABC) confer an activated noncytotoxic microglial phenotype that is associated with protection in experimental autoimmune encephalomyelitis(*62*), and spinal cord injury for example(*61*).

The ECM can be partitioned into structural subtypes based on organization and composition, which generally include (1) the basement membrane of the BBB, (2) the diffuse ECM found in interstitial and perisynaptic spaces, (3) the condensed, reticular ECM that ensheathes neuronal subsets and their perisomatic synapses to form structures known as perineuronal nets (PNNs), and (4) the perinodal ECM that surrounds nodes of Ranvier within axons and that displays compositional resemblance to PNNs(*63, 64*). Along with synaptic terminals and glial cells, the diffuse perisynaptic matrix and the synaptic ECM of PNNs constitute the fourth compartment and most recent addition to the conventional model of synaptic function, the tetrapartite synapse(*60, 65*), and recent

studies report that both structures are dynamically regulated by microglia in the homeostatic adult brain.

Although PNNs are associated primarily with fast-spiking parvalbumin (PV)-expressing GABAergic interneurons, particularly in the cortex of the brain, they are evident throughout the CNS and across a variety of neuronal subsets(*63, 66*). These formations serve as a molecular scaffold to stabilize and regulate the synapses they surround and reach adult levels during the closure of critical periods of neuroplasticity(*66, 67*), and the genetic or enzymatic removal of PNNs or their components are capable of reinstating critical period-like plasticity. Strikingly, we observed that PNN abundance is dramatically upregulated throughout the healthy adult brain following microglial depletion(*68*). While neurons and glia may both express components that contribute to PNNs, neurons can express the core components of nets themselves and are capable of forming PNNs in vitro in the absence of glia(*69*). Therefore, our findings suggest that microglia basally regulate PNN density in the homeostatic brain, whether via direct or indirect enzymatic degradation and/or phagocytosis, such that their absence allows PNN components to accumulate. PNN enhancements induced by microglial depletion are also associated with increased excitatory and inhibitory synaptic connections to excitatory cortical neurons, as well as augmented neural activity in both cortical excitatory neurons and PV^+ interneurons as assessed by in vivo calcium imaging(*68*). Synaptic connectivity and neural activity are both normalized following microglial repopulation(*68*), which is consistent with the normalization of PNN densities we observed under similar conditions of inhibitor cessation following microglial elimination.

The vast majority (98%) of CSPGs within the CNS are found in the general diffuse ECM, including the perisynaptic matrix. Research by several groups in the past decade has begun to shed light on the comparative composition of perisynaptic and PNN matrices in the CNS. The discovery of axonal coats (ACs) serves as one such example of a well-characterized perisynaptic matrix structure that exists as a separate entity from classical PNNs(*70*). These round structures of aggrecan- and brevican-based ECM enwrap individual synaptic boutons contacting neuronal dendrites and somata and sometimes comingle with PNN components on associated neurons(*70*), with hypothesized roles at the synapse in restricting neurotransmitter spillover and receptor localization(*71*). It has been shown that targeted perisynaptic matrix degradation induces structural plasticity of dendritic spines (e.g., enhanced spine motility and formation of spine head protrusions)(*72*) and similar structural changes are associated with increased functional plasticity as measured by LTP(*73*), and as such, CSPGs appear to restrict plasticity in either case. Thus, changes in upstream perisynaptic ECM could lead to downstream signaling-dependent changes in synaptic plasticity and further alterations in associated ECM in an increasingly complex, circuit-level process.

Suggesting a direct role for microglia in the regulation of perisynaptic matrix-controlled synaptic plasticity, a recent study by Nguyen et al. determined that, in response to neuronal IL-33, microglia in the adult brain phagocytose and clear perisynaptic ECM components to promote dendritic spine formation, synaptic plasticity, and fear memory precision(*74*). Importantly, they found that inhibition of this pathway decreased microglial engulfment of aggrecan and consequently enhanced aggrecan puncta density and deposition at the synapse, in addition to increasing total intact brevican while reducing

levels of proteolyzed brevican. Thus, as in our work, loss of microglial function results in enhanced ECM deposition in the homeostatic brain. The occurrence of this phenomenon across multiple ECM compartments (i.e., the perisynaptic matrix(*74*) and perineuronal nets(*75, 76*)) together suggests a fundamental homeostatic role for microglia in ECM degradation and remodeling, which may be required for subsequent remodeling of synapses surrounded and stabilized by such ECM. However, the molecular mechanism(s) by which such alterations occur in disease or under conditions of homeostasis are as of now unclear.

As observed with synapses during developmental pruning, microglia may directly engulf and phagocytose ECM components. Indeed, aggrecan colocalizes with lysosomal CD68 in microglia, a marker of phagocytosis, and disrupting IL-33-based ECM engulfment by microglia reduces $CD68^{+}$ lysosome number(*74*). However, it is likely that microglial release of degradative enzymes is also involved in ECM turnover processes, especially as it applies to the remodeling of PNNs, in which CSPGs, tenascins, hyaluronan, and link proteins are more tightly woven together compared to the diffuse matrix.

Microglial-Synapse Interactions

Thorough monitoring of the CNS parenchyma by microglia aptly positions these cells to respond rapidly to changes in the synaptic microenvironment. In the healthy brain, they interact with pre- and postsynaptic compartments, perisynaptic astrocytes, and the local extracellular milieu(*77-79*). This has thus far been best studied during development when microglia prune excess synapses(*80, 81*) to promote the removal of extranumerous or weak synapses in the refinement of neuronal networks(*82, 83*). Accumulating evidence has implicated traditionally immune-associated molecules as critical elements in synaptic

refinement, describing synaptic pruning as an activity dependent mechanism. For example, complement cascade elements (e.g., C1q and C3) localize to synaptic compartments to tag synapses for elimination(*84, 85*), inducing phagocytosis by complement receptor 3 (CR3)-expressing microglia in a neural activity-dependent manner(*80*). On the other hand, genetic loss of CX3CR1, a receptor primarily expressed by microglia in the brain, is also associated with synaptic pruning deficits, resulting in an excess of dendritic spines, immature synapses, and immature brain circuitry in development(*81, 86, 87*) that persists as impaired synaptic transmission and functional brain connectivity in adults(*88*).

Microglia can also induce synapse formation, as shown by the addition of developing microglia to cultured hippocampal neurons in vitro, which increases dendritic spines and excitatory and inhibitory synapses via microglial IL-10 (*89*). While this process did not require direct microglial contact, a recent study utilizing in vivo two-photon imaging of early postnatal (P8-P10) mouse brains observed microglial contact-induced filopodia formation on dendrites, which was reduced following minocycline treatment (*90*). Decreased dendritic spine densities were observed in the same study following microglial depletion (*90*), which resembled the reduced spine formation reported by another group under similar circumstances (*91*). However, caution must be taken regarding the interpretation of this result, as both studies utilized diphtheria toxin-based models of microglial ablation, which are associated with inflammation (e.g., upregulation of TNF-α, IL-1β (*92*) or an interferon response (*93*)) that is not seen with genetic- or inhibitor-based models due to the manner in which microglial death is achieved (*94*). Accordingly, IL-1β attenuates synaptic formation induced by IL-10 (*89*), and postnatal CSF1R inhibitor-

based microglial depletion instead results in excess synapses (*95*) that are normalized following microglial repopulation (*96*). Interestingly, loss of CSPG-5 (neuroglycan C), which normally localizes to the perisynaptic space (*97*), results in impaired presynaptic maturation as well as synaptic elimination that occurs earlier than normal in cerebellar Purkinje cells (*98*), which microglia survey and regulate (*99-101*). As early developmental synaptic deficits are observed in other brain regions with CSPG-5 deficiency (*102*), together, this suggests a role for perisynaptic matrix remodeling during synaptic pruning and maturation. Interestingly, the modulation of the synaptic landscape by microglia is not solely restricted to developmental time points. We recently demonstrated that elimination of microglia in healthy adult mice with CSF1R inhibitors increases the total density of hippocampal dendritic spines and enhances PSD95 and synaptophysin immunolabeling(*103*), confirming that microglia continue their roles as synaptic sculptors throughout adulthood. This suggests that perturbations in microglia homeostasis, even in adulthood, could affect synapse and overall CNS health.

Microglia-Neuron Interactions

In addition to synaptic modulation, microglia play a role in CNS homeostasis by regulating neuronal proliferation, survival, and death(*104, 105*). In the absence of microglia, cultured neural precursor cells (NPCs) exhibit decreased proliferation, however, the addition of exogenous microglia rescues this effect(*106*). *In vivo* studies in the developing mouse cortex revealed that microglia provide trophic support to neurons promoting neuronal survival(*105, 107*), whereas inhibition of microglial activity via minocycline treatment or microglial ablation increased neuronal apoptosis during early postnatal development(*105, 108*). Contrasting their role in neuronal survival, microglia are also capable of instructing

neuronal cell death. Approximately half of the neurons originally born in the developing brain undergo apoptosis, with microglia making physical contact with the dying neurons(*109-111*). In addition, deficiencies in DAP12, which is selectively expressed by microglia, reduced numbers of apoptotic neurons in hippocampal regions(*112*), implicating these molecules in the regulation of neuronal death. Additionally, the coordinated anti- and pro-apoptotic mechanisms induced by microglia establish proper CNS homeostasis. By actively mediating cell survival and proliferation through synaptic sculpting, microglia can affect CNS functioning on a global scale. Thus, alterations to microglia-related pathways could exert detrimental effects on neuronal populations, culminating in neurodegenerative phenotypes.

Microglia can also directly contact neurons to regulate neuronal functioning. Microglial processes continually contact developing and mature neurons while surveying their environment. This close physical proximity can be indicative of their phagocytic response; however, recent evidence suggests that microglia also actively mediate cell death through contact-mediated cues and the secretion of soluble factors(*112-114*). Furthermore, these contact points are associated with changes in neuronal excitation(*115*), thereby regulating CNS activity. In larval zebrafish, live imaging revealed that neuronal activity attracted resting microglia processes toward the soma of active neurons. Formation of microglial-neuron contacts was shortly followed by the suspension of spontaneous and evoked activity on these neurons(*116*). These data indicate that microglia could regulate neuronal network activity and excitation following brain injury. Such cell-to-cell contact may initiate a local signaling cascade responsible for the downregulation of neuronal activity. Inducing repetitive action potentials, for example, led to axonal swelling and prolonged

depolarization of the cell, resulting in the rapid migration of microglia to these axons(*117*). The proper function of microglia and its interactions with neurons thus becomes a critical component of CNS homeostasis. Altogether, these data indicate that microglia regulate neuronal network activity and excitation under homeostatic conditions. Whether these roles continue under conditions of duress remains to be determined.

Despite recent studies on microglia-induced modulation of neuronal activity and functioning, the molecular mechanisms behind these phenomena, and how microglia integrate multiple signals from multiple neurons at once, are still not well understood. While it is well-established that dysregulated functioning of microglia and their influence on neuronal populations impairs CNS development and homeostasis, it is also possible that disrupted CNS homeostasis could involve interactions occurring between microglia and other glial cells.

Microglial induction of CNS pathology

Under certain disease states, the immune response fails to achieve effective immune resolution, resulting in a perpetual and chronic inflammatory environment. Among different neurodegenerative disorders, emerging evidence links microglia-mediated neuroinflammation to the progression of pathology The ubiquitous observation of microglial activation and/or dysfunction in various neurodegenerative diseases, such as PD(*118-120*), Multiple Sclerosis (MS)(*118-121*), and Amyotrophic Lateral Sclerosis (ALS)(*122, 123*), strongly implicates microglia in conferring broad detrimental effects to the brain.

Age-related changes in microglial function can also gradually perturb CNS homeostasis, ultimately heightening the reactivity of glial cells(*124-128*). In turn, abnormal reactivity of microglia favors a cytotoxic response; as such, a recurring theme during disease progression is elevated microglial release of neurotoxic species(*129-132*). This dysfunctional immune response mediated by microglia is reported to contribute to the initiation of neuronal damage through the production of inflammatory molecules, including TNF-α, nitric oxide (NO), IL-1β, and ROS. In line with this, we recently demonstrated that pharmacological elimination of microglia in a mouse model of AD prevented neuronal loss(*120*), indicating that chronically activated microglia contribute to this aspect of neurodegeneration. Therefore, tight regulation of these signaling pathways is crucial to avoiding pathological neuroinflammation. The exact pathways and mechanisms involved are still under investigation; however, the influence of microglia on the development of many neuropathologies is well-described.

Disease Associated Microglia

Transcriptomic studies of sorted microglial populations from disease mouse models found common significant increases of microglial transcripts in the distressed CNS, further highlighting the plastic nature of microglia. The reactive microglia found in brains of neurodegenerative disorders, termed disease-associated microglia (DAM), were described as cells displaying increased expression of markers of general macrophage activation with a concomitant downregulation of homeostatic microglial genes. This upregulated DAM gene module has since been described in mouse models of frontotemporal dementia tauopathy(*17*), AD(*18, 114*), ALS(*133*), and cuprizone-induced demyelination(*134*). Transcriptionally, this includes genes involved in interferon

response, lysosomal and phagosome function, and lipid metabolism. The transcriptional signature of DAM includes the expression of the genes: *Axl, Clec7a, Cst7, CD11c, MHCII, CD14, CD86* and *CD274, CSF1*(*18, 135, 136*).

Microglia are equipped to recognize a myriad of signals throughout the lifespan, sensing any deviations in CNS homeostasis. DAM signatures could thus be indicative of responses to stimuli that occurs with chronic disease, perhaps reacting to apoptotic cells, damaged myelin, as well as protein aggregates irrespective of disease etiology. Accordingly, a complete DAM signature can only be attained in a TREM2 dependent manner - without TREM2 activity, microglia only achieve an intermediate state(*18*). TREM2, importantly, recognizes a broad spectrum of danger-related signals, ranging from damaged myelin to lipoproteins that form complexes with amyloid beta (Aβ)(*35, 134, 137, 138*). In this regard, TREM2 is positioned to act as the receptor linking DAM to multiple unique neurodegenerative disorders. Despite giving a transcriptional signature, the involvement of DAMs in disease is still not well understood. However, given the importance of TREM2 for the transition from homeostasis to a DAM signature, and the reported exacerbation of pathology in AD(*11, 139, 140*) and NHD(*24, 27*) caused by TREM2 mutations, it is likely that the DAM is, at least initially, a protective immune response.

Aberrant ECM reorganization

Previous studies have suggested that microglia may drive PNN loss in certain disease contexts due to their inherent ability to secrete matrix-degrading enzymes (e.g., matrix metalloproteinases; MMPs) and/or their molecular activators or inhibitors (*141-144*). Indeed, we have recently shown that microglial depletion prevents disease-associated

PNN reductions in models of Huntington's (*75*) and Alzheimer's disease (*76*). PNN components were evident in microglia in both AD mouse and human brain tissue (*76*). That we observed similar effects on PNN abundance in the relative absence of microglia across these models is striking, both due to their differential etiologies—intracellular vs. extracellular protein accumulation in the R6/2 HD (*145*) and 5xFAD model of AD (*146*), respectively—and the variable microglial phenotypes we observed, which resembled "classical activation" in 5xFAD (*76*) but not R6/2 brains (*75*), where they instead were associated with an interferon signature marked by enrichment of type I (IFNα, IFNβ) and type II (IFNγ) signaling pathways.

A recent study also reported that depletion of the microglial pool with the CSF1R inhibitor PLX5622 prevented PNN loss caused by ketamine or 60 Hz light entrainment (*147*). It appears then that microglia have the capacity to drive PNN loss in disease, which is further supported by temporal analyses of microglial activation and their accumulation of net material in prion disease (*141, 148, 149*) as well as following infection with human or simian immunodeficiency virus (HIV or SIV), which preferentially infect microglia and cause downstream PNN degradation (*143, 150, 151*). PNN deficits/decreases have also been observed across more diverse diseases, many if not all of which are also generally associated with microglial activation including multiple sclerosis, stroke and epilepsy. Loss of PNNs with disease thus likely reflects a toxic gain-of-function in microglia of this newly identified homeostatic role, wherein augmented or complementary PNN-degradative processes are activated. Such processes can occur either via enhanced or alternative secretion of ECM-cleaving proteases or their modulators, and/or increased phagocytosis. Importantly, such proteases implicated in remodeling ECM, are similarly

implicated in remodeling synapses as well (*152, 153*), underscoring the functional relationship between the ECM and synapses—to sculpt synapses, an increasingly salient role of microglia, the matrix in which they are embedded would presumably also have to be restructured. Ongoing research continues to elucidate the bidirectional interactions between the ECM and synapses, but the involvement of microglia in this process has just begun to be examined.

Aberrant synapse elimination

Synaptic loss, as opposed to neuronal loss, serves as the most accurate indicator of cognitive decline. While synapse elimination is known to be a normal process in brain development, the dysregulation of this process is recognized as an early feature of neurodegeneration(*154-157*). Under neurodegenerative conditions, microglial-induced synapse loss may be viewed as a toxic gain-of-function with respect to normal synaptic-regulating processes as in AD where microglial-induced synapse loss involves the dysfunctional activation and upregulation of complement proteins C1q and C3. These pathways are responsible for synaptic pruning during development, with their overactivation leading to aberrant synaptic loss and excessive phagocytosis of synaptic elements(*158*). Elimination of microglia, however led to improved functional outcomes accompanied by restoration in spine number and synaptic surrogates(*103, 120*), further emphasizing the important role of healthy microglia in maintaining synapse density. In addition to complement components, synapse loss can also result from the release of soluble synaptotoxic factors. *In vitro* experiments demonstrated that conditioned media containing TNF-α, nitric oxide, and IL-6 from activated microglia was sufficient to induce synaptic loss(*159, 160*). Microglia thus play an important role in the maintenance and

elimination of synaptic elements during disease pathogenesis where maintenance is hindered or aberrant pruning occurs due to the dysfunction of microglia.

Neuropsychiatric disorders

The hypothesis for an immunological contribution to major psychiatric disorders initially arose from evidence drawing parallels between core symptoms of depressive disorders and sickness behaviors resulting from inflammatory conditions(*161*). As sentinels of the brain parenchyma, microglia are more likely to sense the psychological stress induced by different paradigms. In support of this hypothesis, patients diagnosed with depression present with increased levels of circulating cytokines TNF-α and IL-6(*162*) and innate immunity-related genes in the blood(*163*). Consistently, the anterior cingulate cortex and the dorsal prefrontal white matter in postmortem tissue of depressed patients displayed increased density and enlargement of microglia(*164, 165*). In accordance with these studies, murine models of chronic stress-induced depression mirrored aspects of immunological alterations found in the human patients. Recent studies have linked microglia to the development of depression and anxiety demonstrating that chronic mild stress activated microglia and subsequently upregulated inflammatory mediators, such as IL-1β and IL-6(*166-171*). Inactivating microglia through minocycline treatment reduced depressive and anxiety-like behavior(*170, 171*). Similarly, the induction of pro-inflammatory phenotypes in stress-induced paradigms also promotes a state of glucocorticoid insensitivity in microglia, which prevents glucocorticoid-induced suppression of inflammation(*172-174*). This feedback loop then has potential to further propagate microglial damage to the local brain environment. As indicated by reduced Fos B labeling in neurons, minocycline treatment also attenuated neuronal activation induced

by restraint stress(*167*). Thus, one method by which microglia could advance dysfunctional neurobiological stress responses, and ultimately neuropsychiatric disorders, is by also further dysregulating neuronal activity. Indeed, it has been proposed that dysfunctional microglia-neuron crosstalk is the primary source of neuroinflammatory signaling after a stress response(*175*). To date, the exact molecular mechanisms by which neuropsychiatric disorders develop is still not well understood. Regardless of the true mechanism(s) in action, microglia are implicated as mediators to some capacity of depressive and anxiety-related behavioral changes associated with ALSP.

Demyelination

One of the main pathological hallmarks in ALSP is the severe demyelination of axonal tracts primarily found in the subcortical white matter of the frontal lobes and the corpus collosum(*176, 177*). White matter changes including reductions in volume and integrity(*178, 179*), bulging of myelin sheaths(*180*), and a separation of myelin from axons(*181*) have been observed in normal aging individuals. Similarly, multilamellar myelin fragments have been observed in brains of aged mice(*182, 183*). These fragments can be phagocytosed by microglia raising the possibility that they can actively remove myelin. Indeed, aged microglia accumulate material reminiscent of lipofuscin that represent indigestible myelin within their lysosomes(*183*). Inclusion of indigestible material could contribute to microglial dysfunction found in aged individuals. The precise role microglia play during dysfunctional demyelination in the adult is still under investigation, however, microglia have been implicated in the clearance of myelin debris in several CNS disorders such as MS and progressive multifocal leukoencephalopathy(*184-188*).

Myelin clearance through the involvement of macrophage-associated complement, scavenger, and Fc, receptors(*189*), pointing towards indicating that the failure of proper microglial phagocytosis could may be involved as a mechanism for myelin loss. Active demyelination is associated with the accumulation of microglia at the site of axonal lesioning(*190, 191*). As is the case in other neurodegenerative diseases, the increase in microglia density precedes the appearance of white matter pathology, implicating microglia as primary mediators of axonal damage. Microglial activation induces the loss of myelin, even prior to astrocytosis, further suggesting these cells may drive the eventual demyelination found in these diseases. A recent study demonstrated that the loss of homeostatic signature in microglia in MS, as evident by a loss in P2RY12 expression, was associated with the progression of disease at active lesion sites(*121*) . Additional characterization at these sites showed increased expression of phagocytic and oxidative responses linked specifically to microglia - in line with other studies reporting similar characterizations(*121, 192-195*)

Recent advances showing the cellular interdependence of microglia and oligodendrocytes indicate that myelin dysfunction should be understood in the broader context of CNS pathology. As such, microglia could play a role in white matter loss and myelin integrity through their actions on oligodendrocyte homeostasis. Oligodendrocytes and oligodendrocyte precursor cells (OPCs) are involved in the myelination of the CNS , but both of these cell types are particularly susceptible to damage in the presence of reactive oxygen species, excitotoxicity, and cytokine signaling(*196-201*) . Indeed, in a mouse model of MS, the upregulation of microglial inflammatory mediators p22phox and gp21phox in lesion sites was positively correlated with the extent of DNA oxidation in

oligodendrocytes(*184, 194*). Furthermore, inefficient microglial phagocytosis of myelin debris is reported to inhibit oligodendrocyte-derived remyelination and the maturation of OPCs into myelinating oligodendrocytes(*202*), impairing myelination processes. This cascade of disorganized clearance and subsequent oligodendrocyte pathology may induce a vicious cycle, sustaining microglial activation processes and resulting in further demyelination, which could lead to the development of white matter brain diseases.

Roles of CSF1R in Myeloid Cells

Differentiation and Proliferation

CSF1R is expressed on myeloid-lineage cells. Signaling through the receptor is involved in the differentiation of these cells to the microglial compartment in the brain – mice lacking the receptor are born without microglia(*203, 204*). During development, CSF1R is upregulated in myeloid precursor cells in two phases. During the first phase, transcription factors such as PU.1, Runx1, and C/EBP assemble, leading to the remodeling of chromatin at the macrophage promoter(*205*). The second phase involves assembly of transcription factors, such as Egr1 and Egr2, that simultaneously promotes the expression of macrophage genes and represses the transcription of neutrophil genes(*206*), ultimately resulting in the development of myeloid progenitors with restricted developmental potential. Upregulating CSF1R in two phases ensures that CSF1R is only expressed at high levels in differentiated cells that respond to CSF1 alone and not in multipotent cells that require synergistic growth factors like IL-3(*207, 208*).

In addition to differentiation, CSF1R signaling has known roles in macrophage proliferation. Activation of CSF1R signaling pathways induces CSF1 dose-dependent

increases in protein synthesis(*209, 210*). CSF1R activation also phosphorylates ITAMs of the cytoplasmic domain of DAP12. The cascade of signals resulting from this activation leads to the eventual phosphorylation and nuclear translocation of β-catenin, subsequently activating cell cycle genes. DAP12 deficiency impairs CSF1R-mediated proliferation and the subsequent transduction of DAP12 into DAP12 deficient bone marrow-derived macrophages restored wild type cell cycle signatures(*39, 211*).

Survival

CSF1 mediates macrophage survival (*209, 210*) largely through Akt/PI3K pathways. In an *in vitro* study of macrophage survival, inhibition of PI3K with specific inhibitors prevented increases of macrophages in cell culture. Despite the inhibition in proliferation, there was no change in DNA synthesis reported, suggesting that the pathways involved were related to cell survival rather than proliferation. Independent of PI3K, CSF1R-mediated PLC activity enhances macrophage survival by altering glucose uptake. Upon stimulation via CSF1, glucose transporters are translocated to the cell membrane and glucose uptake is enhanced(*212*).

Our lab has performed extensive studies on CSF1R function in CNS homeostasis and also found that microglia are dependent on its signaling for survival(*103, 119, 120, 213-215*). We have identified several brain-penetrant CSF1R inhibitors (PLX3397, PLX5622) that can be orally administered to mice, resulting in the elimination of up to ~99% of microglia for the duration of treatment(*103, 119, 120, 213-215*). Despite extended CSF1R inhibitor treatments/microglial elimination of up to six months, no deleterious effects on cognition have been observed(*119, 120, 213*). These data inform us that we can eliminate the entire microglial population in the adult brain with no detrimental effects. These

inhibitors are currently in clinical use for oncology indications; however, as a result of our work, CSF1R inhibitors are now being developed for CNS disorders. Microglial elimination via CSF1R inhibitor administration is a unique tool that provides us with a tremendous amount of exploratory freedom, as we can now begin to answer fundamental questions about microglial function, homeostasis, and involvement in disease.

Chapter Two:

Microglial dyshomeostasis drives perineuronal net and synaptic loss in a CSF1R $^{+/-}$ mouse model of ALSP, which can be rescued via CSF1R inhibitors

INTRODUCTION

Adult Onset Leukoencephalopathy with Axonal Spheroids and Pigmented Glia (ALSP), also reported as hereditary diffuse leukoencephalopathy with spheroids (HDLS), is a rare autosomal dominant neurodegenerative white matter disease. Pathologically, this disease is characterized by the presence of patchy cerebral white matter lesions, predominantly in frontal and parietal white matter areas, which induce early thinning of the corpus collosum (cc) followed by subsequent cortical atrophy in the affected regions (*1-4*). Genome-wide linkage analyses (GWLAs) have provided a genetic origin of the disease by identifying mutations that affect the tyrosine kinase domain of CSF1R in families with ALSP. In the adult brain, CSF1R is primarily expressed by microglia, and mutations discovered in the GWLAs have been shown to effectively eliminate the kinase activity of this receptor (*5, 6, 15*). Indeed, *in vitro* models demonstrate that autophosphorylation of the tyrosine residues in the kinase domain is impaired in cells with mutated *Csf1r* (*2, 6*). However, the cellular biology underlying detrimental ALSP phenotypes induced by mutations in *Csf1r* (e.g. cellular source(s) of pathology) remains unclear. Where some studies argue for a dominant-negative effect in which expression of the mutant CSF1R suppresses autophosphorylation of the wild type CSF1R (*6, 216*), others argue for a predominantly functional haploinsufficiency genetic mechanism (*7, 217*). However, the discovery that *Csf1r* haploinsufficiency alone could cause ALSP in the clinical population without requiring the expression of mutated protein (*2, 218*) lead to

subsequent development of CSF1R$^{+/-}$ mice as a model of disease. This mouse model develops behavioral and histopathological deficits similar to those found in ALSP patients including depression, seizures, cognitive deficits, abnormal myelination and neurodegeneration (*16*), highlighting the validity of using these mice to investigate disease-related mechanisms. In addition to *Csf1r*, mutations in other genes highly expressed in microglia (*Trem2*, *Tyrobp*) are known to cause progressive leukodystrophies and neurodegenerative disorders aside from ALSP, broadly termed microgliopathies (*11, 13*).

As CNS resident macrophages, microglia modulate CNS homeostasis by orchestrating inflammatory responses (*219*), clearing cellular debris (*24, 220*), restructuring synapses (*80, 221*), and regulating perineuronal nets (PNNs) (*74, 75, 221*). Understanding how changes in microglial function that result from *Csf1r* haploinsufficiency, or other factors, can affect these various modalities may inform us about how microglia cause neurodegeneration in related microgliopathies. Importantly, this information can be extended to understand how altered microglial functions can affect CNS stability and contribute to neurodegeneration in other disorders such as Alzheimer's disease, Parkinson's disease, tauopathies, stroke and injury, as well as aging itself. Whether microglial gain of function or loss of function results in ALSP phenotypes, however, is still up for debate. Of relevance, microglia are dependent on CSF1R signaling for their survival, and sustained pharmacological inhibition of CSF1R, or absence of *Csf1r* expression (*222*), results in microglial death (*213*). As such, it has been postulated that ALSP could result from loss of homeostatic microglial numbers due to a decreased amount of CSF1R expression during the aging process, as has been shown in a *Csf1r*

genetic knock-out zebrafish model (*223*). However, long-term CSF1R inhibitor-dependent microglial elimination in mice (up to 6 months of treatment) does not cause any overt impairments as related to ALSP, and in fact improves cognition in some cases, as assessed by Contextual Fear Conditioning, Morris Water Maze, Barnes Maze, and Elevated Plus Maze (EPM) (*119, 213*). Nonetheless, given the primary role of CSF1R in both microglial survival and ALSP, and of the frequent microglial gene-specific etiology of leukodystrophies in general, it is likely that pathological alterations in microglial function contribute to ALSP onset and/or progression.

In this study, we aimed to investigate how loss of one *Csf1r* allele would affect microglial and parenchymal homeostasis. Here, we found that myeloid-specific ablation of one copy of the *Csf1r* gene in adult mice resulted in a general loss of microglial homeostasis as evident by loss of P2RY12 expression. Accompanying this microglial dyshomeostasis, we observed a decrease in synaptic surrogates, as well as dysregulation of extracellular matrix (ECM) components, in particular a loss of perineuronal nets (PNNs), confirming an adult microglial origin for these downstream phenotypes. Using a constitutive $CSF1R^{+/-}$ mouse model of ALSP we noted an increase in microglia densities, due to developmental defects in the establishment of the adult microglial population, and a similar loss of P2RY12 expression and microglial hyper-ramification in $CSF1R^{+/-}$ mice. Accompanying this loss in microglial homeostasis, we observed impaired behavioral output assessed by Novel Object and Novel Place Recognition tasks, along with similar decreases in synaptic surrogates and PNNs. Accordingly, complete elimination of microglia from adult $CSF1R^{+/-}$ mice reverses PNN and synaptic deficits. We further compared the genetic monoallelic loss of *Csf1r* with low-grade chronic CSF1R inhibition (CSF1Ri) and found significant

overlap in gene expression changes, suggesting that partial disruptions to CSF1R signaling, whether pharmacological or genetic in nature, lead to similar downstream signaling abnormalities. Unexpectedly, low-grade CSF1Ri in CSF1R$^{+/-}$ mice was able to reverse microglial dyshomeostasis and restore cognition, as well as prevent the loss of synaptic surrogates and perineuronal nets in affected mice, rather than exacerbate these alterations.

MATERIALS AND METHODS

Compounds:

PLX5622 was provided by Plexxikon Inc. and formulated in AIN-76A standard chow at a dose of 150 ppm or 1200 ppm by Research Diets Inc.

Mice:

All mice were obtained from The Jackson Laboratory. Mice were mixed sex C57BL/6 (000664) mice. Animals were housed with open access to food and water under 12h/12h light-dark cycles. All mice were aged to 8 months unless otherwise indicated. *Csf1r*$^{+/-}$ mice were generously provided by Dr. Karina Cramer (University of California – Irvine; Department of Neurobiology and Behavior) and were maintained and genotyped as described previously (*224*). For genotyping *Csf1r*$^{+/-}$ mice the following primers were used: Forward, 5' ATCCAGCATTAGGCAGCCT; reverse, 5' GCCACCATGTGTCCGTGCTT. For inducible CSF1R haploinsufficiency experiments the following mice were obtained from The Jackson Laboratory: CSF1R$^{fl/fl}$ (B6.Cg-*Csf1r*$^{tm1.2Jwp}$/J; Stock No: 021212) and Cx3Cr1$^{cre\text{-}ert2/cre\text{-}ert2}$ (B6.129P2(C)-Cx3cr1$^{tm2.1(cre/ERT2)Jung}$; Stock No: 020940). Progeny from these mice were bred to produce groups of interest. For genotyping *Csf1r*$^{+}$/*Csf1r* ^{fl}

mice the following primers were used: Forward, 5' CTGGACTCATCCACCACCTT; reverse, 5' CGTTGGCTACCCGTGATATT). For genotyping *Cx3cr1*$^{cre\text{-}ert2}$ mice, the following primers from The Jackson Laboratory were used: Wild type Forward, 5' AGCTCACGACTGCCTTCTTC; Common, 5' ACGCCCAGA CTAATGGTGAC; Mutant Forward, 5' GTTAATGACCTGCAGCCAAG

Animal treatments:

All rodent experiments were performed in accordance with animal protocols approved by the Institutional Animal Care and Use Committee (IACUC) at the University of California, Irvine. The CSF1R$^{+/-}$ mouse model (*16, 225*) has been previously described in detail. For LPS experiments, 9-month-old male and female Wild-Type mice were intraperitoneally (IP) injected with 0.5 mg/kg LPS, as described before, (*213*)(L4130, Sigma) and BrdU (000103, Thermo Fisher Scientific) or saline and BrdU every other day for a week followed by euthanasia 24hr after the last dose. BrdU injections were administered intraperitoneally to all mice at a dose of 1 ml/100 g body weight (*213*) (per manufacturer's instructions) twice daily. At the end of treatments, mice were euthanized via CO2 inhalation and transcardially perfused with 1X phosphate buffered saline (PBS). For all studies, brains were removed, and hemispheres separated along the midline. Brain halves were either flash frozen for subsequent biochemical analysis, drop-fixed in 4% Paraformaldehyde (PFA; Thermo Fisher Scientific, Waltham, USA) for subsequent immunohistochemical analysis. Half brains collected into 4% PFA for 48 hrs and then transferred to a 30% sucrose solution with 0.02% sodium azide for another 48-72 hrs at 4C. Fixed half brains were sliced at 40 µm using a Leica SM2000 R freezing microtome. The flash-frozen hemispheres were microdissected into cortical, hippocampal, and

thalamic/striatal regions and then ground with a mortar and pestle to yield a fine powder. For RNA analyses, half of the powder was processed with an RNA Plus Universal Mini Kit (Qiagen, Valencia, USA) according to the manufacturer's instructions.

Behavioral assays:

The following behavioral paradigms were carried out in the following order (*213*) WT and CSF1R+/- underwent behavioral assessment six weeks after being placed on their respective diet beginning at 6 mo.

Elevated plus maze (EPM)

Mice were placed in the center of an elevated plus maze for 5 minutes to assess anxiety. Unless otherwise stated, ANY-Maze software was employed to video-record and track animal behavior. The total number of open and closed arm entries, as well as the time spent in each arm was determined.

Open field (OF)

In brief, mice were placed in a white box for 5 min to assess anxiety. The amount of time spent in the center versus the perimeter of the arena was obtained. Measurements on distance traveled as well as average speed of the mice were also observed. Of note, the same arena was used for OF, Novel Object, Novel Place and Social Interaction tasks.

Novel object recognition (NOR)

Mice were allowed to freely explore two identical objects (either small glass beakers or plastic building blocks; counterbalanced for treatment) and exploratory behavior was recorded for 5 min. 24 hrs later, one familiar object is replaced with a novel object (either

beaker or block) and behavior is recorded for 3 min. The amount of time spent investigating the novel object was determined by calculating the discrimination index (time investigating novel object—time investigating old object / total time) and is presented as a percentage, where chance level of investigation for each object is 50%.

Novel place recognition (NPR)

Mice were allowed to freely explore two identical objects (either small glass beakers or plastic building blocks; counterbalanced for treatment) and exploration behavior is recorded for 5 min. 24 hrs later, one familiar object is moved to a new location and behavior is recorded for 3 min. The amount of time spent investigating the novel object was determined by calculating the discrimination index (time investigating novel place—time investigating old place / total time) and is presented as a percentage, where chance level of investigation for each place is 50%.

Social Interaction Task

Mice we allowed to freely explore the arena for 5 minutes. After habituation, a control mouse of the same sex was placed inside a wire containment cup that is located to the side of the arena. Subject mouse was allowed free access to the arena and control mouse for 5 minutes. Number of direct contacts between the subject mouse and the containment cup housing a control mouse were quantified as active contacts. Duration of active contact points were measured and determined by calculating the discrimination index (time of active contact points / total time) and is presented as a percentage.

Rotarod

The motor capabilities of the mice were tested using an accelerating rotarod (Ugo Basile). Each mouse was placed on the rotarod beam for a maximum of 5 min while it accelerated from 8 to 40 rpm. The experimenter stopped the timer when either the mouse fell off the beam or the mouse held on to the beam and its body completed two full rotations. A total of 5 trials were performed per mouse, each with a 15-min intertrial interval.

Oral gavage of adult mice with tamoxifen:

Tamoxifen (Sigma, T5648) was dissolved in corn oil (Sigma, C8267) at a concentration of 50 mg/ml. For adult induction of CSF1R haploinsufficiency, tamoxifen (5 mg/25g body weight) was orally gavaged daily for 5 days. Tamoxifen administration began at 2 mo and brains were harvested at 8 months.

Histology and confocal microscopy:

For immunostaining of P2RY12, Aggrecan, CSPG CS-56, and Ctip2 antigen retrieval was performed by heating the sections in citrate buffer (10 mM [pH 6.0]) for 30 minutes at 80C followed by 10 minute cooling period and 5 minute 1X PBS wash. Fluorescent immunolabeling followed using a standard indirect technique as described previously (*119*). Brain sections were stained with primary antibodies against: ionized calcium binding adaptor molecule 1 (IBA1; 1:1000; 019-19741, Wako and ab5076, Abcam), wisteria floribunda agglutinin (WFA; 1:1000, B1355, Vector), Aggrecan (1:200; ab1031 Millipore), CSPG CS-56 (1:200; ab11570 Abcam), S100β (1:200; Abcam), glial fibrillary protein (GFAP; 1:1000; Abcam), Ki67 (1:200; Cell Signaling), BrdU (1:500; Abcam), NeuN (1:1000; Millipore), MBP (1:200; Millipore), PDGFR□ (1:200; Thermofisher Scientific), Olig2 (1:200; Abcam), Synaptophysin (1:1000; Sigma Aldrich), PSD95 (1:500; Abcam

and Cell Signaling), Bassoon (1:1000; Synaptic Systems), P2RY12 (1:200; Sigma-Aldrich), Ctip2 (1:200; Abcam), SV2A (1:200; Synaptic Systems), CD206 (1:200; Thermofisher Scientific), CD163 (1:200; Abcam) and CUX1 (1;200; Abcam).

For TUNEL staining the Promega Dead End TUNEL Assay Kit (Cat No: G3250) was used following manufacturer's instructions. Briefly, samples were washed in PBS, incubated in Equilibration Buffer for 10 minutes, and covered with plastic coverslips. Slides were then immersed in incubation buffer made of Equilibration Buffer (180 μL), Nucleotide Mix (20 μL), and rTdT Enzyme(4 μL) at 37 °C for 1h not exposed to light. Slides were dipped in 2X saline sodium-citrate (SSC) buffer for 10 minutes at room temperature. DNase I was used to generate strand breaks in DNA to provide a positive TUNEL reaction control. Negative control sections were incubated in incubation buffer without rTdT Enzyme.

For RNAscope In-Situ Hybridization we followed manufacturer's instructions. Briefly, tissue sections were mounted onto slides and warmed at 60℃ for 30 minutes. Sections were dehydrated with 50%, 70%, and 100% ethyl alcohol gradients for 5 minutes each at room temperature and followed by hydrogen peroxide (Cat No.322335 ACDBio) at room temperature for 10 minutes each and then washed with Deionized (DI) water. Tissue sections were placed in boiling 1X Target Retrieval Reagent (Cat No.322380 ACDBio) for 15 minutes then immediately transferred to DI water and washed in 100% Ethyl Alcohol and allowed to dry. Slides were covered in Protease III (Cat No.322337 ACDBio) for 30 minutes at 40℃. Probes were then added for 2 hrs at 40℃ within a humidity control chamber. Signal amplification and detection reagents (Cat No.322310 ACDBio) were applied sequentially and incubated in AMP 1, AMP 2, and AMP for 30 minutes each. Before adding each AMP reagent, samples were washed twice with washing buffer (Cat

NO.310091 ACDBio). Respective HRPs were placed on slides for 15 minutes at 40℃ followed by 30 minutes of respective Opal dye (FP1487001KT Akoya Biosciences) for 30 minutes at 40℃ and HRP blocker for 15 minutes at 40℃.

High resolution fluorescent images were obtained using a Leica TCS SPE-II confocal microscope and LAS-X software. For confocal imaging, one field of view (FOV) per brain region was captured per mouse using the Allen Brain Atlas to capture comparable brain regions. For synaptic quantifications three FOVs per brain region were captured and quantifications for each animal was averaged. Total cell counts and morphological analyses were obtained by imaging comparable sections of tissue from each animal at the 20X objective, at multiple z-planes, followed by automated analyses using Bitplane Imaris 7.5 spots and filaments respectively, as described previously (*214*). Colocalization analyses were conducted using Bitplane Imaris 7.5 colocalization and surfaces modules. For hemisphere stitches automated slide scanning was performed using a Zeiss AxioScan.Z1 equipped with a Colibri camera and Zen AxioScan 2.3 software. Cell quantities were determined using the spots module in Imaris. Integrated density measurements were determined in ImageJ (NIH).

RNA sequencing:

Whole transcriptome RNA sequencing (RNA-Seq) libraries were produced from Wild-type (WT), CSF1Ri, CSF1R$^{+/}$, and CSF1Ri-CSF1R$^{+/-}$ mice treated from 6 – 8 months, brains that were microdissected to extract cortical tissue (n=6/group). Briefly, 100-600ng of RNA were depleted of ribosomal RNA, fragmented, reverse transcribed and ligated to indexed sequencing adapters using the KAPA RNA HyperPrep Kit with RiboErase. Amplified libraries were combined into 4 pools of 12 libraries and sequenced on 4 lanes of a

HiSeq4000 producing 50bp single-end reads. Reads were mapped to the reference mouse genome (mm10) using STAR (*226*) aligner and quantified with the featureCounts function of the *Rsubread* (*227*) package in R (*228*). After filtering out low-count genes, count distributions were scaled using the calcNormFactors function of the *edgeR* (*229*) package.

Weighted correlation network analysis: Network analysis was performed using weighted gene co-expression analysis (WGCNA) package in R (*230*). First, bi-weighted mid-correlations were calculated for all gene pairs, and then used to generate an eigengene network matrix, which reflects the similarity between genes according to their expression profiles. This matrix was then raised to power β (β=20). Modules were defined using specific module cutting parameters (minimum module size = 100 genes, deepSplit = 4 and threshold of correlation = 0.2). Modules with a correlation greater than 0.8 were merged. We used first principal component of the module, called signed bicor network, to correlate brain region, irradiation, and treatment. Hub genes were defined using intra-modular connectivity (kME) parameter of the WGCNA package. *Gene enrichment analysis:* Gene-set enrichment analysis was done using enrichR (*231*)

Quantitative PCR:

cDNA was prepared using an iScript cDNA synthesis kit following manufacturer's instructions (Bio-Rad; 1708890). Quantitative real-time polymerase chain reaction was performed to determine the relative expression of *Csf1r* as well as *Gapdh* as a control. The primer pairs for each were obtained as part of the PrimePCR-PreAMP SYBR Green Assay (Bio-Rad; unique assay ID: qMmuCID0016567, qMmuCED0027497). Real-time polymerase chain reactions were performed in 20 μL volume reactions using the

SsoAdvanced Universal Supermix SYBR Green system (Bio-Rad). Real-time polymerase chain reaction conditions were 95℃ for 2 minutes for 1 cycle followed by 95℃ for 10 seconds and 60℃ for 30 seconds for 40 cycles on a Bio-Rad CFX96 Touch thermocycler.

Data analysis and statistics

Statistical analysis was performed with Prism Graph Pad (v.8.0.1; La Jolla, USA). To compare two groups, the unpaired or paired Student's t-test were used. Behavioral, biochemical, and immunohistological data were analyzed using Two-way ANOVA (Diet: Control vs. PLX5622 and Genotype: WT vs. $CSF1R^{+/-}$) using GraphPad Prism Version 8. Tukey's post hoc tests were employed to examine biologically relevant interactions from the two-way ANOVA regardless of statistical significance of the interaction. For all analyses, statistical significance was accepted at $p < 0.05$. and significance expressed as follows: *$p < 0.05$, **$p< 0.01$, ***$p < 0.001$. n is given as the number of mice within each group. Statistical trends are accepted at $p<0.10$ ($^{\#}$). Data are presented as raw means and standard error of the mean (SEM).

RESULTS

Microglia-specific monoallelic *Csf1r* KO in adult mice induces loss of presynaptic markers, disruption to the ECM compartment, and microglial dyshomeostasis

While CSF1R is exclusively expressed in microglia in the adult brain (*232*), expression of this receptor has also been reported in specific neuronal populations during brain development (*233, 234*) . As $CSF1R^{+/-}$ mice lack one *Csf1r* allele in all cells throughout their lifespan, we sought to fully establish the microglial and adult origin of any disruptions

induced by *Csf1r* haploinsufficiency which may be relevant to ALSP pathogenesis. *To this end,* we crossed *Cx3cr1*-Cre$^{ERT2/+}$ mice with floxed *Csf1r*$^{+/fl}$ mice to generate mice in which we could inducibly and specifically ablate a *Csf1r* allele from adult microglia. Progeny from this pairing resulted in two groups: **CX3CR1^{Cre}-CSF1R$^{+/+}$** (**Con)** and **CX3CR1^{Cre}-CSF1R$^{+/fl}$ (iCSF1R$^{+/-}$)** mice. At 2 months of age (*i.e.*, in adult mice) we administered tamoxifen to excise a single CSF1R allele selectively from microglia/myeloid cells, and animals were subsequently sacrificed at 8 months old (mo) (Fig. 1a). Because events leading up to overt CNS pathology in ALSP are still poorly understood, we chose to focus our study on a time point at which cognitive deficits are detectable, but white matter and axonal damage is not yet apparent, based on published data from global *Csf1r* haploinsufficient mice (*16*). To confirm the efficient recombination and knockdown of *Csf1r* expression, we quantified *Csf1r* mRNA via RNAscope *in situ* hybridization and found 40-50% reduced levels of *Csf1r* RNA in iCSF1R$^{+/-}$ mice compared to Con mice (Fig. 1b, c). Notably, *Csf1r* mRNA was absent in neurons at this time point. Since *Csf1r* is a primarily microglia-expressed gene in the adult brain, and studies of post-mortem ALSP brains report microglial dysregulation preceding axonal pathology (*3*) further suggesting microglial involvement during early disease onset, we first analyzed cortical microglial densities. Despite apparent *Csf1r* downregulation, cortical microglial numbers were unaffected in iCSF1R$^{+/-}$ animals (Fig. 1d,e), in contrast to the reported ~25% elevation in microglial densities reported in global *Csf1r* haploinsufficient mice (*16, 225*), and no overt morphological signs of microglial reactivity were seen (i.e. de-ramified enlarged cell bodies, retracted and condensed processes). Because *Csf1r* can be expressed by perivascular macrophages (PVM) we immunostained for these with antibodies against

CD206 and found no changes to the number of PVMs between Con and iCSF1R$^{+/-}$ groups (Supplemental Fig. 1a,b).

Under homeostatic conditions, the microglial transcriptome is characterized by expression of genes such as *Sall1, Hexb, Cx3cr1, Tmem119, Trem2, P2ry12, Mertk,* and *SiglecH* (*18, 235*) *. While these genes are uniquely and highly expressed by microglia during homeostasis, under states of duress or neurodegeneration this subset of genes is downregulated* (*235-237*) *. This downregulation, however, is transient in some cases – during periods of recovery, microglia have been observed to upregulate these same genes* (*238*)*. A recent study noted reduced expression of P2RY12 in ALSP patients* (*238*)*, as such, we stained for P2RY12 to examine the homeostatic status of microglia and observed reduced microglial expression of this marker in iCSF1R$^{+/-}$ mice* (Fig. 1f, g). Similarly, we observed reduced expression of the homeostatic maker TMEM119 in iCSF1R$^{+/-}$ mice (Supplemental Fig. 2a,b).

Previous studies have shown that dysfunctional microglia are active participants in the structural and functional alteration of synapses that culminates in synaptic impairment and degradation (*157, 159*) . Therefore, we investigated cortical synaptic integrity by quantifying known pre- and post- synaptic markers (*239-241*). Interestingly, iCSF1R$^{+/-}$ mice showed significant reductions in presynaptic markers (Synaptophysin, SV2A, and Bassoon; Fig. 1h-m; Fig 1h' example Imaris-quantified puncta), but no changes in the postsynaptic marker PSD95 (Fig. 1n, o).Within the framework of the tetrapartite synapse model(*242*), the extracellular matrix (ECM) has emerged as a vital component involved in the modulation of synaptic plasticity (*67, 243*), stabilization of synaptic contacts (*67, 244*) , and overall learning and memory (*67, 243*) . Recently, we demonstrated that

microglia in mouse models of Huntington's disease (HD) and Alzheimer's disease (AD) induced profound changes in the ECM – including notable reductions in specialized interneuron-associated structures known as perineuronal nets (PNNs) that occurred concomitant with the accumulation of chondroitin sulfate proteoglycans (CSPGs) in the general ECM (*75, 76*). iCSF1R$^{+/-}$ mice show robust reductions in SS Ctx PNNs, via stains for both *Wisteria Floribunda Lectin* (WFA), a plant lectin commonly used to label PNNs, and aggrecan, a CSPG selectively expressed by PNNs necessary for their construction and maintenance (*245*) (Fig. 1p-t), indicating that loss of a single *Csf1r* allele in adult microglia is sufficient to induce PNN degradation and/or loss.

We next explored the presence of CSPGs with chondroitin-6 sulfate patterns via the CS-56 antibody (*246*) While aggrecan is primarily found in PNNs, CS-56^{+} staining presents as "dandelion clock-like structures" (DACS) distinct from PNNs (*247*) . In ketamine models of schizophrenia, the prefrontal cortex exhibits reduced levels of PNNs and increased intensity of DACS staining (*248*) , similar in pattern to what we reported in HD, wherein elimination of microglia rescued the increased accumulation of DACS (*75*). Here, we find that iCSF1R$^{+/-}$ mice show dramatically increased CS-56^{+} staining throughout the brain (Fig. 1u, w). Importantly, while these CSPG structures are primarily produced by astrocytes(*249*) , and we often observed astrocytes at the center of these deposits (Fig. 1v, arrows), it should be noted that we did not detect any changes to astrocyte density as assessed by S100b^{+} cell number across groups (Fig. 1x). Interestingly, it has been reported that CS-56^{+} upregulation occurs around reactive astrocytes in physical proximity to activated microglia/macrophages (*250*) . Crucially, these results show that loss of one *Csf1r* allele from adult *Cx3cr1*-expressing resident myeloid cells (i.e. microglia) is

sufficient to induce disturbances in microglial homeostasis as reflected in the loss of P2RY12 immunofluorescence, presynaptic dysfunction, and dysregulation of the ECM.

Microglial depletion reverses presynaptic and ECM alterations induced by *Csf1r* haploinsufficiency

Our results show that microglial loss of a *Csf1r* allele in adult mice leads to cellular dyshomeostasis, concomitant with a loss of presynaptic puncta and remodeling of the ECM. To further confirm the microglial origin of these CSF1R-associated phenotypes and to complement with a more clinically relevant model of ALSP, and to determine the extent to which pathology can be rescued, we next sought to eliminate virtually all microglia from adult CSF1R$^{+/-}$ mice (i.e. global CSF1R haploinsufficiency), which can be achieved by administration of the CSF1R inhibitor PLX5622 (1200 ppm in chow) (*119*). WT and CSF1R$^{+/-}$ mice were treated for 2 months beginning at 6 mo (Fig. 2a) to align with the 8-month old iCSF1R$^{+/-}$ mice. This paradigm generated four groups: **WT** and **CSF1R$^{+/-}$** groups as well as their microglia depleted (MD) counterparts **MD-WT** and **MD-CSF1R$^{+/-}$**. Quantification of IBA1^{+} cells confirmed depletion of >90% of microglia in MD-WT and MD-CSF1R$^{+/-}$ mice (Fig. 2b, c; Interaction: $F(1, 15) = 21.88$, $p = .0003$; post hoc significance between groups displayed on graph), with CSF1R$^{+/-}$ mice showing elevated densities of microglia compared to WT mice, in accordance with prior studies (*16, 225*). This is in contrast to what we observed in adult microglia-specific *Csf1r* haploinsufficient mice (iCSF1R$^{+/-}$ mice; Fig 1d), suggesting that elevated microglial densities may be established during development (e.g. prior to tamoxifen-induced *Csf1r* excision) further explored in our developmental time course experiment (Fig 4). Despite this, and in accordance with iCSF1R$^{+/-}$ mice, Synaptophysin^{+}, SV2a^{+}, and Bassoon^{+} puncta were all significantly reduced in CSF1R$^{+/-}$ mice (Fig. 2d-i). Elimination of microglia in CSF1R$^{+/-}$ mice increased

synaptic puncta density for all markers (Interaction: (1,18) = 3.924 p = 0.06; F(1,19) = 9.058 p = .0072; and F(1,18) = 8.738 p = .0085 for Synaptophysin, SV2a, and Bassoon respectively significance between groups displayed on graph). Additionally, CSF1R$^{+/-}$ mice displayed a marked reduction in PNNs as assessed by WFA and aggrecan

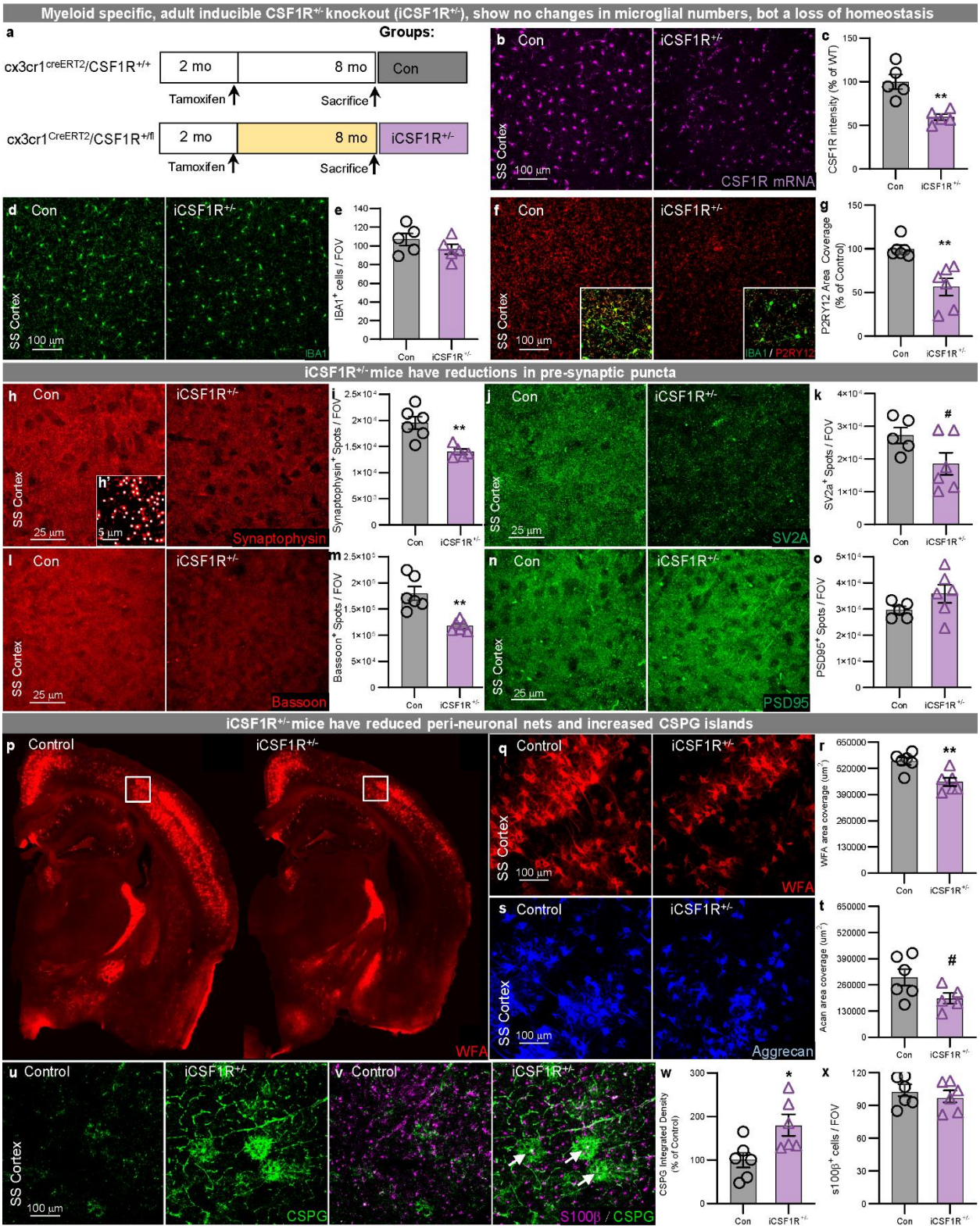

Fig. 2.1*:* **Myeloid-specific CSF1R$^{+/-}$ (iCSF1R) in adult mice confirm loss in homeostasis, reductions in synaptic surrogates and alterations in ECM structures. (a)** Experimental paradigm whereby

tamoxifen was introduced via oral gauvage to cx3cr1^{cre}-CSF1R$^{+/fl}$ and cx3cr1^{cre}-CSF1R$^{+/+}$ mice at two months – well after microglial development. Mice were sacrificed at 8 months. **(b,c)** Representative image of 20x in situ hybridization of CSF1R RNA reveals a 40-50% reduction in CSF1R expression throughout. **(d,e)** Representative 20x image of IBA1^{+} immunofluorescence in the *Somatosensory Cortex (ss ctx)* revealed no significant changes to IBA1^{+} cell number. **(f,g)** Representative 20x image of ss ctx revealed significant decrease in P2RY12 expression by microglia. Myeloid-specific CSF1R knockout mice presented with losses of pre-synaptic puncta **(h,i)** Synaptophysin, **(j,k)** SV2A, **(l,m)** and Bassoon. **(h')** Example Imaris quantification of Synaptophysin^{+} spots digitally zoomed in 5x from 63x image **(n,o)** No differences found in PSD-95 puncta number, however. **(p)** Whole brain stitches of half brains of myeloid-specific CSF1R haploinsufficient mice immunostained for WFA. **(q,r)** Representative 20x images of WFA and Aggrecan immunostaining in ss ctx, respectively **(s,t)** Quantification confirmed significant decrease in WFA and Aggrecan area coverage found in global CSF1R$^{+/-}$ haploinsufficient mice. **(u,v)** Representative 20x confocal images of ss ctx immunostained for *CSPG* and S100 **(w)** display a significant increase in *CSPG* accumulation as measured by integrated density. Statistical analysis for inducible CSF1R$^{+/-}$ comparisons used a two-tailed t-test. Significance indicated as * $p< 0.05$; ** $p < 0.01$; # $0.05 < p < 0.1$.

immunostaining, which are also restored upon microglial elimination (Fig. 2j-m; Interaction: $F(1,19) = 3.380$ $p = 0.08$ and $F(1,19) = 3.727$ $p = 0.06$ for WFA and aggrecan respectively significance between groups displayed on graph). Finally, similar disease-associated CS-56^{+} CSPG upregulation was evident in the CSF1R$^{+/-}$ brain as in iCSF1R$^{+/-}$, and was reduced with microglial depletion (Fig. 2n, o; Interaction: $F(1,20) = 57.751$ p-value = 0.02 significance between groups displayed on graph). These data further suggest a disease phenotype primarily driven by malfunctioning microglia and the downstream detrimental effects they exert on neuronal populations, which, importantly, may be mitigated by pharmacological targeting of the former, at least in early stages of disease.

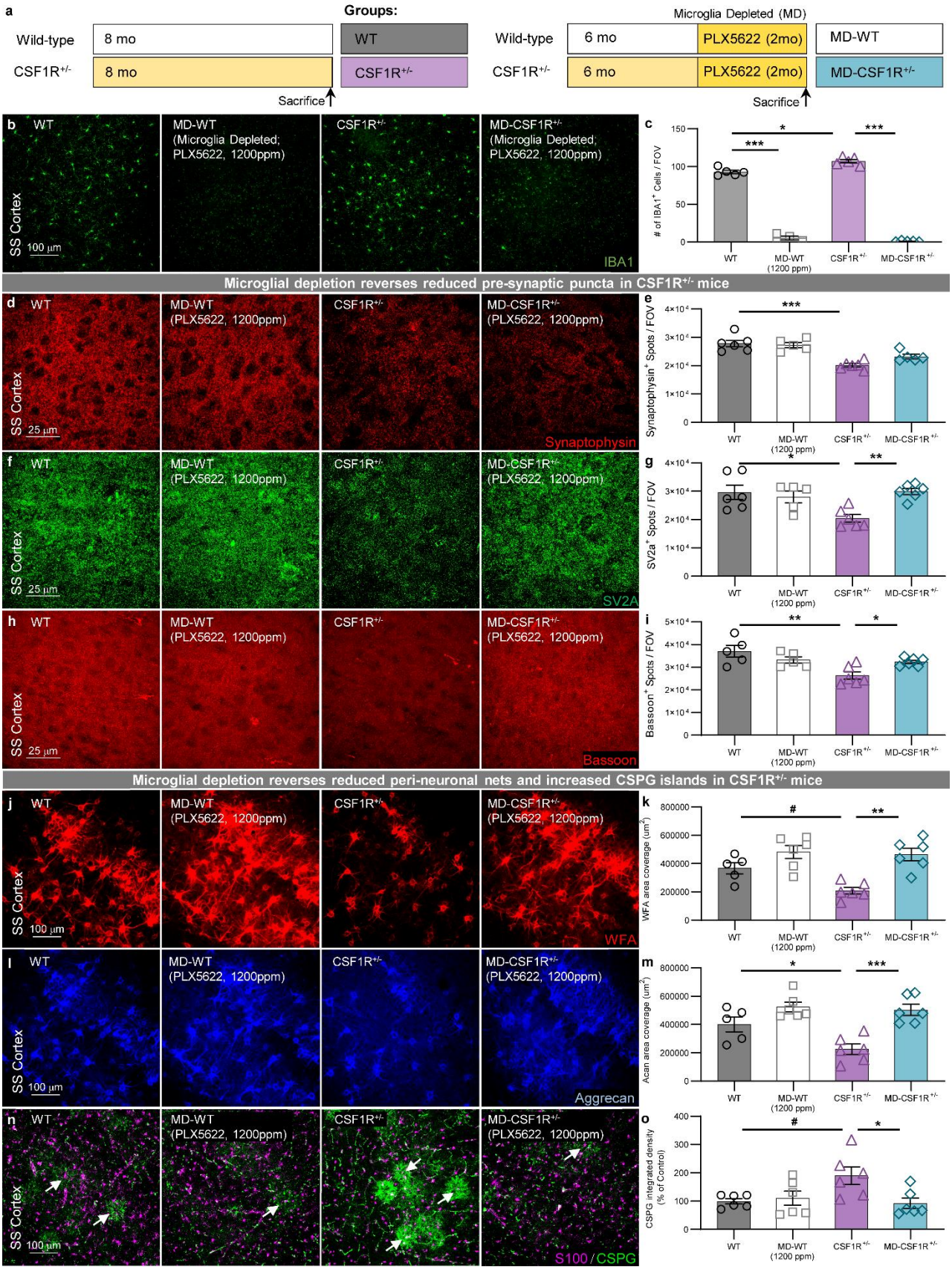
a
Groups:
Wild-type
8 mo
WT
CSF1R+/-
8 mo
CSF1R+/-
Sacrifice
Microglia Depleted (MD)
Wild-type
6 mo
PLX5622 (2mo)
MD-WT
CSF1R+/-
6 mo
PLX5622 (2mo)
MD-CSF1R+/-
Sacrifice
b
WT
MD-WT (Microglia Depleted; PLX5622, 1200ppm)
CSF1R+/-
MD-CSF1R+/- (Microglia Depleted; PLX5622, 1200ppm)
SS Cortex
100 μm
IBA1
c
# of IBA1+ Cells / FOV
WT
MD-WT (1200 ppm)
CSF1R+/-
MD-CSF1R+/-
Microglial depletion reverses reduced pre-synaptic puncta in CSF1R+/- mice
d
WT
MD-WT (PLX5622, 1200ppm)
CSF1R+/-
MD-CSF1R+/- (PLX5622, 1200ppm)
SS Cortex
25 μm
Synaptophysin
e
Synaptophysin+ Spots / FOV
f
SV2A
g
SV2a+ Spots / FOV
h
Bassoon
i
Bassoon+ Spots / FOV
Microglial depletion reverses reduced peri-neuronal nets and increased CSPG islands in CSF1R+/- mice
j
100 μm
WFA
k
WFA area coverage (um2)
l
Aggrecan
m
Acan area coverage (um2)
n
S100 / CSPG
o
CSPG integrated density (% of Control)

Fig. 2.2: **Elimination of microglia with 1200 ppm PLX5622 restored synaptic and ECM alterations induced by CSF1R haploinsufficiency (a)** WT and $CSF1R^{+/-}$ mice were placed on a high dose PLX5622 diet (1200 ppm) for 2 months beginning at 6 mo to completely eliminate microglia from the brain parenchyma. **(b)** Immunofluorescent image of $IBA1^{+}$ cells in the ss ctx **(c)** quantification of which showed significant decrease (~90-95% elimination) of microglia in WT and $CSF1R^{+/-}$ treated mice. **(d, f, h)** Representative 63x immunofluorescent images of presynaptic elements Synaptophysin, SV2A, and Bassoon, respectively. **(e, g, i)** Quantification of these showed significant decreases in the number of puncta in $CSF1R^{+/-}$ ss ctx and recovery of puncta number in $CSF1R^{+/-}$ mice in which microglia were completely eliminated, with the exception of synaptophysin. **(j-m)** Immunostaining of WFA and Aggrecan displayed decreased PNN area coverage in ss ctx of $CSF1R^{+/-}$ mice. Elimination of microglia restored ECM composition in $CSF1R^{+/-}$ mice. **(n,o)** Immunostaining and quantification of CSPG revealed increased immunostaining of CS-56 in $CSF1R^{+/-}$ parenchyma that was restored by elimination of microglia. Statistical analysis used a two-way ANOVA with Sidak multiple comparisons correction. Significance indicated as * $p< 0.05$; ** $p < 0.01$; *** $p < 0.001$; # $0.05 < p < 0.1$.

$CSF1R^{+/-}$ mice display cognitive deficits that are rescued by sustained low-grade CSF1R inhibition (CSF1Ri)

The elimination of the microglial compartment for extended periods of time via CSF1R inhibitors is unlikely to be clinically feasible in ALSP patients, therefore we sought to identify potential treatments that could mitigate disease by modulating, rather than removing, the microglial phenotype. Notably, lower doses of CSF1R inhibitors that do not eliminate the microglial compartment have been shown to nonetheless alter disease-related microglial phenotypes and provide protection in animal models of Alzheimer's disease (*251, 252*), Prion disease (*253*), and tauopathies (*254*). To that end, we developed a CSF1Ri regimen that led to reduced effects of CSF1R inhibition such that

there was modest microglial death compared to higher dosages which eliminate more than 95% of microglia (Supplemental Fig. 3a). WT and CSF1R$^{+/-}$ mice were treated with the specific CSF1R inhibitor PLX5622 (150 ppm in chow) for 2 months starting at 6 mo to induce CSF1Ri. Thus, 4 groups were generated: **WT, CSF1Ri, CSF1R$^{+/-}$,** and **CSF1Ri-CSF1R$^{+/-}$** (Fig. 3a). This dosage of PLX5622 was determined in a separate subset of mice to provide microglial CSF1R inhibition that eliminates <25% of microglia under either homeostatic or inflammatory conditions (Supplemental Fig. 3b,c). Quantitative PCR confirmed half the level of *Csf1r* transcripts in CSF1R$^{+/-}$ mice compared to WT mice (Fig. 3b).

ALSP is characterized by executive dysfunction, memory decline, motor impairments, and a lack of social inhibitions. In studies characterizing phenotypes of *Csf1r* haploinsufficient mice, cognitive deficits are reported to begin at 7 mo (*16*) that resemble the clinical presentation of ALSP (*4, 6*), but overt white matter damage is not observed until 14 mo. To characterize behavioral phenotypes in our cohort of mice (n=8-10), we performed a battery of tasks consisting of EPM, Open Field (OF), Novel Object Recognition (NOR), Novel Place Recognition (NPR) Given the motor impairments, including gait dysfunction, and social withdrawal noted in ALSP patients we also included a Rotarod and Social Interaction Task. Behavioral assessments began 6 weeks after mice were placed on diet and continued for two weeks, at which point mice were euthanized. While we found no significant changes in mobility or anxiety measures in any group as determined by performance in EPM, OF, Social Interaction and Rotarod Tasks (Supplemental Fig. 4a-f), we observed impairments in cognitive domains as measured by NOR and NPR Tasks in CSF1R$^{+/-}$ mice (Fig. 3c, d). However, no impairments were evident in CSF1Ri mice by

any of these measures (Interaction: $F(1,42) = 4.126$ $p = 0.06$ and $F(1,42) = 1.688$ $p = 0.2$ for NOR and NPR tasks respectively significance between groups displayed on graph). These results show that life-long loss of a *Csf1r* allele induces cognitive deficits detectable by 8 months in mice, and that such deficits are not similarly evident following sustained (at least 2 months) low-grade CSF1Ri in the healthy adult. Surprisingly, however, CSF1Ri did rescue cognitive deficits in $CSF1R^{+/-}$ mice in the NOR task (Fig. 3c), revealing that altered CSF1R signaling can induce, and be targeted to rescue, cognitive impairments.

CSF1Ri restores $CSF1R^{+/-}$ microglia number, morphology, and homeostatic marker expression

To better understand the role of CSF1R signaling in cognition, we performed immunohistochemical (IHC) analyses of myeloid cell attributes in the brain. Here, we found robust increases (~25%) in cortical and hippocampal microglia in $CSF1R^{+/-}$ mice, as shown via immunostaining with antibodies against IBA1 (Fig. 3e, f), consistent with previous data (*16*). Notably, CSF1Ri treatment of $CSF1R^{+/-}$ mice normalized microglial densities to WT numbers (Fig. 3e, f). Additionally, $IBA1^{+}$ cell quantification showed a consistent ~25% reduction in microglia following CSF1Ri in both $CSF1R^{+/-}$ and WT mice, as CSF1Ri-treated $CSF1R^{+/-}$ mice exhibit the same ~25% decrease in $IBA1^{+}$ cell number as CSF1Ri-treated WT animals relative to their respective controls (Fig. 3f), revealing that despite partial loss of CSF1R signaling in $CSF1R^{+/-}$ mice, microglia remain dependent on this signaling pathway for survival. Again, given the expression of *Csf1r* by PVMs, we explored PVM cell populations in our cohorts of mice. Immunostaining of CD206 revealed similar number of PVMs between WT and $CSF1R^{+/-}$ mice and an expected reduction in

CSF1Ri treated groups (Supplemental Fig. 1c,d; Interaction: F(1,17) = 0.0019 p = 0.9 significance between groups displayed on graph).

Microglial reactivity is a highly dynamic process encompassing a spectrum of phenotypic changes, and under conditions of activation such changes include an increase in cell size and a loss of process ramification (e.g. amoeboid microglia) (*255*). We found no changes in cell soma size between microglia in WT and CSF1R$^{+/-}$ mice, whereas CSF1Ri in WT, but not CSF1R$^{+/-}$ mice, induced significant increases in this measure (Fig. 3g; Interaction: F(1,13) = 6.095 p = 0.02; F(1,14) = .9976 p = 0.33; F(1,14) = 5.573 p = 0.03 for Cortex, Hippocampus, and Thalamus respectively significance between groups displayed on graph). Analysis of microglial process diameter and average process length revealed no differences between groups (Fig. 3h, I; Interaction: F(1,30) = 2.232 p = 0.14 and F(1,29) = 2.645 p = 0.11 for diameter and process length respectively significance between groups displayed on graph). On the other hand, measures of microglial ramification (i.e., primary, secondary, and tertiary branching of microglia processes) showed that CSF1R$^{+/-}$ microglia adopt a hyper-ramified state compared to WT microglia, while CSF1Ri reduced ramification in both WT and CSF1R$^{+/-}$ groups (Fig. 3j; Interaction: F(1,30) = .8740 p = 0.35; F(1,29) = .8646 p = 0.36; and F(1,30) = 3.117 p = 0.08 for primary, secondary and tertiary branching respectively significance between groups displayed on graph). Examination of microglial P2RY12 revealed decreases *in both CSF1Ri and CSF1R$^{+/-}$ microglia (Fig. 3k, l), as in iCSF1R$^{+/-}$ microglia (Fig. 1f,g). Rather than further reducing expression, CSF1Ri increased microglial P2RY12 in CSF1R$^{+/-}$ mice (Interaction: F(1,17) = 55.87 p = 0.0001* significance between groups displayed on graph*). This same pattern was observed with TMEM119 expression (Supplemental Figure 2c,d; Interaction: F(1,18)*

= 54.59 p = 0.0001 significance between groups displayed on graph*). Together,* these data illustrate the deviation of CSF1R$^{+/-}$ microglia from homeostasis, although more subtle than activation, and suggest that certain biophysical properties of microglia in ALSP (e.g. process ramification, elevated population densities) may be amenable to CSF1Ri treatment, in turn potentially contributing to the rescue of cognitive deficits in *CSF1Ri-CSF1R$^{+/-}$ mice.*

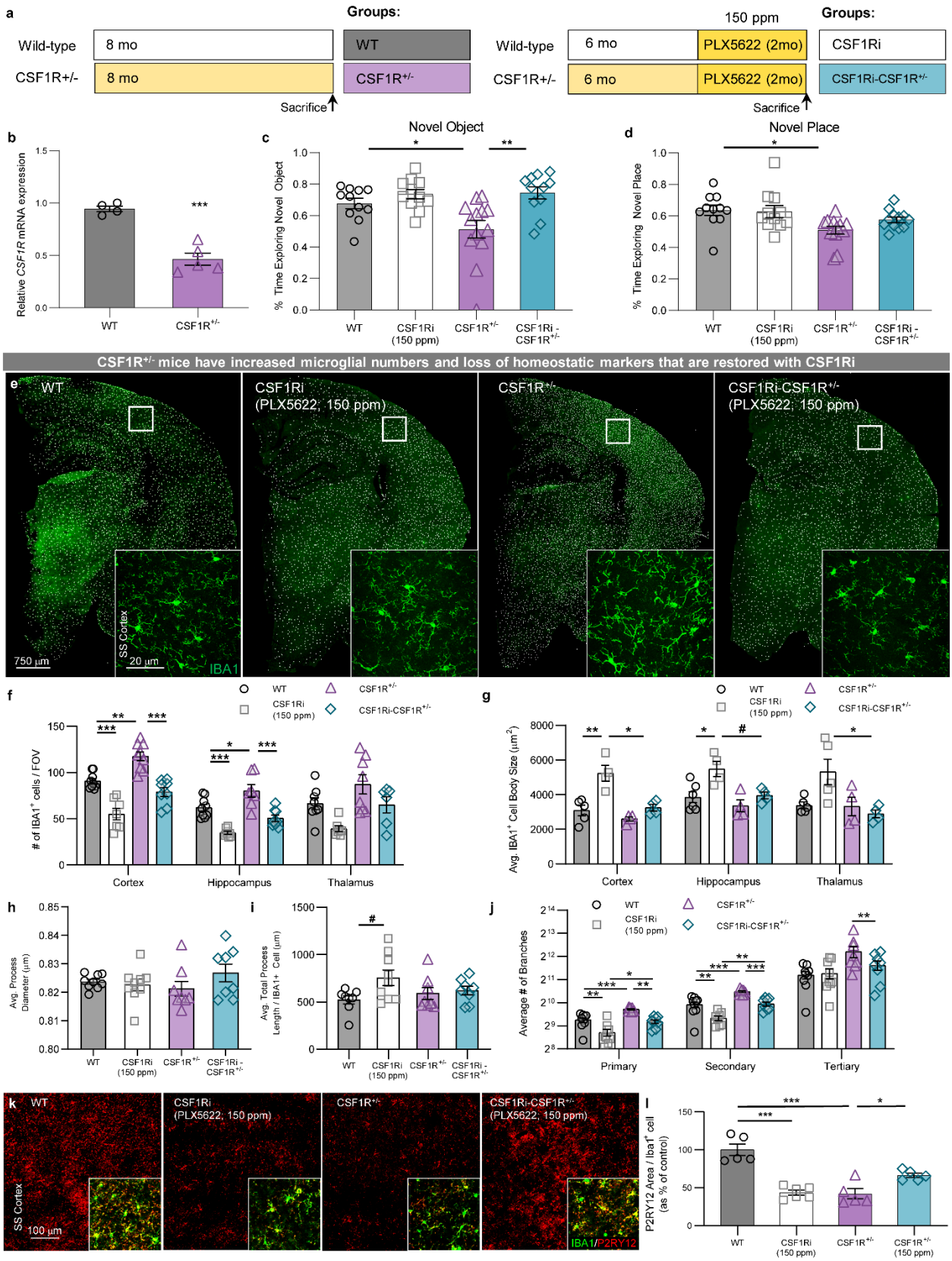
a
Groups:
Wild-type
8 mo
WT
CSF1R+/-
8 mo
CSF1R+/-
Sacrifice
150 ppm
Groups:
Wild-type
6 mo
PLX5622 (2mo)
CSF1Ri
CSF1R+/-
6 mo
PLX5622 (2mo)
CSF1Ri-CSF1R+/-
Sacrifice
b
Relative CSF1R mRNA expression
WT
CSF1R+/-
c
Novel Object
% Time Exploring Novel Object
WT
CSF1Ri (150 ppm)
CSF1R+/-
CSF1Ri - CSF1R+/-
d
Novel Place
% Time Exploring Novel Place
WT
CSF1Ri (150 ppm)
CSF1R+/-
CSF1Ri - CSF1R+/-
CSF1R+/- mice have increased microglial numbers and loss of homeostatic markers that are restored with CSF1Ri
e
WT
CSF1Ri (PLX5622; 150 ppm)
CSF1R+/-
CSF1Ri-CSF1R+/- (PLX5622; 150 ppm)
SS Cortex
750 µm
20 µm
IBA1
f
WT
CSF1Ri (150 ppm)
CSF1R+/-
CSF1Ri-CSF1R+/-
# of IBA1+ cells / FOV
Cortex
Hippocampus
Thalamus
g
Avg. IBA1+ Cell Body Size (µm2)
Cortex
Hippocampus
Thalamus
h
Avg. Process Diameter (µm)
WT
CSF1Ri (150 ppm)
CSF1R+/-
CSF1Ri - CSF1R+/-
i
Avg. Total Process Length / IBA1+ Cell (µm)
WT
CSF1Ri (150 ppm)
CSF1R+/-
CSF1Ri - CSF1R+/-
j
Average # of Branches
Primary
Secondary
Tertiary
k
WT
CSF1Ri (PLX5622; 150 ppm)
CSF1R+/-
CSF1Ri-CSF1R+/- (PLX5622; 150 ppm)
SS Cortex
100 µm
IBA1/P2RY12
l
P2RY12 Area / Iba1+ cell (as % of control)
WT
CSF1Ri (150 ppm)
CSF1R+/-
CSF1R+/- (150 ppm)

Fig. 2.3: **CSF1R$^{+/-}$ mice display behavioral and morphological deviations from WT counterparts which are restored by CSF1Ri (a)** Experimental paradigm: WT and CSF1R$^{+/-}$ mice were treated with 150 ppm PLX5622 for two months beginning at 6 mo. Mice were sacrificed at 8 mo (n=8-10/group) **(b)** Relative expression levels of CSF1R normalized to GAPDH via qPCR. Expression levels of CSF1R in CSF1R$^{+/-}$ was reduced ~50% compared to WT mice ($p < 0.0001$). Statistical analysis used two-tailed t-test **(c)** CSF1R$^{+/-}$ mice spent significantly less time exploring the novel object compared to WT mice. Treatment with 150 ppm PLX5622 rescued performance comparable to WT counterparts **(d)** CSF1R$^{+/-}$ mice spent significantly less time exploring an object moved to a novel place compared to WT mice. **(e)** Whole-brain stitches of half-brains from WT, CSF1Ri, CSF1R$^{+/-}$, and CSF1Ri-CSF1R$^{+/-}$ mice. Each white dot represents a microglial cell. Representative 63x image of ss ctx IBA1 immunofluorescence **(f)** Quantification of IBA1^{+} cells / FOV in cortex, Hippocampus, and Thalamus. 25-30% increase in IBA1^{+} cells were found in ss ctx, Hippocampus, and Thalamus. Treatment with 150 ppm PLX5622 reduced IBA1^{+} cells by 25% in both WT and CSF1R$^{+/-}$ mice. **(g)** Average soma size of IBA1^{+} cells reveal significant increase in soma size in CSF1Ri microglia. WT IBA1^{+} cells had comparable soma size to CSF1R$^{+/-}$ and CSF1Ri-CSF1R$^{+/-}$. **(h)** Average process diameter measurements show no changes between groups (**i)** No changes to Average total process length found between groups however a trending increase in CSF1Ri microglia was found when comparing WT and CSF1Ri. **(j)** Morphological analysis of branch patterns revealed decreased number of primary and secondary branches in CSF1Ri microglia compared to WT. CSF1R$^{+/-}$ microglia had increased numbers of primary, secondary, and tertiary branching which were reduced to WT levels by CSF1Ri. **(k, l)** Representative 20x image of the SS Cortex reveals a marked decrease in microglial P2RY12 immunopositivity in CSF1Ri and CSF1R$^{+/-}$ mice. CSF1Ri of CSF1R$^{+/-}$ mice revealed an increased expression in P2RY12 expression. Statistical analysis used a two-way ANOVA with Sidak multiple comparisons correction. Significance * $p< 0.05$; ** $p < 0.01$, *** $p < 0.001$, # $0.05 < p < 0.1$

Increased microglial density is established during early postnatal development

Given the discrepancy between global *Csf1r* haploinsufficiency and adult microglia-specific *Csf1r* haploinsufficiency, whereby only the former results in increases in adult

microglial densities, we next explored steady-state turn-over of microglia in both adult and developing CSF1R$^{+/-}$ mice. Analysis of adult *CSF1R$^{+/-}$ mice* revealed no changes in either proliferation (via Ki67 staining; Fig. 4a, b) or apoptosis (via TUNEL; Fig. 4c, d) of microglia compared to WT, suggesting that steady-state microglial turnover in the adult CSF1R$^{+/-}$ mouse brain parallels that of adult WT microglia. As expected, CSF1Ri treatment in both WT and CSF1R$^{+/-}$ mice increased the number of TUNEL^{+} microglia (Fig. 4c, d), confirming that CSF1Ri acts by inducing microglia death (*213*). As one copy of *Csf1r* is absent throughout development in *CSF1R$^{+/-}$ mice, and as adult microglial turnover remained similar between* WT and CSF1R$^{+/-}$ mice*, we next explored* the establishment of CSF1R$^{+/-}$ microglial densities during brain development. Early microglia proliferate extensively during the first two postnatal weeks, reaching maximal numbers at P14 (*256*), whereafter this rapid proliferation is followed by a period of selective microglial die-off to establish the final densities of adult microglia by ~P28 (*256*). Quantification of microglia in developing *CSF1R$^{+/-}$ mice revealed similar increases in microglial densities due to proliferation between P7-14 as seen in WT mice, but this proliferation was followed by decreased reductions in the CSF1R$^{+/-}$ microglial population by P26 (Fig. 4e-g). Importantly, this occurred despite equivalent Ki67^{+} proliferation at all developmental timepoints measured, suggesting that elevated microglial densities in adult CSF1R$^{+/-}$ mice could be due to developmental defects in the establishment of the adult microglial compartment (e.g. impaired microglial die-off). This data is in line with recent evidence wherein constitutive microglial Csf1r haploinsufficiency resulted in increased microglial density* (*257*)*, consistent with the lack of differences we observed in iCSF1R$^{+/-}$ mice, in which monoallelic knockdown of microglial Csf1r was induced only after development.*

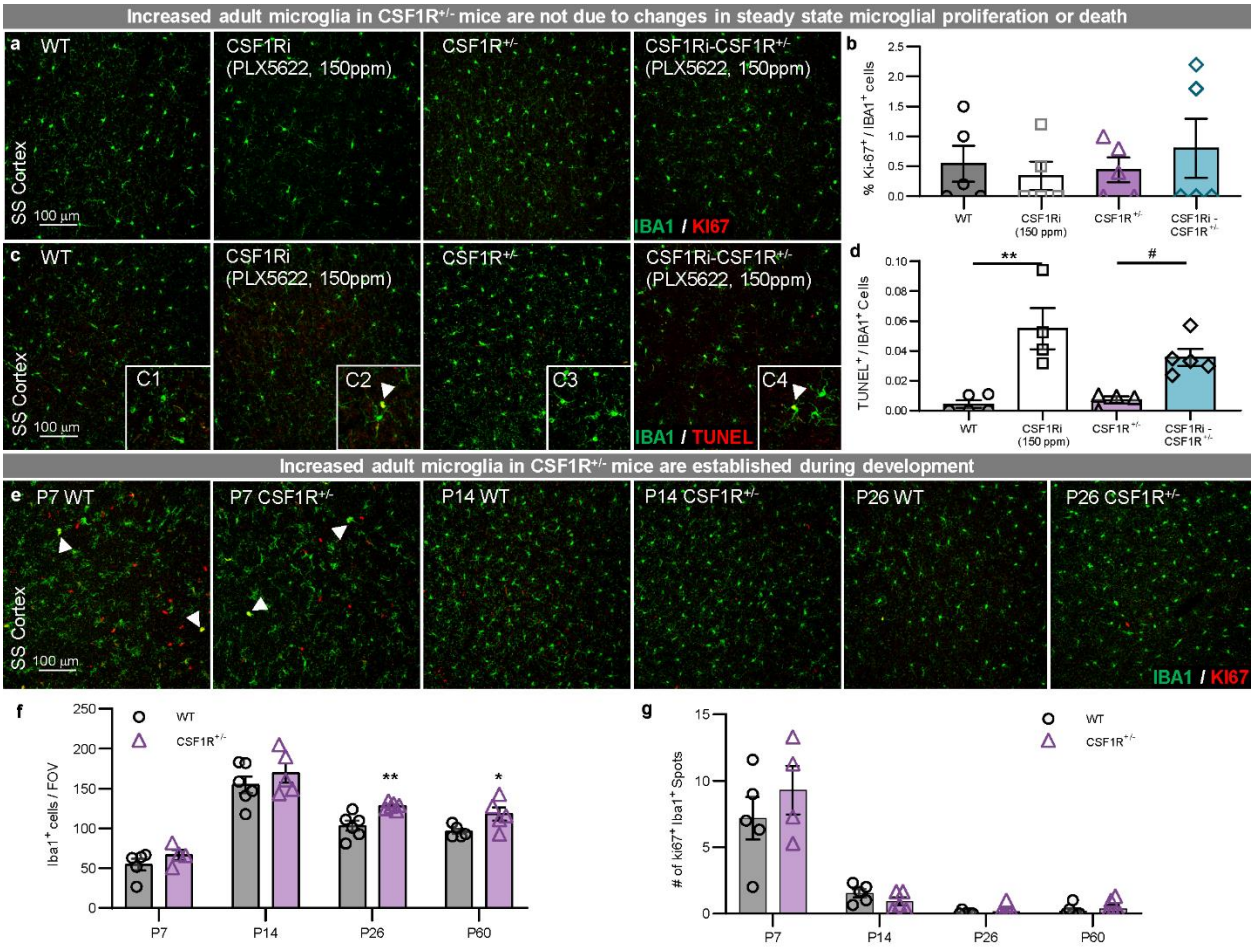

Fig. 2.4: **Increased microglial population established during development; Microglial-specific excision of one CSF1R reveals decreases in microglial molecular markers as well as dysfunction of a presynaptic marker (a)** Representative 20x image of the SS Ctx immunostaining for ki67 and IBA1^{+} cells revealed **(b)** no changes to proliferation in any group when compared to WT mice suggesting that proliferation in the adult cannot account for increased number of IBA1^{+} cells found in 8 month old CSF1R$^{+/-}$ mice. **(c)** Representative 20x image of SS Ctx immunostaining for TUNEL and IBA1 revealed that **(d)** CSF1Ri induced an increase in TUNEL IBA1 double positive cells. **(c1-c4)** Arrows indicate presence of TUNEL^{+} / IBA1^{+} cells. **(e)** Representative 20x images of the SS Ctx of WT and CSF1R$^{+/-}$ mice at P7, P14, P26. Immunostaining for IBA1 and ki67 showed **(f)** no changes in microglial number between WT and CSF1R$^{+/-}$ mice at P7 or P14 but a significant increase in CSF1R$^{+/-}$ at P26 and P60. **(g)** No changes in ki67 IBA1 double positive cells were found throughout the time course however; arrows indicate location of ki67 IBA1 double positive cells. Statistical analysis used a two-way ANOVA with Sidak multiple comparisons

correction or two-tailed t-test for developmental study. Significance indicated as * p< 0.05; ** p < 0.01; *** p < 0.001; # 0.05 < p < 0.1.

CSF1Ri restores CSF1R$^{+/-}$ synaptic and extracellular matrix deficits without changes to neuronal populations

Confirming the synaptic deficits in the prior cohort of CSF1R$^{+/-}$ and iCSF1R$^{+/-}$ mice, we found that CSF1R$^{+/-}$ mice again displayed significant reductions in presynaptic markers (i.e., synaptophysin, SV2A, and Bassoon), but not the postsynaptic marker PSD95 (Fig. 5a-h). Treatment of WT mice with CSF1Ri had similar effects to the loss of one *Csf1r* allele, with reductions seen in both SV2A and Bassoon, but not Synaptophysin, puncta (Fig. 5a-h). Treatment with the higher, microglia-depleting dose of PLX5622 (Fig 2f-i) did not induce these same reductions in cortical SV2a^{+} or Bassoon^{+} puncta number, illustrating the difference between altering microglial function with partial CSF1R inhibition via low dose CSF1Ri (150 ppm PLX5622) and completely eliminating the microglial compartment with more extensive CSF1R inhibition (1200 ppm PLX5622). As with the restorative effects on behavior and microglial phenotype, CSF1Ri increased presynaptic puncta in CSF1R$^{+/-}$ mice (Interaction: $F(1,16) = 3.582$ $p = 0.07$; $F(1,20) = 110.5$ $p = 0.0001$; and $F(1,20) = 24.76$ $p = 0.0001$ for Synaptophysin, SV2a and Bassoon respectively significance between groups displayed on graph). Similarly, CSF1R$^{+/-}$ mice showed robust reductions in SS Ctx PNNs, which were reversed back to WT levels by CSF1Ri in CSF1R$^{+/-}$ mice (Fig. 5i-l; Interaction: $F(1,25)$ p value = 0.48 and $F(1,18)$ $p = 0.0003$ for WFA and aggrecan respectively significance between groups displayed on graph), while CSF1R$^{+/-}$ mice showed dramatically increased CS-56 immunofluorescence

CSPGs throughout the brain that was also normalized to WT levels with CSF1Ri (Fig. 5m, n; Interaction: $F(1,31) = 11.17$ $p = 0.0022$ significance between groups displayed on graph). Again, we noted no changes to astrocyte density or GFAP immunofluorescence throughout the groups (Supplemental Fig. 5m-n).

Given the changes in synaptic densities with CSF1R manipulation, and as cerebral atrophy is a feature of ALSP, we next explored neuronal densities in $CSF1R^{+/-}$ mice. While unexplored in ALSP, CSF1R has been shown to be necessary for the differentiation of $Cux1^{+}$ and $Ctip2^{+}$ neurons as CSF1R null humans (*222*), mice (*233*), and zebrafish (*222*) displayed reductions in these neuronal subtypes. Analysis of neuronal subtype numbers (via $NeuN^{+}$, $Cux1^{+}$, and $Ctip2^{+}$ neurons) revealed no changes between groups (Supplemental Fig. 5a-f) suggesting that neuronal loss is not present in 8-month-old $CSF1R^{+/-}$ mice. Investigation of white matter via immunolabeling for oligodendrocytes, oligodendrocyte precursor cells, and myelin basic protein (MBP) revealed no changes in cell number or integrated signal density between groups (Supplemental Fig. 5g-l).

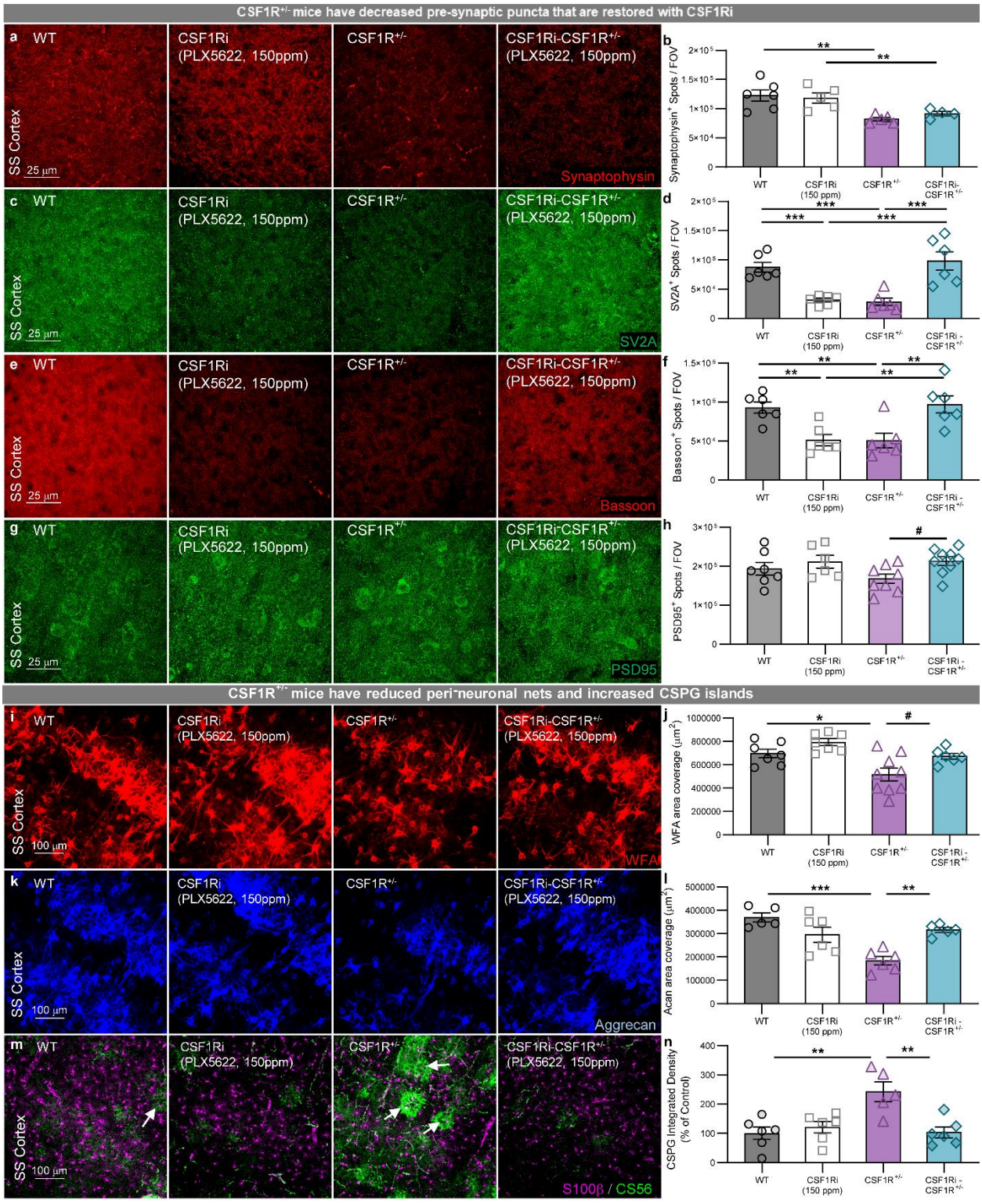

Fig. 2.5: **Microglial dyshomeostasis results deficits in presynaptic elements, perineuronal net loss and CSPG accumulation in CSF1R$^{+/-}$ SS Ctx which is restored by CSF1Ri (a,b)** Representative 63x

images of ss ctx reveals decreases in synaptophysin puncta in CSF1R$^{+/-}$ and CSF1Ri-CSF1R$^{+/-}$ mice **(c,d)**, decreases in SV2A in CSF1Ri and CSF1R$^{+/-}$ mice and recovery in CSF1Ri-CSF1R$^{+/-}$ mice **(e,f),** decreases in Bassoon in CSF1Ri and CSF1R$^{+/-}$ mice and recovery in CSF1Ri-CSF1R$^{+/-}$ mice **(g,h),** and no changes to PSD95 puncta. **(i)** representative 20x images of ss ctx from WT, CSF1Ri, CSF1R$^{+/-}$, and CSF1Ri-CSF1R$^{+/-}$ mice immunostained for WFA. **(j)** Quantification of WFA area coverage revealed significant decrease in WFA coverage in CSF1R$^{+/-}$ ss ctx and a trending recovery in the CSF1Ri-CSF1R$^{+/-}$ group. **(k)** Representative 20x confocal images of aggrecan immunostaining, another component ECM perineuronal nets quantification of which **(l)** revealed similar significant decreases in area coverage in the CSF1R$^{+/-}$ group and significant recovery in CSF1Ri-CSF1R$^{+/-}$ group. **(m)** Immunofluorescence of *CSPG* in the ss ctx and quantification by integrated density **(n)** revealed accumulation of *CSPG* deposits in CSF1R$^{+/-}$ groups that was restored upon CSF1Ri. Statistical analysis used a two-way ANOVA with Sidak multiple comparisons correction. Significance indicated as * $p< 0.05$; ** $p < 0.01$; *** $p < 0.001$; # $0.05 < p < 0.1$.

Partial disruption of CSF1R signaling induces dysregulation of microglial transcripts and downstream changes in neuronal gene expression

To elucidate the mechanisms by which CSF1R signaling could both perturb and rescue cortical-dependent cognition, we performed RNA-seq on microdissected cortices from WT, CSF1Ri, CSF1R$^{+/-}$, and CSF1Ri-CSF1R$^{+/-}$ mice. Fragments Per Kilobase of transcript per Million mapped reads (FPKM) for each gene, as well as FDR values for the relevant comparisons, can be explored at http://rnaseq.mind.uci.edu/green/csf1r_hets/. To explore the relationships of gene expression changes in a network we employed weighted gene co-expression network analysis (WGCNA) and identified 16 independent modules. The correlation of each module to either genotype (Fig. 6d) or CSF1Ri (Fig. 6f) highlighted several modules of interest – in particular the *brown* module was highly correlated to genotype (i.e. CSF1R$^{+/-}$ mice), the *darkgrey* module was highly correlated to

CSF1Ri, and the *midnight blue* module was correlated to both (correlation scores >0.5). Eigengenes were calculated and plotted for each group for each of the three highlighted modules, alongside a heatmap of all of the genes in the module (Fig. 6d,f,h), and gene ontology analyses (Fig. 6e,g,i). The CSF1R$^{+/-}$ associated *brown* module was enriched for neuronally expressed genes, associated with *axonogenesis*, *neuronal morphologies* and *development*, while the *midnight blue* module (associated with CSF1Ri treated CSF1R$^{+/-}$ mice) is strongly enriched for genes associated with *translation*, but not associated with any particular cell type. The CSF1Ri treatment-associated *darkgrey* module is enriched in microglial-expressed and immune-related genes as expected (Fig. 6f,g), and hub genes include homeostatic microglial genes such as *C1qa*, *C1qb*, *Cd53*, *Ctss*, *Gpr34*, *P2ry12*, *Tmem119*, and *Siglech* (Fig. 6j). Normalizing these myeloid-expressed genes to microglial densities reveals a clear downregulation of microglial transcripts in CSF1R$^{+/-}$ mice (Fig. 7k-m), consistent with a loss of homeostasis (Fig. 6m; established homeostatic genes bolded), as well as a group of genes that are upregulated with CSF1Ri (Fig. 6l).

We next compared differentially expressed genes (DEGs) between WT and CSF1Ri mice and WT and CSF1R$^{+/-}$ mice. Notably, thirty-four percent (412 genes) of DEGs were common between the two comparisons, with CSF1R$^{+/-}$ mice having 705 unique DEGs and CSF1Ri only 65 (Fig. 6n), suggesting similar transcriptional effects between genetic *Csf1r* haploinsufficiency and low-grade pharmacological inhibition of CSF1R. Consistent with the *darkgrey* module from the WGCNA analyses, downregulated DEGs in WT vs CSF1Ri (Fig. 6o) or CSF1R$^{+/-}$ mice vs CSF1Ri-CSF1R$^{+/-}$ (Fig. 6q) mice represented myeloid-expressed genes, as expected given the loss of ~20% of microglia with CSF1Ri. However, few myeloid-expressed DEGs were found comparing WT to CSF1R$^{+/-}$ mice

despite CSF1R$^{+/-}$ mice exhibiting ~25% higher microglial densities throughout the brain. In addition to an overall reduction in myeloid-expressed genes, these data also suggest a lack of transcripts canonically expressed by reactive or activated microglia (*i.e. Cst7, Clec7, Tnf, Ldl, Ifitm3)*, further emphasizing that disease microglia do not undergo stereotypical classical activation. Intriguingly, given the microglial expression of CSF1R, these downregulated DEGs were far fewer in number than upregulated DEGs with either CSF1Ri or in CSF1R$^{+/-}$ mice, as shown in volcano plots (Fig. 6o and 6p). Top DEGs were similar for both comparisons, and included the circadian rhythm-associated gene *NOCT*, as well as *LAMP1*, *FAM43b*, *Prr18*, and *Wrnip1*. Gene ontology analyses of DEGs between WT and CSF1R$^{+/-}$ mice highlighted *axonogenesis* (Supplemental Fig. 6b) and similarities to gene changes in *Spinal Cord Injury* and *Huntington's disease* (Supplemental Fig. 6c), both of which have been shown to involve profound ECM remodeling resembling what we see in the context of *Csf1r* haploinsufficiency (*75, 258, 259*). Furthermore, all upregulated DEGs induced by either CSF1Ri in WT mice or comparing WT to CSF1R$^{+/-}$ mice appear to be neuronally-expressed. This data suggests that despite CSF1R being restricted to microglia in the adult brain, altered CSF1R signaling in microglia induces robust gene expression changes in neurons.

To understand how CSF1Ri of CSF1R$^{+/-}$ mice could rescue disease-related impairments in synaptic integrity, ECM remodeling, and cognition, we performed more comprehensive analyses of DEGs between CSF1R$^{+/-}$ and CSF1Ri-treated CSF1R$^{+/-}$ mice (Fig. 6q, r). The most significantly downregulated gene was *MRC1*, a myeloid-expressed gene associated with phagocytosis (*260*). Conversely, most DEGs are upregulated in CSF1Ri treated CSF1R$^{+/-}$ mice, as depicted in Fig. 6r. Gene ontology analyses of these DEGs highlight

their roles in *synaptic function and morphology* (Fig. 6r) confirming changes to synapses that could account for the changes in synaptic landscape that we have observed here. Collectively, from these analyses we conclude that there is a loss of microglial homeostatic signature in CSF1R$^{+/-}$ mice, rather than a reactive or activated signature.

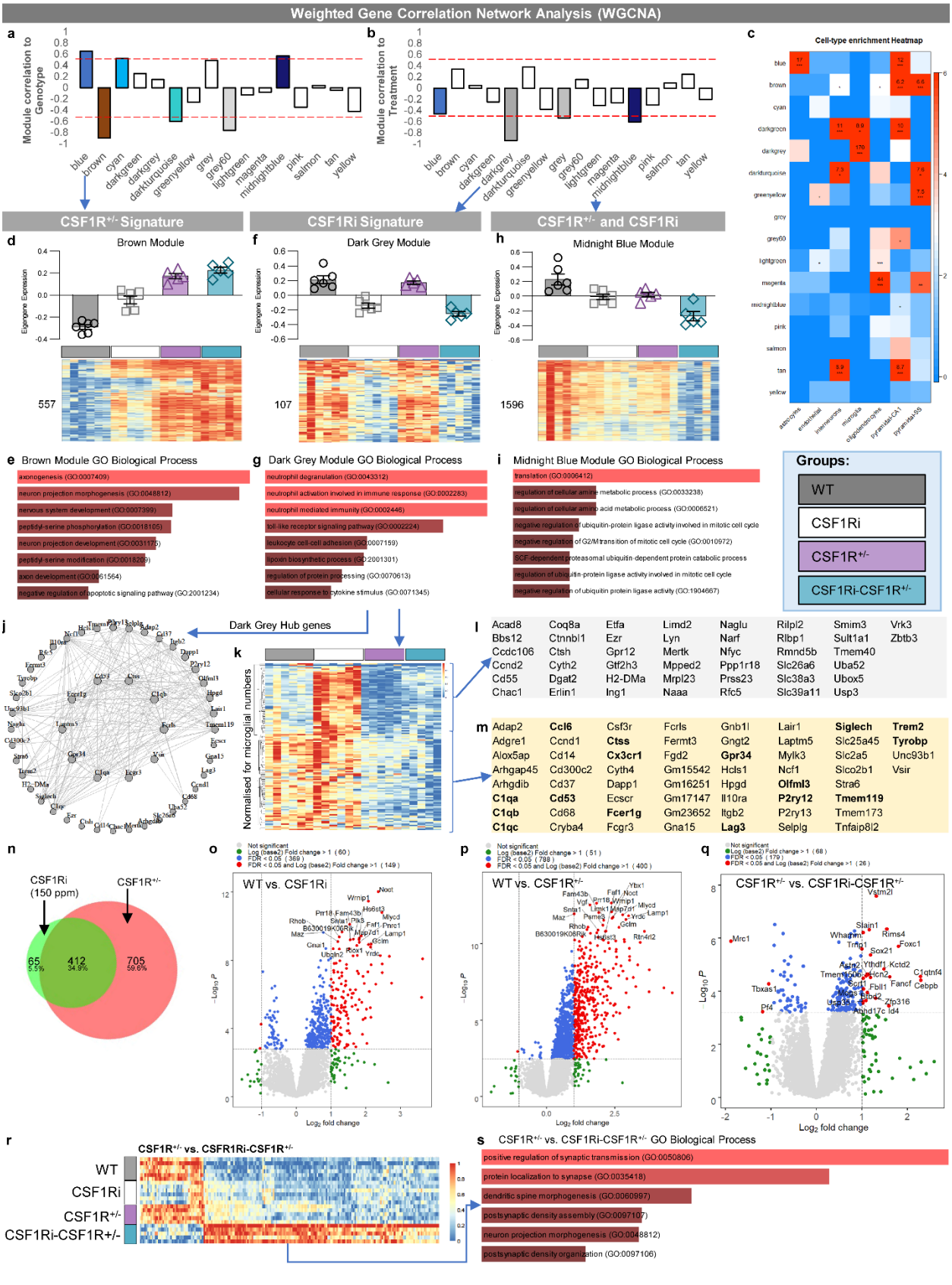
Weighted Gene Correlation Network Analysis (WGCNA)
Module correlation to Genotype
Module correlation to Treatment
blue brown cyan darkgreen darkgrey darkturquoise greenyellow grey grey60 lightgreen magenta midnightblue pink salmon tan yellow
Cell-type enrichment Heatmap
astrocytes endothelial interneurons microglia oligodendrocytes pyramidal-CA1 pyramidal-SS
CSF1R+/- Signature
CSF1Ri Signature
CSF1R+/- and CSF1Ri
Brown Module
Dark Grey Module
Midnight Blue Module
Eigengene Expression
557
107
1596
Brown Module GO Biological Process
axonogenesis (GO:0007409)
neuron projection morphogenesis (GO:0048812)
nervous system development (GO:0007399)
peptidyl-serine phosphorylation (GO:0018105)
neuron projection development (GO:0031175)
peptidyl-serine modification (GO:0018209)
axon development (GO:0061564)
negative regulation of apoptotic signaling pathway (GO:2001234)
Dark Grey Module GO Biological Process
neutrophil degranulation (GO:0043312)
neutrophil activation involved in immune response (GO:0002283)
neutrophil mediated immunity (GO:0002446)
toll-like receptor signaling pathway (GO:0002224)
leukocyte cell-cell adhesion (GO:0007159)
lipoxin biosynthetic process (GO:2001301)
regulation of protein processing (GO:0070613)
cellular response to cytokine stimulus (GO:0071345)
Midnight Blue Module GO Biological Process
translation (GO:0006412)
regulation of cellular amine metabolic process (GO:0033238)
regulation of cellular amino acid metabolic process (GO:0006521)
negative regulation of ubiquitin-protein ligase activity involved in mitotic cell cycle
negative regulation of G2/M transition of mitotic cell cycle (GO:0010972)
SCF-dependent proteasomal ubiquitin-dependent protein catabolic process
regulation of ubiquitin-protein ligase activity involved in mitotic cell cycle
negative regulation of ubiquitin protein ligase activity (GO:1904667)
Groups:
WT
CSF1Ri
CSF1R+/-
CSF1Ri-CSF1R+/-
Dark Grey Hub genes
Normalised for microglial numbers
Acad8 Coq8a Etfa Limd2 Naglu Rilpl2 Smim3 Vrk3
Bbs12 Ctnnbl1 Ezr Lyn Narf Rlbp1 Sult1a1 Zbtb3
Ccdc106 Ctsh Gpr12 Mertk Nfyc Rmnd5b Tmem40
Ccnd2 Cyth2 Gtf2h3 Mpped2 Ppp1r18 Slc26a6 Uba52
Cd55 Dgat2 H2-DMa Mrpl23 Prss23 Slc38a3 Ubox5
Chac1 Erlin1 Ing1 Naaa Rfc5 Slc39a11 Usp3
Adap2 Ccl6 Csf3r Fcrls Gnb1l Lair1 Siglech Trem2
Adgre1 Ccnd1 Ctss Fermt3 Gngt2 Laptm5 Slc25a45 Tyrobp
Alox5ap Cd14 Cx3cr1 Fgd2 Gpr34 Mylk3 Slc2a5 Unc93b1
Arhgap45 Cd300c2 Cyth4 Gm15542 Hcls1 Ncf1 Slco2b1 Vsir
Arhgdib Cd37 Dapp1 Gm16251 Hpgd Olfml3 Stra6
C1qa Cd53 Ecscr Gm17147 Il10ra P2ry12 Tmem119
C1qb Cd68 Fcer1g Gm23652 Itgb2 P2ry13 Tmem173
C1qc Cryba4 Fcgr3 Gna15 Lag3 Selplg Tnfaip8l2
CSF1Ri (150 ppm)
CSF1R+/-
65 5.5%
412 34.9%
705 59.6%
WT vs. CSF1Ri
WT vs. CSF1R+/-
CSF1R+/- vs. CSF1Ri-CSF1R+/-
Not significant
Log (base2) Fold change > 1 (60)
FDR < 0.05 (369)
FDR < 0.05 and Log (base2) Fold change >1 (149)
Not significant
Log (base2) Fold change > 1 (51)
FDR < 0.05 (798)
FDR < 0.05 and Log (base2) Fold change >1 (400)
Not significant
Log (base2) Fold change > 1 (68)
FDR < 0.05 (179)
FDR < 0.05 and Log (base2) Fold change >1 (26)
Log10 P
Log2 fold change
CSF1R+/- vs. CSFR1Ri-CSF1R+/-
WT
CSF1Ri
CSF1R+/-
CSF1Ri-CSF1R+/-
CSF1R+/- vs. CSF1Ri-CSF1R+/- GO Biological Process
positive regulation of synaptic transmission (GO:0050806)
protein localization to synapse (GO:0035418)
dendritic spine morphogenesis (GO:0060997)
postsynaptic density assembly (GO:0097107)
neuron projection morphogenesis (GO:0048812)
postsynaptic density organization (GO:0097106)

Fig. 2.6: **CSF1R signaling disruptions induces loss of microglial homeostasis but primarily affects neuronal gene expression (a)** Correlation of modules generated by weighted gene correlation network analysis (WGCNA) to the genotype (Z-score cut-off: +/-0.5). **(b)** Correlation of modules generated by WGCNA to the treatment (Z-score cut-off: +/-0.5) **(c)** Cell-type enrichment heatmap displays genes associated with specific cell types within a given color module. Values provided indicate the number of genes within the network associated with that a specific cell type. *** = 6+ genes. ** = 3+ genes. **(d,e)** $CSF1R^{+/-}$ signature: Module eigengene trajectory and heatmap of gene expression value in brown **(d)**, as well as gene ontology (GO) term enrichment for brown **(e)**. **(f,g)** CSF1Ri signature: Module eigengene trajectory and heatmap of gene expression value in dark grey **(f)**, as well as gene ontology (GO) term enrichment for dark grey **(g)**. **(h,i)** CSF1Ri signature: Module eigengene trajectory and heatmap of gene expression value in midnight blue **(h)**, as well as gene ontology (GO) term enrichment for midnight blue **(i)**. Curated gene ontology grids were ranked based on pathway p-value where cutoff was 0.05. Colors are associated with an adjusted p-value cut off of 0.1 herein pathways with lighter color had lower adjusted p-value than darker colors. **(j)** Interactive plot between hub genes extracted from the dark grey module showing a distinct CSF1Ri signature. **(k)** Heatmap of genes found in the dark grey module normalized to the average microglial numbers found within a group. **(l)** List of genes displaying increased expression in mice that are upregulated CSF1Ri-$CSF1R^{+/-}$ compared to $CSF1R^{+/-}$ mice. **(m)** List of downregulated genes between WT and $CSF1R^{+/-}$ mice normalized for number of microglia. **(n)** Venn diagram displaying the number of differentially expressed genes (DEGs, numbers provided) generated in transcriptional comparisons between CSF1Ri mice and $CSF1R^{+/-}$ mice in comparison with WT mice. **(o-q)** Volcano plots displaying the fold change of genes (log2 scale) and their p-values (-log10 scale) between WT vs CSF1Ri mice **(o)**, WT vs $CSF1R^{+/-}$ mice **(p)** and $CSF1R^{+/-}$ vs CSF1Ri-$CSF1R^{+/-}$ **(q)**. **(r)** Heatmap of DEGs between $CSF1R^{+/-}$ and CSF1Ri-$CSF1R^{+/-}$ mice. **(s)** Top biological processes gene ontology (GO) term enrichment for upregulated genes from the heatmap **(r)**.

MMP-14 is a putative mediator of perineuronal net loss

Our results repeatedly link altered microglial phenotypes with PNN disruption and synaptic loss, and therefore we next sought to explore the molecular mechanism by which this occurs. To accomplish this, we used a candidate-driven approach utilizing our RNA-seq data to identify potential genes that could be linked to regulation of the ECM. We observed *Mrc1* mRNA significantly decreased by CSF1Ri in CSF1R$^{+/-}$ cortices (Fig. 6Q). Immunostaining revealed increased expression of MRC1 by microglia in CSF1R$^{+/-}$ mice with normalization to WT expression in CSF1Ri-CSF1R$^{+/-}$ mice (Fig. 7a, b). Similarly, iCSF1R$^{+/-}$ mice displayed an increase in microglial MRC1 expression(Fig. 7e, f), suggesting alternative microglia activation (*258*). It has been proposed that cooperative actions between MMPs and phagocytic receptors, such as MRC1, can lead to cleavage of ECM components into manageable fragments for subsequent phagocytosis and degradation (*259, 260*). We similarly found that *Mmp-14* mRNA was increased in CSF1R$^{+/-}$ mice. Supporting this, a recent study investigating the microglial modulation of perisynaptic ECM and downstream changes in dendritic spine density also observed increased *Mmp-14* gene expression associated with ECM disruption, proposing that such proteases could be integral to remodeling of the ECM compartment (*74*). Furthermore, MMP-14 has been associated with degradation of the ECM either by directly cleaving components associated with PNNs, such as aggrecan (*261*), or by activating other MMPs, such as MMP-2 (*262, 263*). Accordingly, immunostaining for MMP-14 revealed increased microglial expression in CSF1R$^{+/-}$ mice, with subsequent normalization to WT levels with CSF1Ri (Fig. 7c, d). In addition, microglial MMP-14 expression was significantly increased in iCSF1R$^{+/-}$ mice (Fig. 7g, h). After confirming the association between

increased microglial MMP-14 and PNN loss in disease, we next sought to investigate whether MMP-14 could directly degrade PNNs. To this end, recombinant MMP-14 was injected into one cortical hemisphere of 4-month-old WT mice and Penicillinase, a β–lactamase that does not degrade PNNs, was injected into the contralateral cortex as a control, after which mice were euthanized 10 days post-injection. (Fig. 7i). Immunofluorescent staining of these tissue revealed marked decreases in the general marker WFA and core PNN component aggrecan in MMP-14 injected hemispheres (Fig. 7j-m). These data reinforce the concept that MMPs can influence the structure of the ECM *in vivo,* and suggest a possible mechanism by which microglia induce ECM degradation via elevated expression of MMP-14. Taken together, these results indicate that targeting microglia with elevated MMP-14 expression may at least partly prevent the aberrant modulation of ECM components during disease or injury, presenting a novel and attractive therapeutic approach for CNS diseases and disorders in which ECM dysregulation (specifically PNN loss) is a hallmark feature (*75, 76, 264*).

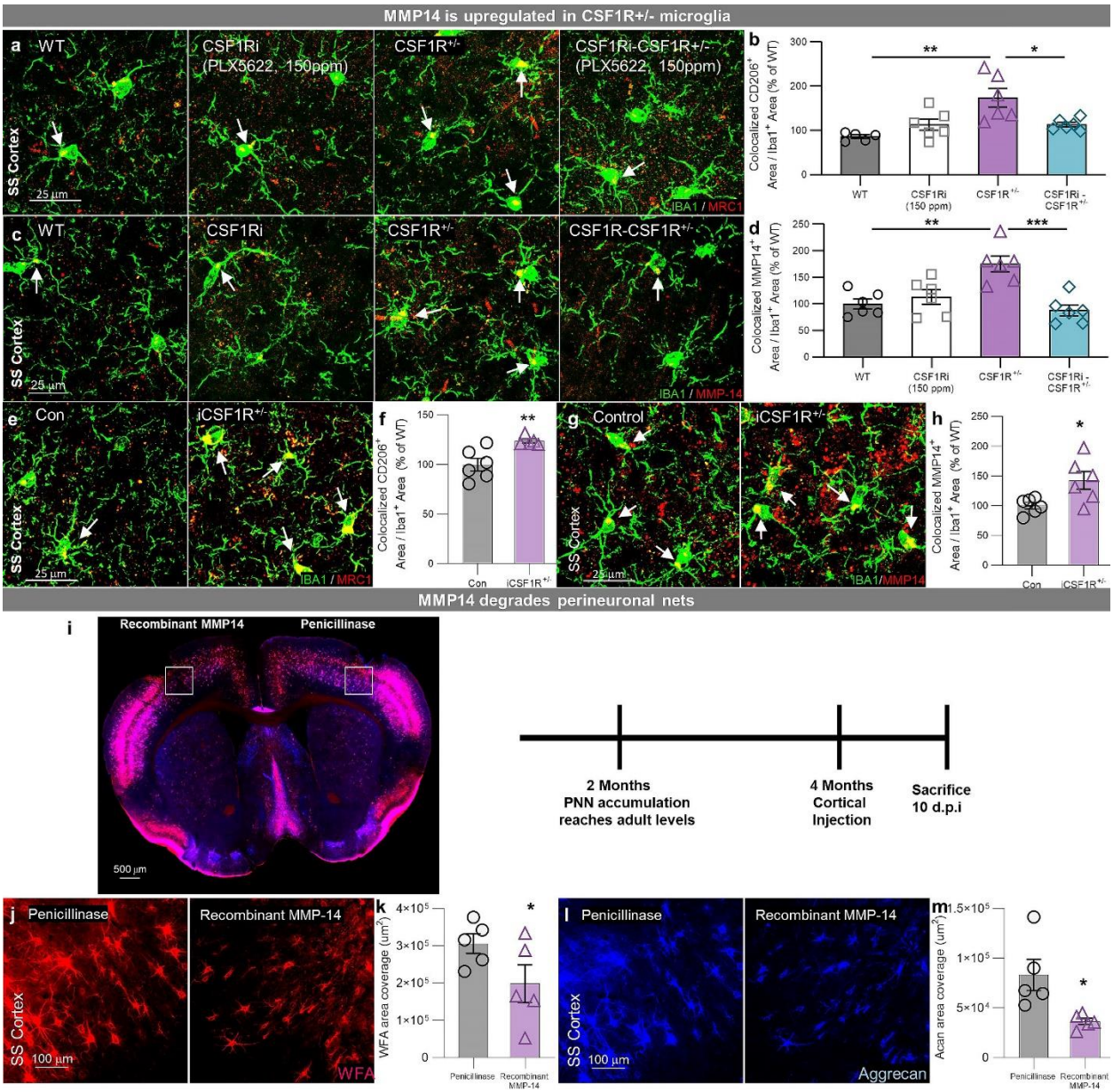

Fig. 2.7*:* **Microglia increase expression of MMP-14 and intracortical injection of recombinant MMP-14 is sufficient to induce PNN breakdown (a)** Representative 63x immunofluorescent images of MRC1^{+} and IBA1^{+} cell in ss ctx of WT, CSF1Ri, CSF1R$^{+/-}$, and CSF1Ri-CSF1R$^{+/-}$ mice **(b)** Quantification of colocalized MRC1^{+} IBA1^{+} area displayed significant increases in colocalized area in CSF1R$^{+/-}$ that was restored to WT levels in CSF1Ri-CSF1R$^{+/-}$ microglia. **(c)** Representative 63x immunofluorescent images of MMP-14^{+} and IBA1^{+} cells in ss ctx of WT, CSF1Ri, CSF1R$^{+/-}$, and CSF1Ri-CSF1R$^{+/-}$ mice **(d)** Quantification of colocalized MMP-14^{+} IBA1^{+} area displayed significant increases in colocalized area in CSF1R$^{+/-}$ that was

restored to WT levels in CSF1Ri-CSF1R$^{+/-}$ microglia. **(e)** Representative 63x immunofluorescent images of MRC1^{+} and IBA1^{+} in Control and iCSF1R$^{+/-}$ ss ctx. **(f)** Quantification of colocalized area displayed increased area of colocalized MRC1 in iCSF1R$^{+/-}$ microglia. **(g)** Representative 63x immunofluorescent images of MMP-14^{+} and IBA1^{+} in Control and iCSF1R$^{+/-}$ ss ctx. **(h)** Quantification of colocalized area displayed increased area of colocalized MMP-14 in iCSF1R$^{+/-}$ microglia. **(i)** WT mice were aged to 4 months at which point they received injection of recombinant MMP-14 and Penicillinase in contralateral cortices. 10 days post injection (d.p.i.) mice were sacrificed and brains were harvested. **(j)** Representative 20x confocal immunofluorescent staining of WFA or **(l)** Aggrecan in the respective injection area. **(k)** Quantification of WFA^{+} area and **(m)** Aggrecan^{+} area revealed significant decreases in MMP-14 injection site compared to Penicillinase injection site. Statistical analysis used a two-way ANOVA with Sidak multiple comparisons correction or Two-Tailed T-Test. Statistical analysis used a two-tailed paired T-Test for MMP-14 injection comparisons. Significance indicated as * $p< 0.05$; ** $p < 0.01$; *** $p < 0.001$

DISCUSSION:

Accumulating evidence indicates that microglia are critically involved in neurodegenerative disease progression. However, it remains unclear whether these cells play a causative role in driving disease pathology and neurodegeneration, a reactive role by responding harmfully to existing pathology, or both. CNS disorders that present genetic etiologies linked to microglia-specific genes provide unique opportunities to investigate and answer these questions (e.g. how microglia drive brain disease). While such disorders have been reported, the cellular mechanisms by which these underlying genetic disturbances lead to overt CNS pathology remain largely unknown. In this study, we conditionally induced microglial Csf1r haploinsufficiency in adult mice to explore the role of partially disrupted CSF1R signaling on microglial homeostasis and CNS function. Additionally, we used a constitutive mouse model of Csf1r haploinsufficiency and explored the consequences of low-grade modulatory and high-grade microglia-depleting doses of the pharmacological CSF1R inhibitor PLX5622. It is important to stress that CSF1R inhibition is highly dynamic – sustained, potent inhibition can eliminate the entire microglial compartment for the duration of treatment, while low-grade inhibition modulates microglial activity/function in a dose-dependent manner, with less extensive depletion of the microglial population (62). For this reason, and because sustained loss of the adult microglial pool is not clinically viable in the long-term, a modulatory dose of PLX5622 for low-grade CSF1R inhibition (CSF1Ri) was utilized to assess how pharmacologically impairing CSF1R signaling in healthy adult mice (or further inhibiting this pathway in Csf1r haploinsufficient mice) influences CNS homeostasis in the presence of microglia.

To establish whether post-developmental Csf1r haploinsufficiency in microglia was sufficient to induce pathology, we utilized a tamoxifen-inducible Cre recombinase system in which one floxed copy of the Csf1r allele was conditionally excised in adult CX3CR1+ microglia (iCSF1R$^{+/-}$ mice). As human ALSP patients are Csf1r haploinsufficient from birth, we validated our findings in an additional constitutive CSF1R$^{+/-}$ model. We noted a loss of microglial P2RY12 expression following iCSF1R$^{+/-}$ tamoxifen recombination and in CSF1R$^{+/-}$ mice, conventionally reflective of a loss of microglial homeostasis in disease (30-32) and similar to the downregulation of P2RY12 expression in human ALSP patients harboring Csf1r mutations (34). Accordingly, our RNA-seq data revealed a general downregulation of canonical microglial gene expression, consistent with a departure from homeostasis. We were also unable to detect an enrichment of inflammatory gene transcripts associated with microglial activation (e.g., Cst7, Axl, or Ldl, as seen in damage-associated microglia (DAM)) (30). Interestingly, the phenotypes of CSF1R$^{+/-}$ microglia we describe here resemble those we recently reported in a mouse model of HD (20), as supported by GO analysis of WT vs CSF1R$^{+/-}$ gene enrichment (Supplemental Fig. 6c). These results suggest that phenotypic states of microglia independent from traditional paradigms of immune activation may also contribute negatively to disease outcome. It should be noted that CSF1Ri did not rescue deficits in NPR tasks (Fig. 3d). NPR memory has been critically linked to hippocampal activity(70), as opposed to the cortical dependence of tasks like NOR(71, 72). These results informed our decision to specifically focus on cortical regions for subsequent analyses. However, future studies should explore the divergent effects of CSF1Ri on myeloid populations among various regions of the CNS especially with regard to their effects on CNS health.

Further, our data emphasize the concept of the tetrapartite synapse as a particularly disease-relevant neurological unit, in which synaptic structure and function are regulated by four key elements: pre- and post-synaptic compartments, glial cells, and the ECM. With regards to this, we observed a consistent downregulation or elimination of presynaptic markers (Sv2a, Bassoon, Synaptophysin) in iCSF1R$^{+/-}$ (Fig. 1) and CSF1R$^{+/-}$ mice (Fig. 5), while post-synaptic proteins (PSD95) appeared to be spared. This is consistent with microglial trogocytosis of synaptic elements (e.g. partial engulfment by microglia of target substrate, rather than complete phagocytosis), whereby microglia sculpt presynaptic elements to refine neural circuits, while sparing postsynaptic components (19). In terms of the ECM we observed deficits in PNNs, specialized lattice-like structures composed of CSPGs that provide structural and biochemical stability to proximal synapses (73). Genetic or enzymatic modifications to PNN composition induce changes in synapse number (74, 75), transmission (76), and receptor makeup (77), and as such these structures play a critical role in regulating synaptic connectivity and plasticity (41, 42). Furthermore, PNNS augment neuronal excitability/firing (78) and protect neurons against neurotoxins (79). We recently reported microglia-facilitated loss of PNNs as a general feature of neurodegeneration in HD (20) and AD (45). Here, we highlighted a loss of microglial homeostasis following induction of Csf1r haploinsufficiency, whether genetic (iCSF1R$^{+/-}$ or CSF1R$^{+/-}$) or pharmacological, that was concomitant with reductions in presynaptic puncta and disruptions to ECM structures, strongly supporting a microglial origin for these deficits.

In support of this microglial basis of pathology, we found that elimination of the microglial compartment (with sustained high dose CSF1R inhibition) prevented both loss of

presynaptic surrogates and PNNs, as well as disease-related CSPG deposition in $CSF1R^{+/-}$ mice. Crucially, these results suggest that specific targeting of microglia can prevent Csf1r haploinsufficiency-associated CNS damage and demonstrates how altered microglial phenotypes can exert profound effects on neuronal function. A caveat of our experiments is that we focused our analyses on microglial populations in the CNS. As mentioned previously, macrophages that also express Csf1r, such as PVMs, could theoretically play a role in inducing pathology given their involvement in the maintenance of steady-state tissue (73) and should be explored in future studies. That being said, we believe that microglia are the most likely culprits for the pathology observed here. Our findings also demonstrate that CSF1R signaling deficiency, either via genetic haploinsufficiency or CSF1Ri, leads to microglial dyshomeostasis, further suggesting that CSF1R is a critical regulator of homeostatic function in microglia. Indeed, we observed overlapping phenotypes induced by CSF1Ri in WT mice and genetic haploinsufficiency in CSF1R+/- mice, e.g. down-regulation of P2RY12 expression in microglia, and loss of presynaptic puncta. RNA-seq analyses also showed ~34% overlap in DEG's between CSF1Ri and Csf1r haploinsufficiency and strikingly, most of these genes were of neuronal origin. These data emphasize how changes in microglial phenotype can modulate neuronal gene expression, function, and structure, and link genetic and pharmacological impairments in CSF1R signaling to specific changes in microglial homeostasis synaptic integrity, and ECM organization.

In this study, we also reported paradoxical observations whereby inhibiting CSF1R signaling in a system already deficient in Csf1r lead to recovery, rather than exacerbation, of multiple facets of CNS homeostasis. This included improved cognitive performance

and normalization of microglial phenotypes (densities, morphologies, P2RY12 expression), PNNs, CSPGs, and presynaptic puncta. Furthermore, RNA-seq data highlighted dramatic increases in neuronal- and synaptic-associated genes with CSF1Ri in $CSF1R^{+/-}$ cortices, such as Syn2, Begain, and Rims3. Prior studies using CSF1R inhibitors in mouse models of AD and MS have also shown modulatory effects on neurodegenerative pathologies (55, 80, 81). Importantly, and in parallel with our findings, restoration of microglial homeostasis by genetic knockout of a single Csf2 allele in $CSF1R^{+/-}$ mice, which exhibit increased Csf2 mRNA expression, prevented loss of myelin and reversed $CSF1R^{+/-}$ behavioral deficits in $CSF1R^{+/-}$ mice by reinstating balanced CSF1R/CSF2 signaling (51). While a genetic approach to normalizing microglial homeostasis is attractive in its specificity, the pharmacological approach of CSF1Ri presents an alternative to targeting this pathway with its own unique advantages (e.g. CSF1R inhibitors can be utilized at virtually any time and for any duration, can be titrated as desired, and readily cross the blood-brain barrier). It is important to note that while haploinsufficiency is considered by some to be a valid model of ALSP, given the emergence of human ALSP patients with Csf1r haploinsufficiency (2, 11), there is still debate on how haploinsufficiency may account for all cases of ALSP (82-84). Indeed, a vast number of ALSP mutations result in kinase dead receptors leading to a dominant negative phenotype (8, 83, 85). While in our study, treatment of Csf1r haploinsufficient mice managed to reverse pathology, further studies are necessary to explore how CSF1Ri would affect kinase dead mutations.

Constitutive CSF1R haploinsufficiency resulted in elevated microglial densities in adult mice, in line with prior reports (12, 51), including in microglia-specific CSF1R

haploinsufficient mice (58). In line with an impaired developmental establishment of the microglial population we find that microglial densities were not increased in adult iCSF1R$^{+/-}$ mice; despite this, induction of microglial specific CSF1R haploinsufficiency in the adult was sufficient to cause loss of microglial homeostasis and associated loss of presynaptic puncta and remodeling of the ECM indicating that increased microglial number do not contribute to the pathology observed here. Accordingly, discrepancies exist between microglial densities reported in constitutive CSF1R haploinsufficient mice, and CSF1R haploinsufficient rats (76) and zebrafish (26), which do not show these increases, while studies in post mortem human ALSP brains suggest an initial increase in microglial densities followed by later reductions (3). These data further suggest that changes in microglial densities, at least in mice, are not key drivers of pathology, but that it is altered microglial phenotypes induced by a loss of a Csf1r allele that is important.

It should be highlighted that there is a marked difference in the effects of CSF1Ri that modulate microglial phenotypes vs. microglia depleting doses – none of the neuronal gene changes seen in the context of genetic or pharmacological Csf1r haploinsufficiency are observed in MD-WT mice ((20, 27) ; http://rnaseq.mind.uci.edu/green/ad_plx/), nor are reductions in synaptic puncta seen (Fig. 2d-g). Similarly, elimination of microglia from healthy adult mice in a prior study does not confer ALSP pathology (i.e. cognitive deficits, PNN degradation, synaptic loss), despite 6 months of microglial depletion (27). In fact microglial depletion is generally associated with improved performance in memory and cognitive tasks (25, 27, 86). Moreover, our data with respect to MD-CSF1R$^{+/-}$ pathology recovery provide further evidence of these cells being viable targets for therapeutic intervention especially at early stages of disease onset. The recent development of the

Csf1r$^{\Delta FIRE/\Delta FIRE}$ mouse line (87) and Csf1r$^{-/-}$ rats (88) which do not develop microglia in the brain but are otherwise healthy further suggest at least partial functional redundancy in the maintenance of adult CNS homeostasis by microglia. Collectively, our results indicate that improperly functioning or “dyshomeostatic” microglia are worse for the adult brain under baseline conditions than the lack of microglia altogether (31, 69).

SUPPLEMENTAL FIGURES:

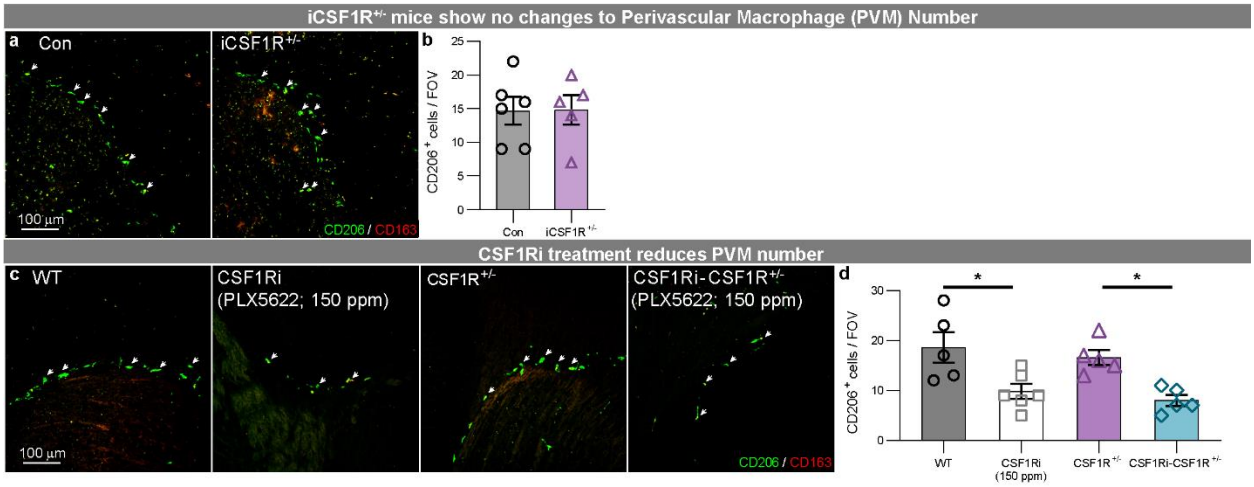

Supplemental Fig. 2.1: **No changes to Perivascular Macrophage (PVM) population via genetic CSF1R haploinsufficiency. CSF1Ri treatment reduces PVM number. (a,b)** Representative 20x confocal images of CD206 and CD163 immunostaining reveals no differences to PVM quantities in iCSF1R$^{+/-}$ mice. **(c,d)** Similarly, 20x representative images of PVMs of CSF1R$^{+/-}$ mice show no differences compared to WT counterparts. CSF1Ri however reduced the number of PVMs in both CSF1Ri and CSF1Ri-CSF1R$^{+/-}$ mice. Statistical analysis used t-test or a two-way ANOVA with Sidak multiple comparisons correction. Significance indicated as * p<0.05.

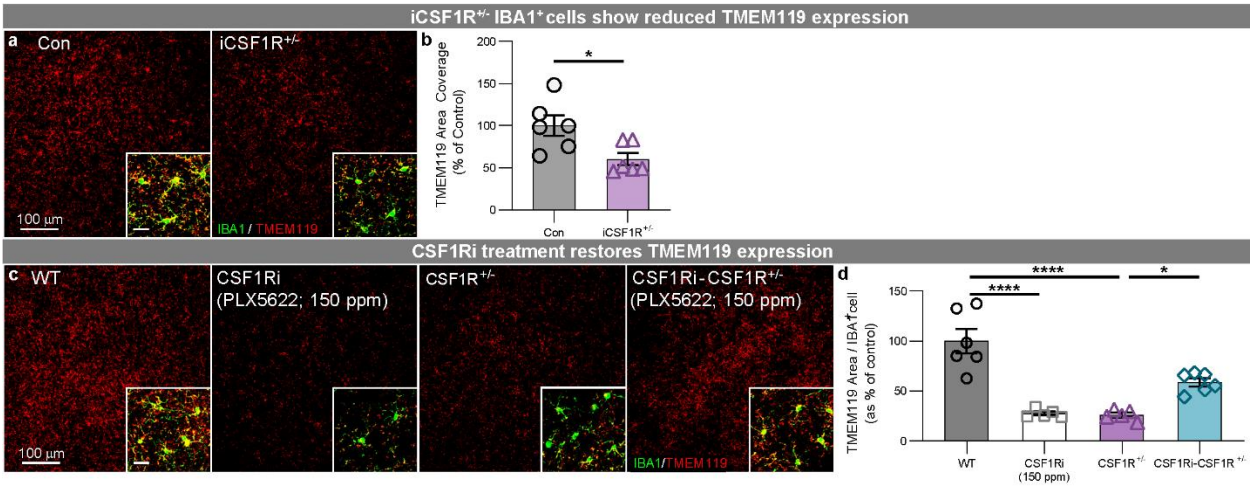

Supplemental Fig. 2.2: **TMEM119 expression is reduced by CSF1R haploinsufficiency. (a)** Representative 20x images in ss cortex immunostaining of TMEM119 **(b)** reveals marked reduction of TMEM119 expression by myeloid cells. Inserts show overlap of IBA and TMEM119 immunopositivity. **(c)** Representative 20x confocal imaging of ss ctx shows **(d)** reduction of TMEM119 expression in CSF1Ri and $CSF1R^{+/-}$ mice. CSF1Ri treatment of $CSF1R^{+/-}$ mice increases TMEM119 immunostaining. Statistical analysis for inducible $CSF1R^{+/-}$ comparisons used a two-tailed t-test. Significance indicated as * $p<0.05$. Statistical analysis used a two-way ANOVA with Sidak multiple comparisons correction. Significance * $p<0.05$; ** $p<0.01$; *** $p<0.001$.

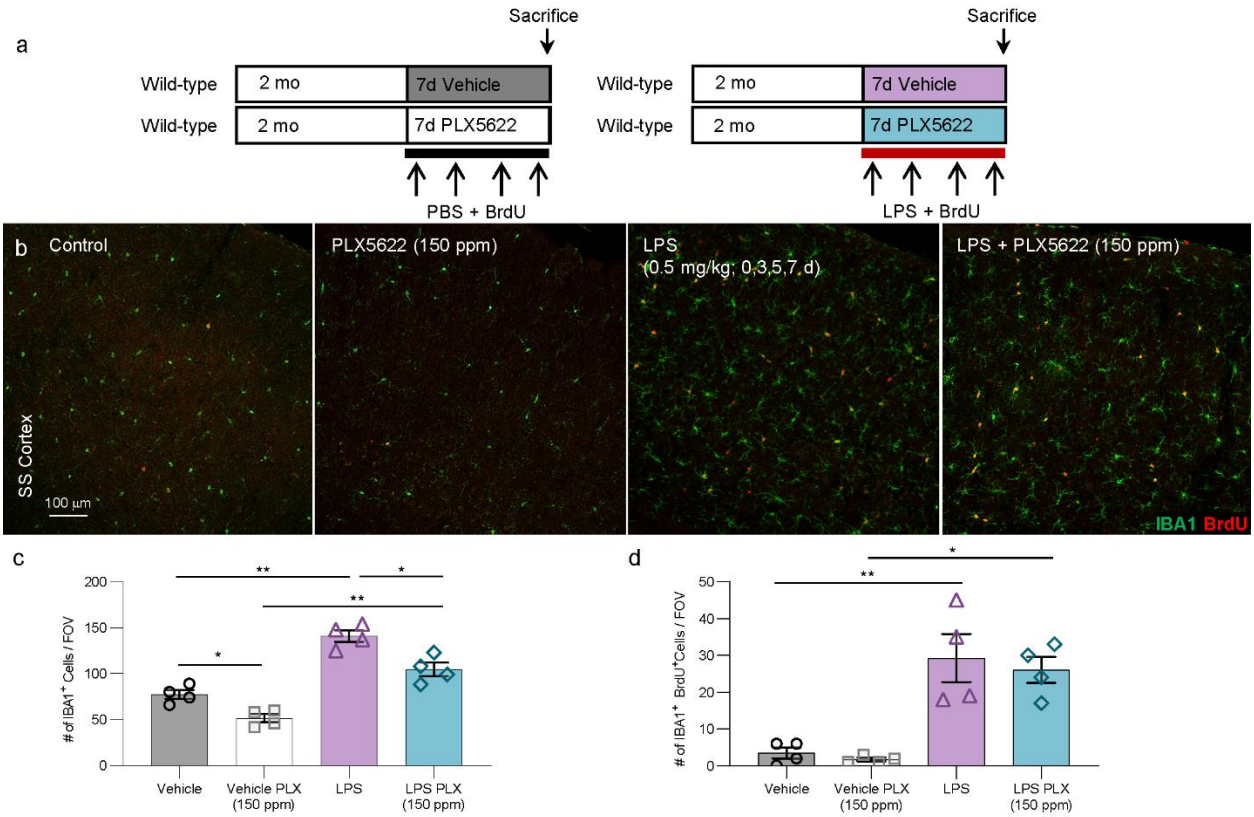

Supplemental Fig. 2.3: **Development of a 150 ppm PLX5622 dosage to eliminate ~25-30% of IBA1$^+$ cells (a)** 2-month-old mice were treated with either PBS + BrdU throughout the course of a week on days 0, 3, 5, and 7. Similarly, each group was treated with either control diet or 150 ppm PLX5622 lasting the duration of that week. **(b)** Representative 20x image of IBA1$^+$ and BrdU$^+$ immunofluorescence in the SS Cortex. **(c)** Quantification of IBA1$^+$ cells in the SS Cortex. Low dose PLX5622 treatment reduced IBA1$^+$ immunofluorescence by 25-30% in both PBS and LPS treated groups. **(d)** Quantification of BrdU$^+$/IBA1$^+$ cells in the SS Cortex. Treatment with PLX5622 did not induce any changes to proliferative capacity as measured by BrdU expression. Statistical analysis used a two-way ANOVA with Sidak multiple comparisons correction. Significance indicated as * p<0.05; ** p<0.01.

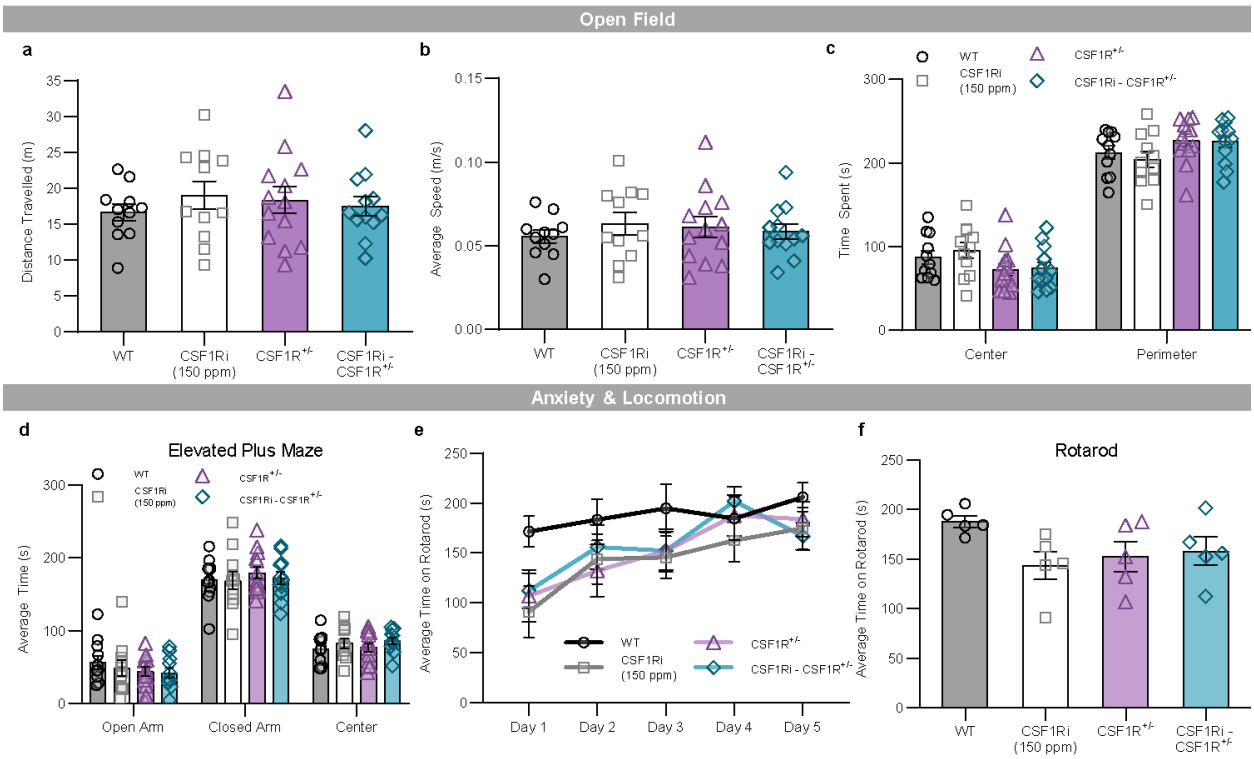

Supplemental Fig. 2.4: **Behavioral analysis of CSF1R$^{+/-}$ mice reveals no locomotor or anxiety changes (a,b)** WT, CSF1Ri, CSF1R$^{+/-}$, and CSF1Ri-CSF1R$^{+/-}$ mice showed no obvious differences in motor capabilities as observed by distance traveled and speed. **(c)** All groups of mice spent similar times in the perimeter and center of the open field testing apparatus. **(d)** No differences were observed between groups in time spend in open or closed arms of the elevated plus maze as a measure of anxiety. **(e)** Performance on a rotarod across five trials showed no differences between groups. **(f)** Time spent on rotarod averaged across five trails revealed no differences amongst the groups. Statistical analysis used a two-way ANOVA with Sidak multiple comparisons correction. Significance indicated as * p<0.05.

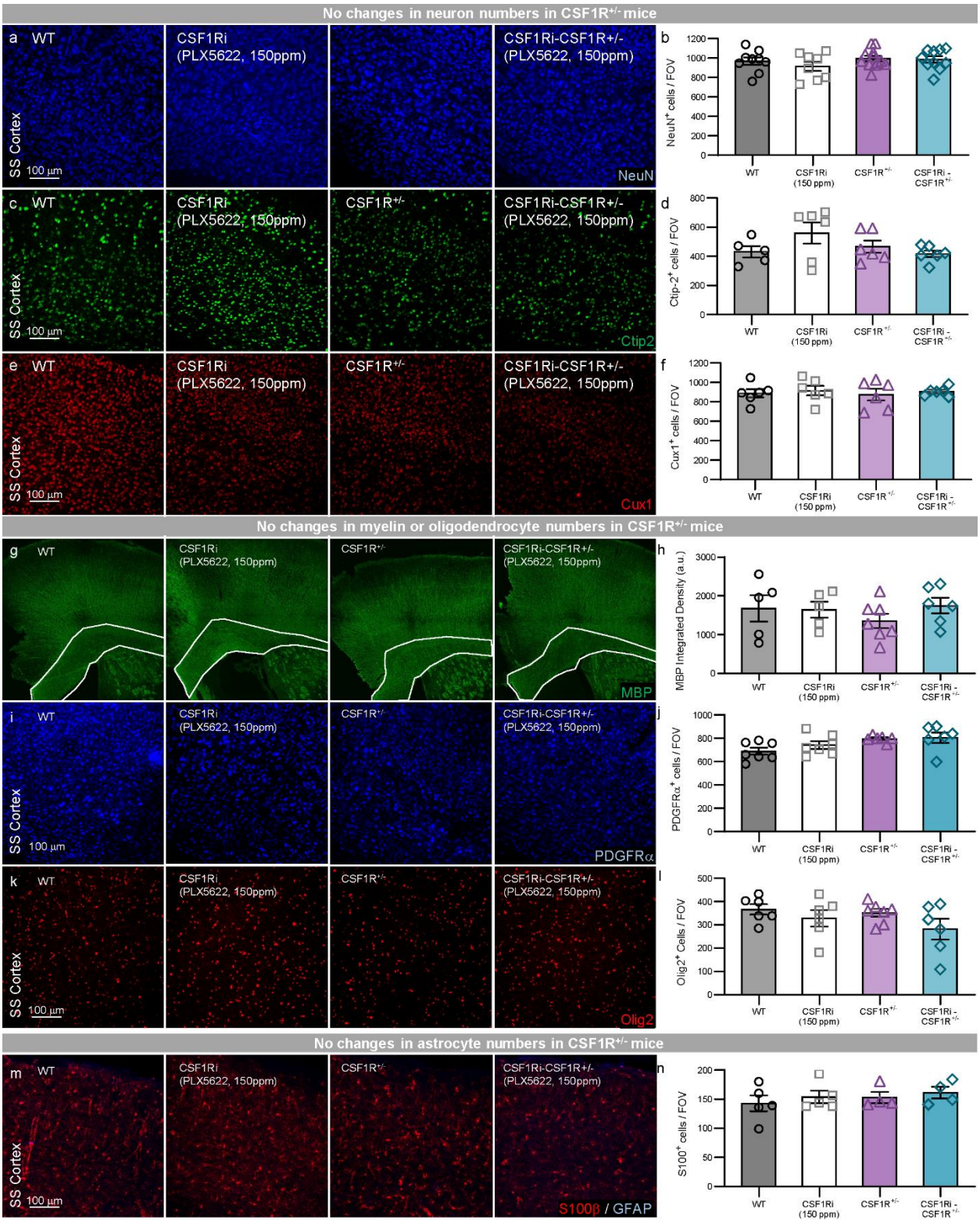

Supplemental Fig. 2.5: **No change in number of various cell types observed in non-microglial cell types in SS Ctx between groups.** Representative 20x image of ss ctx reveals no differences in number of **(a,b)** NeuN$^+$ cells, **(c,d)** Ctip2$^+$ cells or **(e,f)** Cux1$^+$ cells. **(g)** MBP immunofluorescence of the cc found no changes as assessed by Integrated Density via ImageJ **(i)** 20x representative image of PDGFRα marker

for oligodendrocyte progenitor cells and **(k)** Olig2, a marker for mature oligodendrocytes, revealed no changes to either suggesting changes to oligodendrocyte pools are undisturbed by CSF1R alterations. **(m,n)** Similarly, 20x representative images of cortical astrocytes showed no changes in $S100^{+}$ cells and nonexistent GFAP immunofluorescence throughout, suggesting a lack of astroglial activation as a product of dysregulated CSF1R signaling. Statistical analysis used a two-way ANOVA with Sidak multiple comparisons correction. Significance indicated as * $p<0.05$.

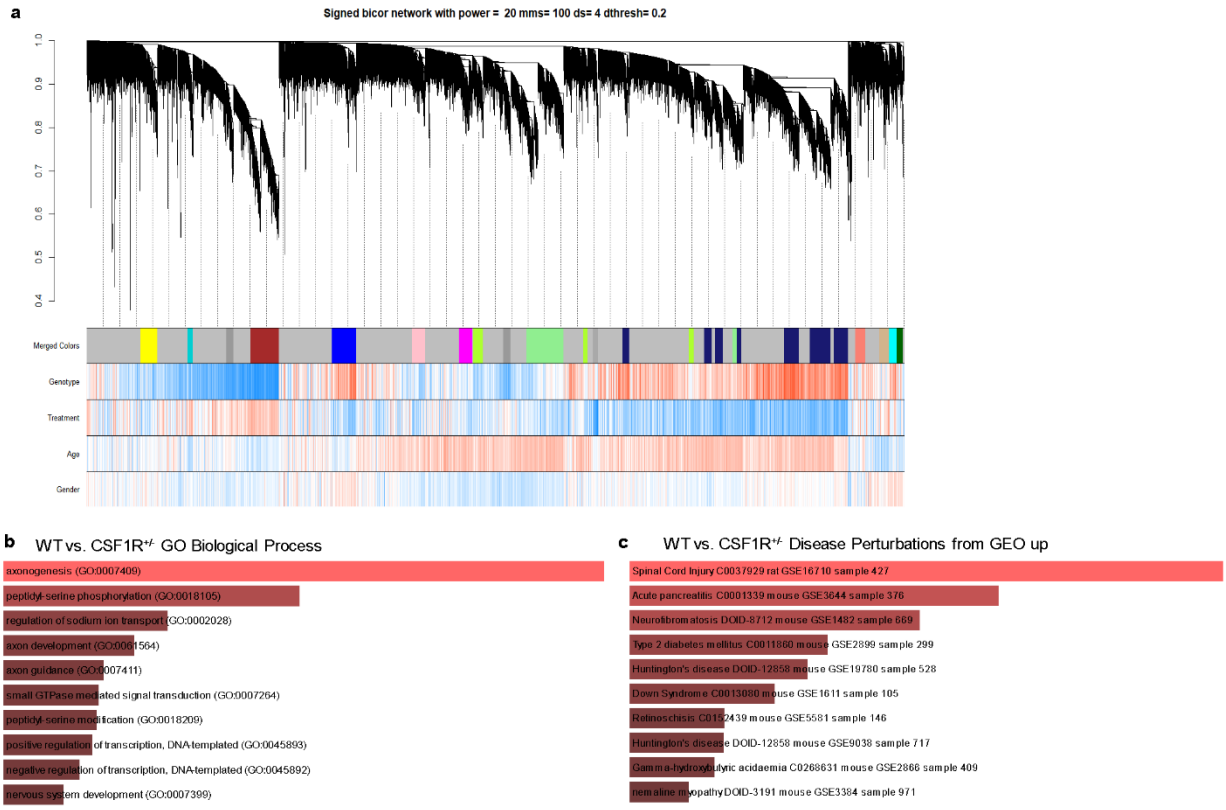

Supplemental Fig. 2.6: **Gene ontology terms for differentially expressed genes WT and $CSF1R^{+/-}$ comparison (a)** Signed bicor network shows the effects of genotype, treatment, age and gender which are separated into distinct colored modules. **(b)** GO terms for biological processes and **(c)** GO Terms for Disease Pathways.

Chapter Three:

Microglial dyshomeostasis in aged CSF1R$^{+/-}$ mice can be restored with CSF1Ri and can partly reduce pathological burden

INTRODUCTION

ALSP is clinically delineated by cognitive dysfunction with motor and neuropsychiatric symptoms including bradykinesia, depression, and personality changes. Symptoms are oftentimes non-specific in the early stages of ALSP and may be difficult to distinguish from other neurological diseases in the absence of CSF1R genetic mutation verification. The diagnosis of ALSP thus requires exclusion of disorders with symptoms that overlap with ALSP, as many neurodegenerative disorders share symptoms with ALSP and further complicate the differential diagnosis of ALSP, confirming the need for genetic testing, such as a leukodystrophy panel or whole exome testing. Efficient and accurate diagnosis of ALSP is further complicated given that there is no major correlation of genotype to phenotype. Indeed, family members with identical CSF1R mutations often do not present with the same clinical phenotype. Similarly, the rate of symptom progression varies among patients and even within family members who carry the same mutations, arguing for the presence of environmental influences and genetic mosaicism that can alter disease penetrance.

In chapter two, we show that the regulation of microglial homeostasis via CSF1Ri treatment of CSF1R$^{+/-}$ mice leads to the amelioration of ALSP pathology as described by the recovery of PNN and synaptic structures. It is important to highlight that these data implicated microglia dyshomeostasis specifically as the driving force for the pathology

observed. However, the paradigm established in our previous study focused on the treatment of mice prior to pathology onset, examining CSF1R haploinsufficient mice at 8 months of age. In the clinical population, patients are diagnosed with ALSP once pathology has set in, given the complexity of the disease, spurring a necessary investigation into whether CSF1Ri treatment can still be used as a pharmacological intervention when treating patients who have already begun developing ALSP pathology. To that end, we extended our prior work exploring the effects of CSF1Ri and CSF1R haploinsufficiency in aged mice. We find that similar to the 8 month cohort, the 16 month $CSF1R^{+/-}$ also displayed evidence of dyshomeostatic microglia, as assessed by decreased expression of P2RY12, as well as increased expression of CD68 and microglial Lamp1, which were restored upon CSF1Ri treatment. This was accompanied by a loss in corpus callosum and cortical MBP immunostaining of $CSF1R^{+/-}$ mice. Measurements of PNN and synaptic structures were also restored upon CSF1Ri, as well as measurements of Nf-L immunoreactivity, a marker for axonal damage in the CNS. Collectively these data suggest that while only modest restorations were found across a variety of measurements, CSF1Ri could still be used as a possible therapeutic for CSF1R haploinsufficiency at more advanced stages of disease.

MATERIALS AND METHODS

Compounds:

PLX5622 was provided by Plexxikon Inc. and formulated in AIN-76A standard chow at a dose of 150 ppm or 1200 ppm by Research Diets Inc.

Mice:

All mice were obtained from The Jackson Laboratory. Mice were mixed sex C57BL/6 (000664) mice. Animals were housed with open access to food and water under 12h/12h light-dark cycles. All mice were aged to 16 months unless otherwise indicated. *Csf1r*$^{+/-}$ mice were generously provided by Dr. Karina Cramer (University of California – Irvine; Department of Neurobiology and Behavior) and were maintained and genotyped as described previously (*224*). For genotyping *Csf1r*$^{+/-}$ mice the following primers were used: Forward, 5' ATCCAGCATTAGGCAGCCT; reverse, 5' GCCACCATGTGTCCGTGCTT.

Animal treatments:

All rodent experiments were performed in accordance with animal protocols approved by the Institutional Animal Care and Use Committee (IACUC) at the University of California, Irvine. The CSF1R$^{+/-}$ mouse model (*16, 225*) has been previously described in detail. At the end of treatments, mice were euthanized via CO2 inhalation and transcardially perfused with 1X phosphate buffered saline (PBS). For all studies, brains were removed, and hemispheres separated along the midline. Brain halves were either flash frozen for subsequent biochemical analysis, drop-fixed in 4% Paraformaldehyde (PFA; Thermo Fisher Scientific, Waltham, USA) for subsequent immunohistochemical analysis. Half brains collected into 4% PFA for 48 hrs and then transferred to a 30% sucrose solution with 0.02% sodium azide for another 48-72 hrs at 4C. Fixed half brains were sliced at 40 µm using a Leica SM2000 R freezing microtome. The flash-frozen hemispheres were microdissected into cortical, hippocampal, and thalamic/striatal regions and then ground with a mortar and pestle to yield a fine powder.

Behavioral assays:

The following behavioral paradigms were carried out in the following order (*213*) WT and CSF1R+/- underwent behavioral assessment six weeks after being placed on their respective diet beginning at 14 mo.

Elevated plus maze (EPM)

Mice were placed in the center of an elevated plus maze for 5 minutes to assess anxiety. Unless otherwise stated, ANY-Maze software was employed to video-record and track animal behavior. The total number of open and closed arm entries, as well as the time spent in each arm was determined.

Open field (OF)

In brief, mice were placed in a white box for 5 min to assess anxiety. The amount of time spent in the center versus the perimeter of the arena was obtained. Measurements on distance traveled as well as average speed of the mice were also observed. Of note, the same arena was used for OF, Novel Object, Novel Place and Social Interaction tasks.

Novel object recognition (NOR)

Mice were allowed to freely explore two identical objects (either small glass beakers or plastic building blocks; counterbalanced for treatment) and exploratory behavior was recorded for 5 min. 24 hrs later, one familiar object is replaced with a novel object (either beaker or block) and behavior is recorded for 3 min. The amount of time spent investigating the novel object was determined by calculating the discrimination index (time investigating novel object—time investigating old object / total time) and is presented as a percentage, where chance level of investigation for each object is 50%.

Novel place recognition (NPR)

Mice were allowed to freely explore two identical objects (either small glass beakers or plastic building blocks; counterbalanced for treatment) and exploration behavior is recorded for 5 min. 24 hrs later, one familiar object is moved to a new location and behavior is recorded for 3 min. The amount of time spent investigating the novel object was determined by calculating the discrimination index (time investigating novel place—time investigating old place / total time) and is presented as a percentage, where chance level of investigation for each place is 50%.

Social Interaction Task

Mice we allowed to freely explore the arena for 5 minutes. After habituation, a control mouse of the same sex was placed inside a wire containment cup that is located to the side of the arena. Subject mouse was allowed free access to the arena and control mouse for 5 minutes. Number of direct contacts between the subject mouse and the containment cup housing a control mouse were quantified as active contacts. Duration of active contact points were measured and determined by calculating the discrimination index (time of active contact points / total time) and is presented as a percentage.

Rotarod

The motor capabilities of the mice were tested using an accelerating rotarod (Ugo Basile). Each mouse was placed on the rotarod beam for a maximum of 5 min while it accelerated from 8 to 40 rpm. The experimenter stopped the timer when either the mouse fell off the beam or the mouse held on to the beam and its body completed two full rotations. A total of 5 trials were performed per mouse, each with a 15-min intertrial interval.

Histology and confocal microscopy:

For immunostaining of P2RY12, Aggrecan and CSPG CS-56 antigen retrieval was performed by heating the sections in citrate buffer (10 mM [pH 6.0]) for 30 minutes at 80C followed by 10 minute cooling period and 5 minute 1X PBS wash. Fluorescent immunolabeling followed using a standard indirect technique as described previously (*119*). Brain sections were stained with primary antibodies against: ionized calcium binding adaptor molecule 1 (IBA1; 1:1000; 019-19741, Wako and ab5076, Abcam), wisteria floribunda agglutinin (WFA; 1:1000, B1355, Vector), Aggrecan (1:200; ab1031 Millipore), CSPG CS-56 (1:200; ab11570 Abcam), S100β (1:200; Abcam), glial fibrillary protein (GFAP; 1:1000; Abcam), Ki67 (1:200; Cell Signaling), NeuN (1:1000; Millipore), MBP (1:200; Millipore), PDGFRα (1:200; Thermofisher Scientific), Olig2 (1:200; Abcam), Synaptophysin (1:1000; Sigma Aldrich), P2RY12 (1:200; Sigma-Aldrich), Nf-L (1:200; Synaptic Systems).

For RNAscope In-Situ Hybridization we followed manufacturer's instructions. Briefly, tissue sections were mounted onto slides and warmed at 60℃ for 30 minutes. Sections were dehydrated with 50%, 70%, and 100% ethyl alcohol gradients for 5 minutes each at room temperature and followed by hydrogen peroxide (Cat No.322335 ACDBio) at room temperature for 10 minutes each and then washed with Deionized (DI) water. Tissue sections were placed in boiling 1X Target Retrieval Reagent (Cat No.322380 ACDBio) for 15 minutes then immediately transferred to DI water and washed in 100% Ethyl Alcohol and allowed to dry. Slides were covered in Protease III (Cat No.322337 ACDBio) for 30 minutes at 40℃. Probes were then added for 2 hrs at 40℃ within a humidity control chamber. Signal amplification and detection reagents (Cat No.322310 ACDBio) were

applied sequentially and incubated in AMP 1, AMP 2, and AMP for 30 minutes each. Before adding each AMP reagent, samples were washed twice with washing buffer (Cat NO.310091 ACDBio). Respective HRPs were placed on slides for 15 minutes at 40℃ followed by 30 minutes of respective Opal dye (FP1487001KT Akoya Biosciences) for 30 minutes at 40℃ and HRP blocker for 15 minutes at 40℃.

High resolution fluorescent images were obtained using a Leica TCS SPE-II confocal microscope and LAS-X software. For confocal imaging, one field of view (FOV) per brain region was captured per mouse using the Allen Brain Atlas to capture comparable brain regions. For synaptic quantifications three FOVs per brain region were captured and quantifications for each animal was averaged. Total cell counts and morphological analyses were obtained by imaging comparable sections of tissue from each animal at the 20X objective, at multiple z-planes, followed by automated analyses using Bitplane Imaris 7.5 spots and filaments respectively, as described previously (*214*). Colocalization analyses were conducted using Bitplane Imaris 7.5 colocalization and surfaces modules. For hemisphere stitches automated slide scanning was performed using a Zeiss AxioScan.Z1 equipped with a Colibri camera and Zen AxioScan 2.3 software. Cell quantities were determined using the spots module in Imaris. Integrated density measurements were determined in ImageJ (NIH).

Data analysis and statistics

Statistical analysis was performed with Prism Graph Pad (v.8.0.1; La Jolla, USA). To compare two groups, the unpaired or paired Student's t-test were used. Behavioral, biochemical, and immunohistological data were analyzed using Two-way ANOVA (Diet: Control vs. PLX5622 and Genotype: WT vs. $CSF1R^{+/-}$) using GraphPad Prism Version 8.

Tukey's post hoc tests were employed to examine biologically relevant interactions from the two-way ANOVA regardless of statistical significance of the interaction. For all analyses, statistical significance was accepted at $p < 0.05$. and significance expressed as follows: *$p < 0.05$, **$p< 0.01$, ***$p < 0.001$. n is given as the number of mice within each group. Statistical trends are accepted at $p<0.10$ ($^{\#}$). Data are presented as raw means and standard error of the mean (SEM).

RESULTS

Aged CSF1R$^{+/-}$ mice display cognitive deficits that are no longer rescued by sustained low-grade CSF1R inhibition

Previous data from pre-pathological mice suggested that CSF1Ri is a viable treatment avenue for restoring microglial homeostasis and downstream pathology (i.e. ECM and synaptic elimination). However, whether CSF1Ri has similar efficacy in advanced stages is still unclear. To that end, WT and CSF1R$^{+/-}$ mice were treated with the specific CSF1R inhibitor PLX5622 (150 ppm in chow) for 2 months starting at 14 mo to induce CSF1Ri generating 4 groups: **WT, CSF1Ri, CSF1R$^{+/-}$,** and **CSF1Ri-CSF1R$^{+/-}$** (Fig. 1a). To characterize the behavioral phenotypes in our cohort of mice (n=8-10), we once again performed a battery of tasks consisting of EPM, Open Field (OF), Novel Object Recognition (NOR), Novel Place Recognition (NPR). Behavioral assessments began 6 weeks after mice were placed on diet and continued for two weeks, at which point mice were euthanized. Herein, we found reduced performance of CSF1R$^{+/-}$ mice in both NOR and NPR tasks. While CSF1Ri treatment did not restore cognitive capacity as in chapter two, there was a trending increase on recognition in the novel place task by the CSF1Ri-CSF1R$^{+/-}$ suggesting a promising effect by CSF1Ri (Fig. 1b,c).

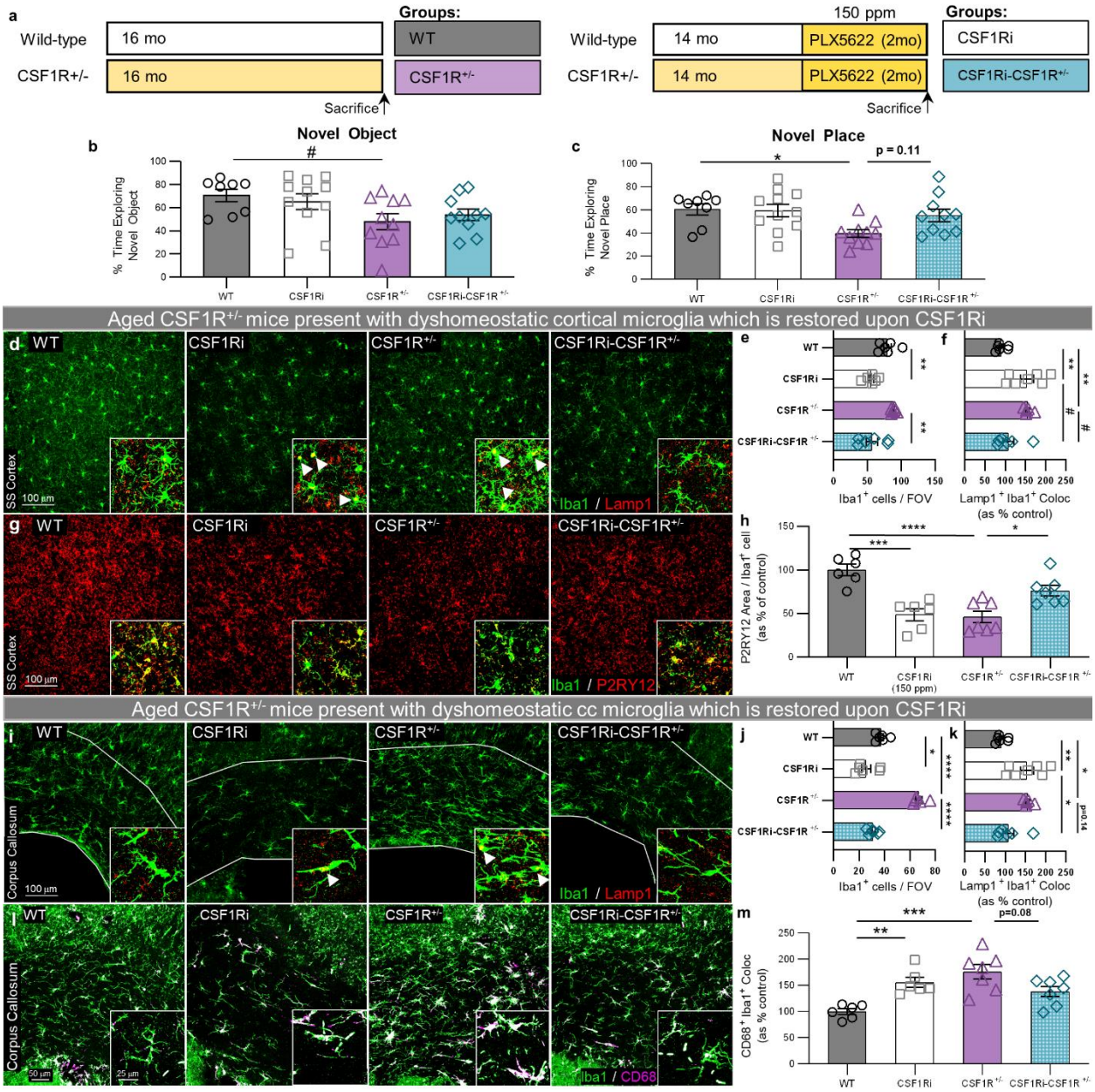

Fig. 3.1: **Aged CSF1R$^{+/-}$ mice display behavioral and phenotypic deviations from WT counterparts of which microglial losses in homeostasis are restored by CSF1Ri (a)** Experimental paradigm: WT and CSF1R$^{+/-}$ mice were treated with 150 ppm PLX5622 for two months beginning at 14 mo. Mice were sacrificed at 16 mo (n=8-10/group) **(b)** CSF1R$^{+/-}$ mice spent significantly less time exploring the novel object compared to WT mice. Treatment with 150 ppm PLX5622 did not rescued performance on this task **(c)** CSF1R$^{+/-}$ mice spent significantly less time exploring an object moved to a novel place compared to WT mice. Treatment with CSF1Ri trended towards rescued performance. **(d)** Representative 20x confocal

image of Iba1 immunostaining in the SS Ctx reveals **(e)** reduced number of Iba1^{+} cells in CSF1Ri treated groups and **(f)** increased microglial immunostaining of Lamp1 which was restored upon CSF1Ri treatment. Intriguingly, CSF1Ri mice showed increased Lamp1 staining that mirrored that seen in CSF1R$^{+/-}$ mice **(g, h)** Representative 20x images of the SS Cortex reveals a marked decrease in microglial P2RY12 immunopositivity in CSF1Ri and CSF1R$^{+/-}$ mice. CSF1Ri of CSF1R$^{+/-}$ mice revealed an increased expression in P2RY12 expression. **(i)** Representative 20x confocal images of cc Iba1 Lamp1 staining reveals **(j)** increased Iba1^{+} cells in CSF1R$^{+/-}$ mice which was normalized in CSF1Ri-CSF1R$^{+/-}$ mice and **(k)** increased Lamp1^{+} Iba1^{+} immunostaining in CSF1Ri and CSF1R$^{+/-}$ mice which was normalized in CSF1Ri-CSF1R$^{+/-}$ mice. Similarly, **(l)** representative 20x imaging of cc Iba1^{+} cells revealed increased CD68 immunopositivity in CSF1Ri and CSF1R$^{+/-}$ mice. CSF1Ri-CSF1R$^{+/-}$ mice showed reduced CD68 immunopositivity. Statistical analysis used a two-way ANOVA with Sidak multiple comparisons correction. Significance * $p< 0.05$; ** $p < 0.01$, *** $p < 0.001$, # $0.05 < p < 0.1$

Aged CSF1R$^{+/-}$ mice display dyshomeostatic microglia can be restored to homeostatic state by sustained low-grade CSF1R inhibition

Given the the trending increases to cognitive faculties, we aimed to clarify whether CSF1Ri treatment managed to restore microglia to a homeostatic status. To this end we immunostained and characterized the Iba1^{+} cell population in the ss ctx and the cc (Fig. 1d-m). Analysis of the brain microglial population in this more advanced cohort of mice revealed that, unlike at 8 months, 16-month-old CSF1R$^{+/-}$ mice did not display an increase in cortical microglial density (Fig. 1d,e). This is not too surprising as in human cases of ALSP microglia densities gradually decline during advanced disease stages (*261*). Once again, we aimed to quantify the expression level of homeostatic markers by microglia and so stained for P2RY12 (Fig. 1g). Quantification of colocalized P2RY12 Iba1 immunostaining revealed similar losses of P2RY12 expression by CSF1Ri and CSF1R$^{+/-}$ as in the previous pre-pathology cohort. Indeed, as before, P2RY12 expression was

increased in CSF1Ri-CSF1R$^{+/-}$ microglia suggesting a restoration of microglial homeostasis.

Examination of the microglia population in the cc revealed marked microgliosis that was ameliorated with CSF1Ri treatment in the CSF1R$^{+/-}$ mice (Fig. 1i,j). Previous studies have observed increased microglial Lamp1^{+} and CD68^{+} immunostaining in dyshomeostatic microglia with enlarged lysosomal vesicles related to CNS white matter pathology induced by increased phagocytosis of myelin (ref: 34433069). To that end, we immunostained for Lamp1 and examined expression in the cortex and cc (Fig. 1d,i) and found increased Lamp1 expression by microglia in both CSF1Ri and CSF1R$^{+/-}$ microglia. In both ctx and cc we observed a trending decrease of Lamp1 expression in CSF1Ri-CSF1R$^{+/-}$. Similarly, immunostaining for CD68 in the cc (Fig. 1l) revealed increased expression of CD68 by CSF1Ri and CSF1R$^{+/-}$ that was trending towards reduction in CSF1Ri-CSF1R$^{+/-}$ mice. Together these data suggest that CSF1Ri treatment still had the capacity to restore functions of homeostatic microglia, albeit to a lesser extent than was achieved with the pre-pathological cohort in chapter two.

Aged CSF1R$^{+/-}$ mice display signs of Corpus Callosum damage which are attenuated upon CSF1Ri

Previous reports on both ALSP patients and CSF1R haploinsufficient mice have shown marked reductions in white matter integrity in the corpus callosum (*16, 218, 225, 262*). Consistent with this, we observed decreased immunostaining of MBP in both the cc (Fig. 2a,b) and the cortex

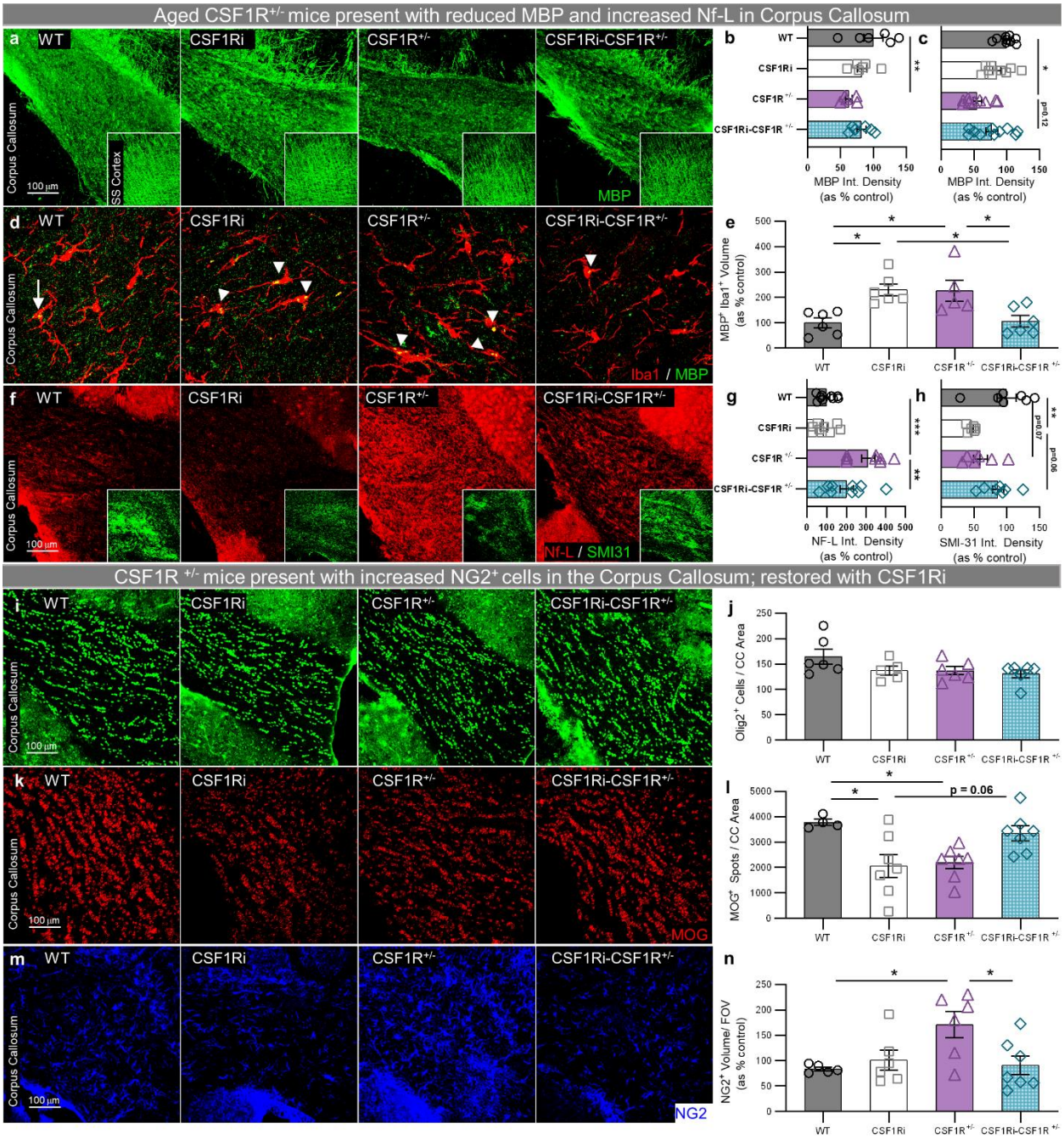

Fig. 3.2: ***CSF1R$^{+/-}$ mice display signs of Corpus Callosum damage which is attenuated upon CSF1Ri***

(a) Representative 20x confocal images of MBP immunostaining in the cc and ctx (insert) show **(b,c)** marked reduction in MBP integrated density of CSF1R$^{+/-}$ mice. **(d)** Representative 63x confocal images of Iba1^{+} MBP^{+} immunostaining revealed **(e)** increased MBP deposits inside Iba1^{+} cells in the cc of CSF1Ri and CSF1R$^{+/-}$ cells which was ameliorated in CSF1Ri-CSF1R$^{+/-}$ microglia. **(f)** Representative 20x images of Nf-L and SMI31 (insert) display **(g)** increased immunofluorescence as measeured by integrated density of cc

Nf-L in CSF1R$^{+/-}$ mice that was partially ameliorated in CSF1Ri-CSF1R$^{+/-}$ mice as well as **(h)** decreased immunostaining of SMI31 in CSF1Ri and CSF1R$^{+/-}$ mice. **(i)** Representative immunofluorescent image of Olig2^{+} cells in the cc showed **(j)** no differences between the groups. **(k)** Representative image of 20x in situ hybridization of MOG RNA revealed **(l)** decreased expression of MOG in CSF1Ri and CSF1R$^{+/-}$ which is trending towards recovery in CSF1Ri-CSF1R$^{+/-}$ mice. **(m)** Representative 20x immunofluorescent images of NG2^{+} cells in the cc of aged mice displayed **(n)** increased amount of NG2^{+} immunostaining in CSF1R$^{+/-}$ mice that was ameliorated with CSF1Ri treatment. Statistical analysis used a two-way ANOVA with Sidak multiple comparisons correction. Significance * $p< 0.05$; ** $p < 0.01$, *** $p < 0.001$, # $0.05 < p < 0.1$

(Fig.2a insert, c). However, CSF1Ri-CSF1R$^{+/-}$ mice showed only marginal recovery in MBP integrated density when compared to CSR1R$^{+/-}$ mice. Recent evidence has implicated microglia in the clearance of myelin debris in several CNS disorders such as MS and progressive multifocal leukoencephalopathy (*184-186*). Given such an ability for myelin control, we next investigated whether CSF1R$^{+/-}$ microglia displayed internalized MBP structures. Indeed, colocalization of Iba1^{+} cells with MBP^{+} immunofluorescence revealed increased colocalization in CSF1Ri and CSF1R$^{+/-}$ groups (Fig. 2d,e) which was normalized in CSF1Ri-CSF1R$^{+/-}$ microglia, suggesting that aged CSF1Ri and CSF1R$^{+/-}$ may have enhanced phagocytic capacity which is mitigated in aged CSF1Ri-CSF1R$^{+/-}$ mice. Given the increasing relevance of neurofilament light chain (Nf-L) as a biomarker for axonal injury we immunostained for Nf-L and noted a marked increase in the intensity of Nf-L in CSF1R$^{+/-}$ mice which was reduced by ~30% in CSF1Ri-CSF1R$^{+/-}$ mice (Fig. 2f,g). Similarly, immunostaining for SMI-31 labeled axons showed reductions in CSF1Ri and CSF1R$^{+/-}$ groups that was ameliorated in the CSF1Ri-CSF1R$^{+/-}$ groups (Fig. 2f (insert),h).

Having seen the burden of white matter pathology in CSF1R$^{+/-}$ mice we next examined whether the oligodendroglial population had similarly been affected by dysregulated CSF1R signaling. To

that end, we immunostained for Olig2, however, we found no differences between the groups with regards to $Olig2^+$ spots throughout the cc (Fig. 2i,j). Intriguingly, RNAscope in-situ hybridization of MOG RNA did reveal a decrease in the amount of MOG^+ RNA in CSF1Ri that mirrored that seen in $CSF1R^{+/-}$ cc. This was recovered in CSF1Ri-$CSF1R^{+/-}$ mice (Fig. 2k,l). Recent studies into spinal cord injuries have found that in response to such lesions, $NG2^+$ cells proliferate(*263*). As such, we immunostained for NG2 and found a marked increase in $NG2^+$ cell density in $CSF1R^{+/-}$ mice compared to their WT counterparts. CSF1Ri-$CSF1R^{+/-}$ mice showed reduced levels of $NG2^+$ immunostaining that was comparable to that found in WT, suggesting that reactivity from these cells to white matter pathology had been assuaged in CSF1Ri-$CSF1R^{+/-}$ mice.

Aged $CSF1R^{+/-}$ mice display signs of ECM dyshomeostasis which are marginally restored upon CSF1Ri

Given the increasing relevance of the ECM in overall CNS health(*264*), as well as prior data from chapter two, we aimed to characterize ECM structural changes in 16 month old $CSF1R^{+/-}$ mice and investigate whether CSF1Ri treatment at this time point could replicate the ameliorative properties seen at 8 months of age. To that end, we immunostained for WFA and Aggrecan and found that 16-month-old $CSF1R^{+/-}$ mice displayed enduring PNN loss that was restored with CSF1Ri (Fig. 3a-d). Reduced PNNs were also evident in CSF1Ri-treated WT mice at 16 months despite no such changes following CSF1Ri at 8 months of age (Fig. 3a-d). Immunostaining for $CS\text{-}56^+$ deposits in the cortex found that $CSF1R^{+/-}$ mice showed dramatically increased CS-56 immunofluorescence CSPGs as before that was normalized in CSF1Ri-$CSF1R^{+/-}$ mice

(Fig. 3e,f). Importantly, these data suggest that, while sustained early intervention with CSF1Ri may be more efficient in preventing the overt CNS damage seen here, treatment during pathological phases still induce beneficial effects to CNS health.

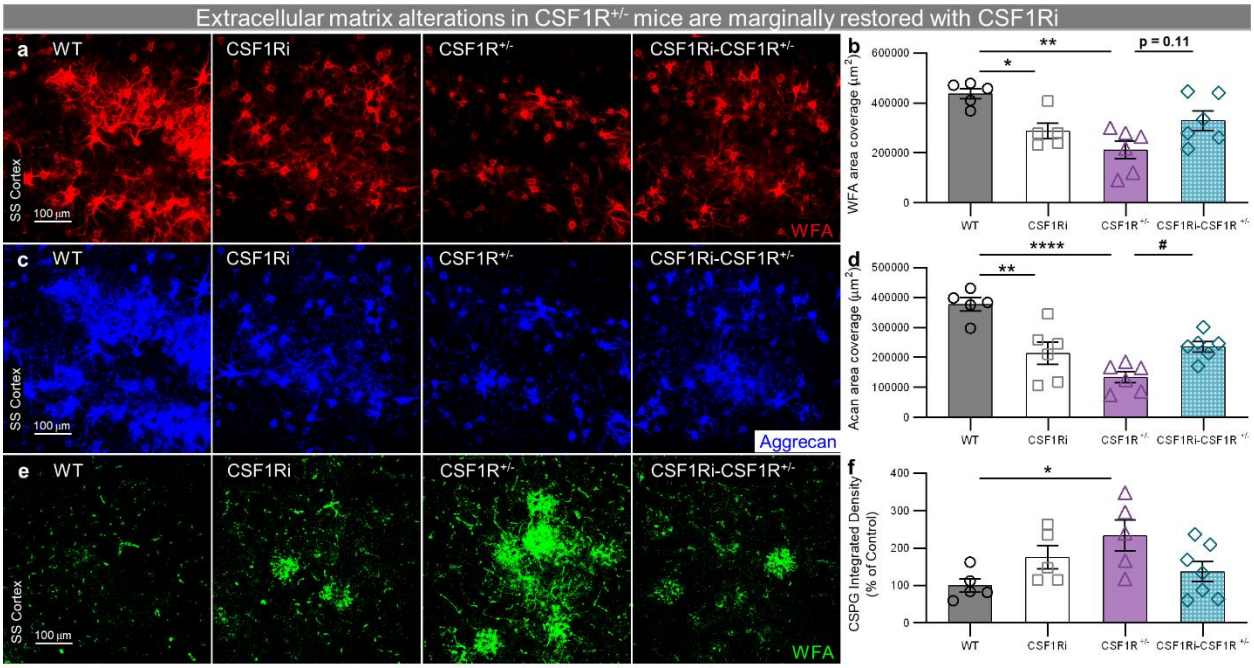

Fig. 3.3: ***CSF1R$^{+/-}$ mice present with diminished perineuronal net density and increased CSPG islands which are modestly restored upon CSF1Ri*** **(a)** Representative 20x confocal image of immunostaining for WFA in aged cohort of mice revealed **(b)** significant reduction in PNN structures in CSF1Ri and CSF1R$^{+/-}$ mice that was trending towards recovery in CSF1Ri-CSF1R$^{+/-}$ mice. **(c)** Representative 20x image of Aggrecan immunofluorescence showed **(d)** similar pattern in Aggrecan expression amongst the groups with CSF1Ri and CSF1R$^{+/-}$ showing reductions in PNNs and trending restoration in CSF1Ri-CSF1R$^{+/-}$ mice. **(e)** Representative 20x confocal image of CS-56 immunostaining revealed **(f)** increased density of DAC structures in CSF1R$^{+/-}$ mice. Statistical analysis used a two-way ANOVA with Sidak multiple comparisons correction. Significance * $p< 0.05$; ** $p < 0.01$, **** $p < 0.0001$, # $0.05 < p < 0.1$

DISCUSSION:

Our previous work had established that CSF1Ri targeting of microglia homeostasis was a valid target for intervention at pre-pathological stages of CSF1R haploinsufficiency induced pathology (i.e. synaptic and PNN downregulation). However, given the rarity of ALSP, human patients with CSF1R genetic mutations are often not diagnosed until symptom onset and pathology has progressed. With that in mind, we designed the experiments in this chapter to address whether CSF1Ri treatment would remain a valid therapeutic approach for the amelioration of pathology associated with ALSP. In line with data from chapter two, we found that $CSF1R^{+/-}$ mice had cognitive deficits as assessed by the NOR and NPR tasks (Fig. 1b,c). CSF1Ri treatment did show promising results with regards to ameliorating these cognitive deficits, however, in 16-month-old $CSF1R^{+/-}$ mice, indeed suggesting that the use of CSF1Ri for treatment of ALSP pathology in advanced stages remains a valid therapeutic approach.

Microglial homeostasis was similarly reintroduced both in the cortex as well as in the corpus callosum (Fig. 1d-m). This notion was emphasized by immunostaining of the homeostatic marker P2RY12, as well as $Iba1^{+}$ $Lamp1^{+}$ colocalized immunostaining. Lamp1 acts as a protein essential for the fusion of phagosomes with lysosomes and their subsequent degradation, here suggesting an enlargement of lysosomal structures by microglial populations in $CSF1R^{+/-}$ mice. Indeed, increased $Lamp1^{+}$ immunostaining in microglia been observed in various models of white matter pathology including mouse models of Frontotemporal Dementia in which microglial lysosomal disfunction contributed heavily towards observed white matter pathology (*265, 266*). Similarly, increased CD68 immunostaining by microglia is often used as a general marker for microglial activation

as its increased expression is related to microglial phagocytic capacity (*267, 268*). Intriguingly, quantification internalized MBP^{+} immunopositive staining in $Iba1^{+}$ cells revealed increased levels of internalized MBP in CSF1Ri and $CSF1R^{+/-}$ mice. This was reduced in CSF1Ri-$CSF1R^{+/-}$ mice to levels that were comparable to the WT controls. These data support the CD68 and Lamp1 immunostaining data as these point toward increased phagocytic capacity by microglia in both investigated regions. Indeed, microglia are active participants in myelin remodeling by way of phagocytic pathways, pathways which could, as hypothesized here, be incurred by dysregulated CSF1R signaling. Further in vitro and in vivo studies should be performed, however, to ascertain the phagocytic capacity of microglia with dysregulated CSF1R signaling. Given the general upregulation in both CD68 and Lamp1 by CSF1R haploinsufficient microglia and subsequent downregulation in CSF1Ri treated $CSF1R^{+/-}$ mice we concluded that CSF1Ri treatment at these late stages remains a viable approach towards reinstating microglial homeostasis.

As white matter degeneration is a significant component of ALSP pathology, we characterized the corpus callosum in our aged cohort of mice. As expected, we found loss of MBP immunostaining that was trending towards recovery in the CSF1Ri-$CSF1R^{+/-}$ mice, again, suggesting that CSF1Ri treatment at these late stages might have some efficacy for improving clinical outcome. Analysis of Nf-L and SMI-31 immunostaining both showed increased axonal damage in $CSF1R^{+/-}$ mice that was mitigated upon CSF1Ri treatment. Nf-L has recently emerged as a clinical biomarker used across a variety of neurodegenerative disorders (*269-272*) as increased levels of Nf-L increase proportionately with levels of axonal damage. In the context of ALSP, human patients with ALSP show similar increased levels of plasma Nf-L (*273*) as those seen in our current

dataset suggesting a replicable and important measure for disease progression monitoring.

Given the intimate relationship between white matter and cells of oligodendrocyte lineage we also analyzed levels of oligodendrocytes here and found no differences in this population as assessed by $Olig2^{+}$ immunostaining. Further characterization of this population is still necessary, however, as OPCs and intermediate stage oligodendrocytes may have been affected. It is interesting to note, however, that the levels of MOG mRNA were vastly reduced in CSF1Ri and $CSF1R^{+/-}$ mice which was restored in CSF1Ri-$CSF1R^{+/-}$ mice. The significance of such altered expression of MOG mRNA necessitates further study but does point towards a non-cell autonomous affect by dyshomeostatic microglia as had been suggested by the bulk RNA-sequencing data in chapter two. Characterization of $NG2^{+}$ cells showed a remarkable increase in NG2 immunostaining in $CSF1R^{+/-}$ mice that was ameliorated upon CSF1Ri treatment. While NG2 cells are still under intense investigation and their roles in CNS homeostasis are still up for debate, this increased number of $NG2^{+}$ cells has been reported by prior studies using different mouse models of white matter damage (*274-276*). Similar studies have found $NG2^{+}$ cells reacting to changes in axonal structure induced by Nf-L knockout studies(*277*) further reinforcing the concept that white matter damage in $CSF1R^{+/-}$ mice can be restored upon CSF1Ri treatment, even at the late stages of pathology. This theme of increased damage was replicated when we characterized the ECM landscape by way of immunostaining for PNNs and DACs. Thus, dyshomeostatic microglia in chapter three similarly showed a capacity to enact profound damage to the CNS at large. Importantly, targeting microglia specifically via CSF1Ri treatment remained a valid therapeutic approach towards

restoring microglial homeostasis and ameliorating downstream pathology. It is important to note, however, that extended treatment at earlier timepoints may allow for improved efficacy in treatment of ALSP-like pathology.

DISSERTATION CONCLUDING REMARKS

Currently, there are no disease-modifying therapies for ALSP. The lack of such treatment options stems from the relatively recent identification of CSF1R mutations as the genetic etiology of ALSP. More importantly, the variable phenotypic presentation of pathology in patients complicates the formation of a collective set of criteria by which ALSP can be identified/treated. As such, rigorous clinical trial methodologies are still evolving. Current treatments for symptoms of ALSP temporarily relieve motor and behavioral ailments as the disorder progresses with the sole intent of maintaining quality of life. Patients with ALSP tend to fail to respond to immunomodulators, however, the effectiveness of pre-symptomatic immunosuppression (*278*) and allogeneic HSCT (*279, 280*) have shown potential efficacy in case reports but still require testing in controlled clinical trials. Although data on HSCT in ALSP are few, given the risks and associated complications of HSCT for the treatment of leukodystrophies, the early detection and therapy of this disorder is highly recommended.

CSF1R is expressed primarily by microglia in the brain (*213*) and mutant CSF1R proteins in ALSP present with suboptimal receptor function that leads to dysfunctional cells with abnormal distribution and physiology (*261*). Microglial replacement thus represents a potential therapeutic avenue for ALSP and so has been the subject of recent research. Microglia are the resident innate immune cells that monitor and maintain the homeostatic environment of the CNS. Aside from their roles in controlling neuroinflammation, microglia respond to various types of cellular signals and regulate responses for the repair and remyelination of white matter tracts, phagocytosis of dead cells, and are largely involved

in the maintenance of synapses and ECM structures. Such key roles in CNS upkeep highlights a potential role for impaired microglia as primary drivers of pathology underlying CSF1R-related leukoencephalopathies.

For my dissertation I sought to explore how dysregulated CSF1R signaling could affect the microglial pool in the CNS and the downstream effects of such altered signaling. To that end, I created a mouse model that excises one *Csf1r* allele under the direction of the *Cx3cr1* promoter. In doing so, I was able to specifically target microglial cells in the CNS. This mouse model was created to emulate CSF1R haploinsufficient human cases of ALSP. CSF1R haploinsufficiency was induced at a post-developmental timepoint, in doing so bypassing any developmental influences of CSF1R dysregulated expression. Data from this initial study identified dysregulated CSF1R signaling as sufficient to induce decreased expression of the homeostatic markers P2RY12 and TMEM119 in microglia, suggesting a loss of homeostatic function in the inducible $CSF1R^{+/-}$ mice.

Having observed a conspicuous downregulation in microglial homeostasis prompted an investigation into the downstream effects of this altered microglial pool on CNS health. Given recent evidence of microglia involvement in synaptic and ECM maintenance under homeostatic conditions, I hypothesized that dysregulated microglia would alter the tetrapartite synaptic landscape. Indeed, inducing a dysregulated microglial state led to a downregulation of presynaptic surrogates as well as PNN structures. The exact mechanism by which such events occur remain elusive. However, investigations into myeloid cell biology do suggest that microglia are equipped with the necessary tools to exert similar controlled effects under homeostatic conditions, whether it be through phagocytosis or the secretion of matrix remodeling enzymes such as MMP9 or MMP14,

and so it is possible that these mechanisms are also used in an unregulated fashion when microglia are dysregulated. Importantly, the observed effects on non-microglial CNS structures were driven solely by microglial dyshomeostasis. Unlike other neurodegenerative disorders where microglia react to protein aggregates, for example, our system clearly delineates the extent to which microglia have the capacity to induce synapse and ECM degeneration independent of external pathology.

Extending these studies, I turned to a global CSF1R haploinsufficient system wherein we pharmacologically depleted the microglial population with a CSF1R inhibitor to investigate whether elimination of dyshomeostatic microglia could restore synaptic and ECM structures. The elimination of dyshomeostatic microglia lead to recovery of both, however, given that elimination of the microglial population is not a clinically feasible option we turned to a microglial modulating approach with a lower dosage of the CSF1R inhibitor. Under this paradigm we treated WT and $CSF1R^{+/-}$ mice for 2 months with the CSF1R inhibitor at which point mice were sacrificed at 8 months of age, before any canonical ALSP pathology has been reported. With the treatment of this modulating dose, we noted an astounding recovery of homeostatic state in $CSF1R^{+/-}$ microglia that resulted in the restoration of synaptic and ECM homeostasis, as well as behavioral output on the Novel Object recognition task suggesting targeting of microglia in CSF1R haploinsufficient organisms as a viable therapeutic, in agreement with another study which restored microglia homeostasis via genetic ablation of *Csf2* which was highly upregulated upon CSF1R haploinsufficiency in both mice and humans.

Intriguingly, WT mice treated with the modulating dose of CSF1R inhibitor showed similar decreases in P2RY12 and TMEM119 expression, which resulted in decreased levels of

presynaptic puncta that mirrored losses seen in genetic CSF1R$^{+/-}$ haploinsufficiency. Moreover, analysis of bulk cortical RNA revealed striking similarities between pharmacological and genetic CSF1R dysregulated signaling raising an important point about the importance of CSF1R signaling in maintaining microglia, and consequently CNS, homeostasis. Contrary to data in which the loss of microglia densities is suggested to lead to ALSP pathology, our data argue that dysregulated CSF1R signaling results in a toxic gain of function status by which microglia begin to exert their pathological effects on the CNS. This idea is supported by my depletion study as well as prior data from our lab showing that extended depletion of microglia in WT mice (up to 6 months of depletion) does not induce ALSP like pathology.

Because ALSP is an extremely rare disorder and correct diagnosis is often achieved once disease pathology is already advanced, it is important to investigate whether CSF1R inhibitor treatment would remain a viable therapeutic avenue. Chapter three of this dissertation thus focused on studying CSF1R haploinsufficient mice at more advanced stages of pathology. To this end, I aged mice to 14 months at which point they underwent similar 2-month pharmacological treatment with the microglia modulating dose of the CSF1R inhibitor. Here, microglia homeostasis was once again restored in CSF1Ri-CSF1R$^{+/-}$ mice as evident by increased P2RY12 expression and reduced CD68 and Lamp1 microglial colocalization. This, however, was not sufficient to completely restore MBP levels in the cortex or corpus callosum. Despite this lack in MBP restoration, Nf-L, SMI-31, Synaptophysin and PNN levels were modestly restored, albeit not to WT levels. This line of evidence suggests that pharmacological treatment at more advanced stages does have the potential to serve as a valid therapeutic, but perhaps the treatment duration

needs to be reconfigured. Given the extent of pathology found in these advanced stages of disease there is only so much that can be restored, once again arguing for the early detection and therapy of patients suffering from ALSP.

Unexpectedly, aged CSF1Ri microglia differed from their younger counterparts in that aged CSF1Ri microglia appeared more detrimental to CNS health. Treatment with CSF1Ri at 8 months did not result in losses of MBP, PNNs nor SMI-31, for example, that was found in the aged cohort. This effect of aging on microglia necessitates further exploration, however, as treatment of non-CSF1R related degenerative disorders are currently undergoing clinical trials. Ultimately, these studies highlight the significance of properly functioning microglia and point towards their critical role for CNS health. Importantly, the restoration of homeostasis through pharmacological means is possible, at least in mice, suggesting the possibility for less invasive treatment options for a clinical population that is already vulnerable. With hope, studies such as those presented in this thesis will accelerate the development of disease-modifying therapies for ALSP that target and modulate microglial function.

References

1. Y. Kondo, A. Matsushima, S. Nagasaki, K. Nakamura, Y. Sekijima, K. Yoshida, Factors predictive of the presence of a CSF1R mutation in patients with leukoencephalopathy. *Eur J Neurol*, (2019).
2. T. Konno, T. Miura, A. M. Harriott, N. Mezaki, E. S. Edwards, R. Rademakers, O. A. Ross, J. F. Meschia, T. Ikeuchi, Z. K. Wszolek, Partial loss of function of colony-stimulating factor 1 receptor in a patient with white matter abnormalities. *Eur J Neurol* **25**, 875-881 (2018).
3. K. Oyanagi, M. Kinoshita, E. Suzuki-Kouyama, T. Inoue, A. Nakahara, M. Tokiwai, N. Arai, J. I. Satoh, N. Aoki, K. Jinnai, I. Yazawa, K. Arai, K. Ishihara, M. Kawamura, K. Ishizawa, K. Hasegawa, S. Yagisita, N. Amano, K. Yoshida, S. Terada, M. Yoshida, H. Akiyama, Y. Mitsuyama, S. I. Ikeda, Adult onset leukoencephalopathy with axonal spheroids and pigmented glia (ALSP) and Nasu-Hakola disease: lesion staging and dynamic changes of axons and microglial subsets. *Brain Pathol* **27**, 748-769 (2017).
4. C. Sundal, Z. K. Wszolek, in *GeneReviews((R)),* M. P. Adam *et al.*, Eds. (Seattle (WA), 1993).
5. A. M. Nicholson, M. C. Baker, N. A. Finch, N. J. Rutherford, C. Wider, N. R. Graff-Radford, P. T. Nelson, H. B. Clark, Z. K. Wszolek, D. W. Dickson, D. S. Knopman, R. Rademakers, CSF1R mutations link POLD and HDLS as a single disease entity. *Neurology* **80**, 1033-1040 (2013).
6. R. Rademakers, M. Baker, A. M. Nicholson, N. J. Rutherford, N. Finch, A. Soto-Ortolaza, J. Lash, C. Wider, A. Wojtas, M. DeJesus-Hernandez, J. Adamson, N. Kouri, C. Sundal, E. A. Shuster, J. Aasly, J. MacKenzie, S. Roeber, H. A. Kretzschmar, B. F. Boeve, D. S. Knopman, R. C. Petersen, N. J. Cairns, B. Ghetti, S. Spina, J. Garbern, A. C. Tselis, R. Uitti, P. Das, J. A. Van Gerpen, J. F. Meschia, S. Levy, D. F. Broderick, N. Graff-Radford, O. A. Ross, B. B. Miller, R. H. Swerdlow, D. W. Dickson, Z. K. Wszolek, Mutations in the colony stimulating factor 1 receptor (CSF1R) gene cause hereditary diffuse leukoencephalopathy with spheroids. *Nat Genet* **44**, 200-205 (2011).
7. S. Hoffmann, J. Murrell, L. Harms, K. Miller, A. Meisel, T. Brosch, M. Scheel, B. Ghetti, H. H. Goebel, W. Stenzel, Enlarging the nosological spectrum of hereditary diffuse leukoencephalopathy with axonal spheroids (HDLS). *Brain Pathol* **24**, 452-458 (2014).
8. C. Wider, Z. K. Wszolek, Hereditary diffuse leukoencephalopathy with axonal spheroids: more than just a rare disease. *Neurology* **82**, 102-103 (2014).
9. D. S. Lynch, Z. Jaunmuktane, U. M. Sheerin, R. Phadke, S. Brandner, I. Milonas, A. Dean, N. Bajaj, N. McNicholas, D. Costello, S. Cronin, C. McGuigan, M. Rossor, N. Fox, E. Murphy, J. Chataway, H. Houlden, Hereditary leukoencephalopathy with axonal spheroids: a spectrum of phenotypes from CNS vasculitis to parkinsonism in an adult onset leukodystrophy series. *J Neurol Neurosurg Psychiatry* **87**, 512-519 (2016).
10. A. Griciuc, A. Serrano-Pozo, A. R. Parrado, A. N. Lesinski, C. N. Asselin, K. Mullin, B. Hooli, S. H. Choi, B. T. Hyman, R. E. Tanzi, Alzheimer's disease risk gene CD33 inhibits microglial uptake of amyloid beta. *Neuron* **78**, 631-643 (2013).
11. R. J. Guerreiro, E. Lohmann, J. M. Bras, J. R. Gibbs, J. D. Rohrer, N. Gurunlian, B. Dursun, B. Bilgic, H. Hanagasi, H. Gurvit, M. Emre, A. Singleton, J. Hardy, Using exome sequencing to reveal mutations in TREM2 presenting as a frontotemporal dementia-like syndrome without bone involvement. *JAMA Neurol* **70**, 78-84 (2013).
12. P. Hollingworth, D. Harold, R. Sims, A. Gerrish, J. C. Lambert, M. M. Carrasquillo, R. Abraham, M. L. Hamshere, J. S. Pahwa, V. Moskvina, K. Dowzell, N. Jones, A. Stretton, C. Thomas, A. Richards, D. Ivanov, C. Widdowson, J. Chapman, S. Lovestone, J. Powell, P. Proitsi, M. K. Lupton, C. Brayne, D. C. Rubinsztein, M. Gill, B. Lawlor, A. Lynch, K. S. Brown, P. A. Passmore, D. Craig, B. McGuinness, S. Todd, C. Holmes, D. Mann, A. D. Smith, H. Beaumont, D. Warden, G. Wilcock, S. Love, P. G. Kehoe, N. M. Hooper, E. R. Vardy, J. Hardy, S. Mead, N. C. Fox, M. Rossor, J. Collinge, W. Maier, F.

Jessen, E. Ruther, B. Schurmann, R. Heun, H. Kolsch, H. van den Bussche, I. Heuser, J. Kornhuber, J. Wiltfang, M. Dichgans, L. Frolich, H. Hampel, J. Gallacher, M. Hull, D. Rujescu, I. Giegling, A. M. Goate, J. S. Kauwe, C. Cruchaga, P. Nowotny, J. C. Morris, K. Mayo, K. Sleegers, K. Bettens, S. Engelborghs, P. P. De Deyn, C. Van Broeckhoven, G. Livingston, N. J. Bass, H. Gurling, A. McQuillin, R. Gwilliam, P. Deloukas, A. Al-Chalabi, C. E. Shaw, M. Tsolaki, A. B. Singleton, R. Guerreiro, T. W. Muhleisen, M. M. Nothen, S. Moebus, K. H. Jockel, N. Klopp, H. E. Wichmann, V. S. Pankratz, S. B. Sando, J. O. Aasly, M. Barcikowska, Z. K. Wszolek, D. W. Dickson, N. R. Graff-Radford, R. C. Petersen, C. M. van Duijn, M. M. Breteler, M. A. Ikram, A. L. DeStefano, A. L. Fitzpatrick, O. Lopez, L. J. Launer, S. Seshadri, C. Berr, D. Campion, J. Epelbaum, J. F. Dartigues, C. Tzourio, A. Alperovitch, M. Lathrop, T. M. Feulner, P. Friedrich, C. Riehle, M. Krawczak, S. Schreiber, M. Mayhaus, S. Nicolhaus, S. Wagenpfeil, S. Steinberg, H. Stefansson, K. Stefansson, J. Snaedal, S. Bjornsson, P. V. Jonsson, V. Chouraki, B. Genier-Boley, M. Hiltunen, H. Soininen, O. Combarros, D. Zelenika, M. Delepine, M. J. Bullido, F. Pasquier, I. Mateo, A. Frank-Garcia, E. Porcellini, O. Hanon, E. Coto, V. Alvarez, P. Bosco, G. Siciliano, M. Mancuso, F. Panza, V. Solfrizzi, B. Nacmias, S. Sorbi, P. Bossu, P. Piccardi, B. Arosio, G. Annoni, D. Seripa, A. Pilotto, E. Scarpini, D. Galimberti, A. Brice, D. Hannequin, F. Licastro, L. Jones, P. A. Holmans, T. Jonsson, M. Riemenschneider, K. Morgan, S. G. Younkin, M. J. Owen, M. O'Donovan, P. Amouyel, J. Williams, Common variants at ABCA7, MS4A6A/MS4A4E, EPHA1, CD33 and CD2AP are associated with Alzheimer's disease. *Nat Genet* **43**, 429-435 (2011).

13. M. E. Meuwissen, R. Schot, S. Buta, G. Oudesluijs, S. Tinschert, S. D. Speer, Z. Li, L. van Unen, D. Heijsman, T. Goldmann, M. H. Lequin, J. M. Kros, W. Stam, M. Hermann, R. Willemsen, R. W. Brouwer, I. W. F. Van, M. Martin-Fernandez, I. de Coo, J. Dudink, F. A. de Vries, A. Bertoli Avella, M. Prinz, Y. J. Crow, F. W. Verheijen, S. Pellegrini, D. Bogunovic, G. M. Mancini, Human USP18 deficiency underlies type 1 interferonopathy leading to severe pseudo-TORCH syndrome. *J Exp Med* **213**, 1163-1174 (2016).

14. A. C. Naj, G. Jun, G. W. Beecham, L. S. Wang, B. N. Vardarajan, J. Buros, P. J. Gallins, J. D. Buxbaum, G. P. Jarvik, P. K. Crane, E. B. Larson, T. D. Bird, B. F. Boeve, N. R. Graff-Radford, P. L. De Jager, D. Evans, J. A. Schneider, M. M. Carrasquillo, N. Ertekin-Taner, S. G. Younkin, C. Cruchaga, J. S. Kauwe, P. Nowotny, P. Kramer, J. Hardy, M. J. Huentelman, A. J. Myers, M. M. Barmada, F. Y. Demirci, C. T. Baldwin, R. C. Green, E. Rogaeva, P. St George-Hyslop, S. E. Arnold, R. Barber, T. Beach, E. H. Bigio, J. D. Bowen, A. Boxer, J. R. Burke, N. J. Cairns, C. S. Carlson, R. M. Carney, S. L. Carroll, H. C. Chui, D. G. Clark, J. Corneveaux, C. W. Cotman, J. L. Cummings, C. DeCarli, S. T. DeKosky, R. Diaz-Arrastia, M. Dick, D. W. Dickson, W. G. Ellis, K. M. Faber, K. B. Fallon, M. R. Farlow, S. Ferris, M. P. Frosch, D. R. Galasko, M. Ganguli, M. Gearing, D. H. Geschwind, B. Ghetti, J. R. Gilbert, S. Gilman, B. Giordani, J. D. Glass, J. H. Growdon, R. L. Hamilton, L. E. Harrell, E. Head, L. S. Honig, C. M. Hulette, B. T. Hyman, G. A. Jicha, L. W. Jin, N. Johnson, J. Karlawish, A. Karydas, J. A. Kaye, R. Kim, E. H. Koo, N. W. Kowall, J. J. Lah, A. I. Levey, A. P. Lieberman, O. L. Lopez, W. J. Mack, D. C. Marson, F. Martiniuk, D. C. Mash, E. Masliah, W. C. McCormick, S. M. McCurry, A. N. McDavid, A. C. McKee, M. Mesulam, B. L. Miller, C. A. Miller, J. W. Miller, J. E. Parisi, D. P. Perl, E. Peskind, R. C. Petersen, W. W. Poon, J. F. Quinn, R. A. Rajbhandary, M. Raskind, B. Reisberg, J. M. Ringman, E. D. Roberson, R. N. Rosenberg, M. Sano, L. S. Schneider, W. Seeley, M. L. Shelanski, M. A. Slifer, C. D. Smith, J. A. Sonnen, S. Spina, R. A. Stern, R. E. Tanzi, J. Q. Trojanowski, J. C. Troncoso, V. M. Van Deerlin, H. V. Vinters, J. P. Vonsattel, S. Weintraub, K. A. Welsh-Bohmer, J. Williamson, R. L. Woltjer, L. B. Cantwell, B. A. Dombroski, D. Beekly, K. L. Lunetta, E. R. Martin, M. I. Kamboh, A. J. Saykin, E. M. Reiman, D. A. Bennett, J. C. Morris, T. J. Montine, A. M. Goate, D. Blacker, D. W. Tsuang, H. Hakonarson, W. A. Kukull, T. M. Foroud, J. L. Haines, R. Mayeux, M. A. Pericak-Vance, L. A. Farrer, G. D. Schellenberg, Common variants at MS4A4/MS4A6E, CD2AP, CD33 and EPHA1 are associated with late-onset Alzheimer's disease. *Nat Genet* **43**, 436-441 (2011).

15. M. Hiyoshi, M. Hashimoto, M. Yukihara, F. Bhuyan, S. Suzu, M-CSF receptor mutations in hereditary diffuse leukoencephalopathy with spheroids impair not only kinase activity but also surface expression. *Biochem Biophys Res Commun* **440**, 589-593 (2013).
16. V. Chitu, S. Gokhan, M. Gulinello, C. A. Branch, M. Patil, R. Basu, C. Stoddart, M. F. Mehler, E. R. Stanley, Phenotypic characterization of a Csf1r haploinsufficient mouse model of adult-onset leukodystrophy with axonal spheroids and pigmented glia (ALSP). *Neurobiol Dis* **74**, 219-228 (2015).
17. B. A. Friedman, K. Srinivasan, G. Ayalon, W. J. Meilandt, H. Lin, M. A. Huntley, Y. Cao, S. H. Lee, P. C. G. Haddick, H. Ngu, Z. Modrusan, J. L. Larson, J. S. Kaminker, M. P. van der Brug, D. V. Hansen, Diverse Brain Myeloid Expression Profiles Reveal Distinct Microglial Activation States and Aspects of Alzheimer's Disease Not Evident in Mouse Models. *Cell Rep* **22**, 832-847 (2018).
18. H. Keren-Shaul, A. Spinrad, A. Weiner, O. Matcovitch-Natan, R. Dvir-Szternfeld, T. K. Ulland, E. David, K. Baruch, D. Lara-Astaiso, B. Toth, S. Itzkovitz, M. Colonna, M. Schwartz, I. Amit, A Unique Microglia Type Associated with Restricting Development of Alzheimer's Disease. *Cell* **169**, 1276-1290.e1217 (2017).
19. E. Croisier, L. B. Moran, D. T. Dexter, R. K. Pearce, M. B. Graeber, Microglial inflammation in the parkinsonian substantia nigra: relationship to alpha-synuclein deposition. *J Neuroinflammation* **2**, 14 (2005).
20. A. D. Bachstetter, L. J. Van Eldik, F. A. Schmitt, J. H. Neltner, E. T. Ighodaro, S. J. Webster, E. Patel, E. L. Abner, R. J. Kryscio, P. T. Nelson, Disease-related microglia heterogeneity in the hippocampus of Alzheimer's disease, dementia with Lewy bodies, and hippocampal sclerosis of aging. *Acta Neuropathol Commun* **3**, 32 (2015).
21. S. Jimenez, D. Baglietto-Vargas, C. Caballero, I. Moreno-Gonzalez, M. Torres, R. Sanchez-Varo, D. Ruano, M. Vizuete, A. Gutierrez, J. Vitorica, Inflammatory response in the hippocampus of PS1M146L/APP751SL mouse model of Alzheimer's disease: age-dependent switch in the microglial phenotype from alternative to classic. *J Neurosci* **28**, 11650-11661 (2008).
22. P. Pey, R. K. Pearce, M. E. Kalaitzakis, W. S. Griffin, S. M. Gentleman, Phenotypic profile of alternative activation marker CD163 is different in Alzheimer's and Parkinson's disease. *Acta Neuropathol Commun* **2**, 21 (2014).
23. J. Paloneva, M. Kestila, J. Wu, A. Salminen, T. Bohling, V. Ruotsalainen, P. Hakola, A. B. Bakker, J. H. Phillips, P. Pekkarinen, L. L. Lanier, T. Timonen, L. Peltonen, Loss-of-function mutations in TYROBP (DAP12) result in a presenile dementia with bone cysts. *Nat Genet* **25**, 357-361 (2000).
24. K. Takahashi, C. D. Rochford, H. Neumann, Clearance of apoptotic neurons without inflammation by microglial triggering receptor expressed on myeloid cells-2. *J Exp Med* **201**, 647-657 (2005).
25. M. M. Bianchin, H. M. Capella, D. L. Chaves, M. Steindel, E. C. Grisard, G. G. Ganev, J. P. da Silva Junior, S. Neto Evaldo, M. A. Poffo, R. Walz, C. G. Carlotti Junior, A. C. Sakamoto, Nasu-Hakola disease (polycystic lipomembranous osteodysplasia with sclerosing leukoencephalopathy--PLOSL): a dementia associated with bone cystic lesions. From clinical to genetic and molecular aspects. *Cell Mol Neurobiol* **24**, 1-24 (2004).
26. E. Chouery, V. Delague, A. Bergougnoux, S. Koussa, J. L. Serre, A. Megarbane, Mutations in TREM2 lead to pure early-onset dementia without bone cysts. *Hum Mutat* **29**, E194-204 (2008).
27. J. Paloneva, J. Mandelin, A. Kiialainen, T. Bohling, J. Prudlo, P. Hakola, M. Haltia, Y. T. Konttinen, L. Peltonen, DAP12/TREM2 deficiency results in impaired osteoclast differentiation and osteoporotic features. *J Exp Med* **198**, 669-675 (2003).
28. P. Garcia-Reitboeck, A. Phillips, T. M. Piers, C. Villegas-Llerena, M. Butler, A. Mallach, C. Rodrigues, C. E. Arber, A. Heslegrave, H. Zetterberg, H. Neumann, S. Neame, H. Houlden, J. Hardy, J. M. Pocock, Human Induced Pluripotent Stem Cell-Derived Microglia-Like Cells Harboring TREM2 Missense Mutations Show Specific Deficits in Phagocytosis. *Cell Rep* **24**, 2300-2311 (2018).

29. C. L. Hsieh, M. Koike, S. C. Spusta, E. C. Niemi, M. Yenari, M. C. Nakamura, W. E. Seaman, A role for TREM2 ligands in the phagocytosis of apoptotic neuronal cells by microglia. *J Neurochem* **109**, 1144-1156 (2009).
30. R. Gawish, R. Martins, B. Bohm, T. Wimberger, O. Sharif, K. Lakovits, M. Schmidt, S. Knapp, Triggering receptor expressed on myeloid cells-2 fine-tunes inflammatory responses in murine Gram-negative sepsis. *Faseb j* **29**, 1247-1257 (2015).
31. G. Kleinberger, Y. Yamanishi, M. Suarez-Calvet, E. Czirr, E. Lohmann, E. Cuyvers, H. Struyfs, N. Pettkus, A. Wenninger-Weinzierl, F. Mazaheri, S. Tahirovic, A. Lleo, D. Alcolea, J. Fortea, M. Willem, S. Lammich, J. L. Molinuevo, R. Sanchez-Valle, A. Antonell, A. Ramirez, M. T. Heneka, K. Sleegers, J. van der Zee, J. J. Martin, S. Engelborghs, A. Demirtas-Tatlidede, H. Zetterberg, C. Van Broeckhoven, H. Gurvit, T. Wyss-Coray, J. Hardy, M. Colonna, C. Haass, TREM2 mutations implicated in neurodegeneration impair cell surface transport and phagocytosis. *Sci Transl Med* **6**, 243ra286 (2014).
32. T. Jiang, L. Tan, X. C. Zhu, Q. Q. Zhang, L. Cao, M. S. Tan, L. Z. Gu, H. F. Wang, Z. Z. Ding, Y. D. Zhang, J. T. Yu, Upregulation of TREM2 ameliorates neuropathology and rescues spatial cognitive impairment in a transgenic mouse model of Alzheimer's disease. *Neuropsychopharmacology* **39**, 2949-2962 (2014).
33. J. A. Hamerman, N. K. Tchao, C. A. Lowell, L. L. Lanier, Enhanced Toll-like receptor responses in the absence of signaling adaptor DAP12. *Nat Immunol* **6**, 579-586 (2005).
34. H. Ito, J. A. Hamerman, TREM-2, triggering receptor expressed on myeloid cell-2, negatively regulates TLR responses in dendritic cells. *Eur J Immunol* **42**, 176-185 (2012).
35. Y. Wang, M. Cella, K. Mallinson, J. D. Ulrich, K. L. Young, M. L. Robinette, S. Gilfillan, G. M. Krishnan, S. Sudhakar, B. H. Zinselmeyer, D. M. Holtzman, J. R. Cirrito, M. Colonna, TREM2 lipid sensing sustains the microglial response in an Alzheimer's disease model. *Cell* **160**, 1061-1071 (2015).
36. L. Zhong, X. F. Chen, Z. L. Zhang, Z. Wang, X. Z. Shi, K. Xu, Y. W. Zhang, H. Xu, G. Bu, DAP12 Stabilizes the C-terminal Fragment of the Triggering Receptor Expressed on Myeloid Cells-2 (TREM2) and Protects against LPS-induced Pro-inflammatory Response. *J Biol Chem* **290**, 15866-15877 (2015).
37. R. Faccio, D. V. Novack, A. Zallone, F. P. Ross, S. L. Teitelbaum, Dynamic changes in the osteoclast cytoskeleton in response to growth factors and cell attachment are controlled by beta3 integrin. *J Cell Biol* **162**, 499-509 (2003).
38. D. W. McVicar, G. Trinchieri, CSF-1R, DAP12 and beta-catenin: a menage a trois. *Nat Immunol* **10**, 681-683 (2009).
39. K. Otero, I. R. Turnbull, P. L. Poliani, W. Vermi, E. Cerutti, T. Aoshi, I. Tassi, T. Takai, S. L. Stanley, M. Miller, A. S. Shaw, M. Colonna, Macrophage colony-stimulating factor induces the proliferation and survival of macrophages via a pathway involving DAP12 and beta-catenin. *Nat Immunol* **10**, 734-743 (2009).
40. W. Zou, J. L. Reeve, Y. Liu, S. L. Teitelbaum, F. P. Ross, DAP12 couples c-Fms activation to the osteoclast cytoskeleton by recruitment of Syk. *Mol Cell* **31**, 422-431 (2008).
41. R. Akiyoshi, H. Wake, D. Kato, H. Horiuchi, R. Ono, A. Ikegami, K. Haruwaka, T. Omori, Y. Tachibana, A. J. Moorhouse, J. Nabekura, Microglia Enhance Synapse Activity to Promote Local Network Synchronization. *eNeuro* **5**, (2018).
42. Z. Chen, B. D. Trapp, Microglia and neuroprotection. *J Neurochem* **136 Suppl 1**, 10-17 (2016).
43. M. E. Choudhury, K. Miyanishi, H. Takeda, A. Islam, N. Matsuoka, M. Kubo, S. Matsumoto, T. Kunieda, M. Nomoto, H. Yano, J. Tanaka, Phagocytic elimination of synapses by microglia during sleep. *Glia*, (2019).
44. E. M. York, L. P. Bernier, B. A. MacVicar, Microglial modulation of neuronal activity in the healthy brain. *Dev Neurobiol* **78**, 593-603 (2018).

45. I. W. Nasr, Y. Chun, S. Kannan, Neuroimmune responses in the developing brain following traumatic brain injury. *Exp Neurol* **320**, 112957 (2019).
46. J. Ye, Z. Jiang, X. Chen, M. Liu, J. Li, N. Liu, The role of autophagy in pro-inflammatory responses of microglia activation via mitochondrial reactive oxygen species in vitro. *J Neurochem* **142**, 215-230 (2017).
47. K. E. Andreou, M. S. Soto, D. Allen, V. Economopoulos, A. de Bernardi, J. R. Larkin, N. R. Sibson, Anti-inflammatory Microglia/Macrophages As a Potential Therapeutic Target in Brain Metastasis. *Front Oncol* **7**, 251 (2017).
48. D. Lobo-Silva, G. M. Carriche, A. G. Castro, S. Roque, M. Saraiva, Interferon-beta regulates the production of IL-10 by toll-like receptor-activated microglia. *Glia* **65**, 1439-1451 (2017).
49. T. Zoller, A. Schneider, C. Kleimeyer, T. Masuda, P. S. Potru, D. Pfeifer, T. Blank, M. Prinz, B. Spittau, Silencing of TGFbeta signalling in microglia results in impaired homeostasis. *Nat Commun* **9**, 4011 (2018).
50. D. R. Green, T. H. Oguin, J. Martinez, The clearance of dying cells: table for two. *Cell Death Differ* **23**, 915-926 (2016).
51. R. Nau, S. Ribes, M. Djukic, H. Eiffert, Strategies to increase the activity of microglia as efficient protectors of the brain against infections. *Front Cell Neurosci* **8**, 138 (2014).
52. S. A. Wolf, H. W. Boddeke, H. Kettenmann, Microglia in Physiology and Disease. *Annu Rev Physiol* **79**, 619-643 (2017).
53. J. R. Appel, S. Ye, F. Tang, D. Sun, H. Zhang, L. Mei, W. C. Xiong, Increased Microglial Activity, Impaired Adult Hippocampal Neurogenesis, and Depressive-like Behavior in Microglial VPS35-Depleted Mice. *J Neurosci* **38**, 5949-5968 (2018).
54. G. C. Brown, J. J. Neher, Microglial phagocytosis of live neurons. *Nat Rev Neurosci* **15**, 209-216 (2014).
55. D. M. Underhill, H. S. Goodridge, Information processing during phagocytosis. *Nat Rev Immunol* **12**, 492-502 (2012).
56. D. Doens, P. L. Fernandez, Microglia receptors and their implications in the response to amyloid beta for Alzheimer's disease pathogenesis. *J Neuroinflammation* **11**, 48 (2014).
57. E. K. Lehrman, D. K. Wilton, E. Y. Litvina, C. A. Welsh, S. T. Chang, A. Frouin, A. J. Walker, M. D. Heller, H. Umemori, C. Chen, B. Stevens, CD47 Protects Synapses from Excess Microglia-Mediated Pruning during Development. *Neuron* **100**, 120-134.e126 (2018).
58. K. M. Lucin, C. E. O'Brien, G. Bieri, E. Czirr, K. I. Mosher, R. J. Abbey, D. F. Mastroeni, J. Rogers, B. Spencer, E. Masliah, T. Wyss-Coray, Microglial beclin 1 regulates retromer trafficking and phagocytosis and is impaired in Alzheimer's disease. *Neuron* **79**, 873-886 (2013).
59. S. Rayaprolu, B. Mullen, M. Baker, T. Lynch, E. Finger, W. W. Seeley, K. J. Hatanpaa, C. Lomen-Hoerth, A. Kertesz, E. H. Bigio, C. Lippa, K. A. Josephs, D. S. Knopman, C. L. White, 3rd, R. Caselli, I. R. Mackenzie, B. L. Miller, M. Boczarska-Jedynak, G. Opala, A. Krygowska-Wajs, M. Barcikowska, S. G. Younkin, R. C. Petersen, N. Ertekin-Taner, R. J. Uitti, J. F. Meschia, K. B. Boylan, B. F. Boeve, N. R. Graff-Radford, Z. K. Wszolek, D. W. Dickson, R. Rademakers, O. A. Ross, TREM2 in neurodegeneration: evidence for association of the p.R47H variant with frontotemporal dementia and Parkinson's disease. *Mol Neurodegener* **8**, 19 (2013).
60. A. Dityatev, C. I. Seidenbecher, M. Schachner, Compartmentalization from the outside: the extracellular matrix and functional microdomains in the brain. *Trends Neurosci* **33**, 503-512 (2010).
61. A. Rolls, R. Shechter, A. London, Y. Segev, J. Jacob-Hirsch, N. Amariglio, G. Rechavi, M. Schwartz, Two faces of chondroitin sulfate proteoglycan in spinal cord repair: a role in microglia/macrophage activation. *PLoS Med* **5**, e171 (2008).

62. A. Rolls, L. Cahalon, S. Bakalash, H. Avidan, O. Lider, M. Schwartz, A sulfated disaccharide derived from chondroitin sulfate proteoglycan protects against inflammation-associated neurodegeneration. *FASEB J* **20**, 547-549 (2006).
63. J. W. Fawcett, T. Oohashi, T. Pizzorusso, The roles of perineuronal nets and the perinodal extracellular matrix in neuronal function. *Nat Rev Neurosci* **20**, 451-465 (2019).
64. L. W. Lau, R. Cua, M. B. Keough, S. Haylock-Jacobs, V. W. Yong, Pathophysiology of the brain extracellular matrix: a new target for remyelination. *Nat Rev Neurosci* **14**, 722-729 (2013).
65. A. Dityatev, M. Schachner, Extracellular matrix molecules and synaptic plasticity. *Nat Rev Neurosci* **4**, 456-468 (2003).
66. A. C. Reichelt, D. J. Hare, T. J. Bussey, L. M. Saksida, Perineuronal Nets: Plasticity, Protection, and Therapeutic Potential. *Trends Neurosci* **42**, 458-470 (2019).
67. T. Pizzorusso, P. Medini, N. Berardi, S. Chierzi, J. W. Fawcett, L. Maffei, Reactivation of ocular dominance plasticity in the adult visual cortex. *Science* **298**, 1248-1251 (2002).
68. Y. J. Liu, E. E. Spangenberg, B. Tang, T. C. Holmes, K. N. Green, X. Xu, Microglia Elimination Increases Neural Circuit Connectivity and Activity in Adult Mouse Cortex. *J Neurosci* **41**, 1274-1287 (2021).
69. S. Miyata, Y. Nishimura, N. Hayashi, A. Oohira, Construction of perineuronal net-like structure by cortical neurons in culture. *Neuroscience* **136**, 95-104 (2005).
70. G. Bruckner, M. Morawski, T. Arendt, Aggrecan-based extracellular matrix is an integral part of the human basal ganglia circuit. *Neuroscience* **151**, 489-504 (2008).
71. C. Jager, D. Lendvai, G. Seeger, G. Bruckner, R. T. Matthews, T. Arendt, A. Alpar, M. Morawski, Perineuronal and perisynaptic extracellular matrix in the human spinal cord. *Neuroscience* **238**, 168-184 (2013).
72. C. Orlando, J. Ster, U. Gerber, J. W. Fawcett, O. Raineteau, Perisynaptic chondroitin sulfate proteoglycans restrict structural plasticity in an integrin-dependent manner. *J Neurosci* **32**, 18009-18017, 18017a (2012).
73. L. de Vivo, S. Landi, M. Panniello, L. Baroncelli, S. Chierzi, L. Mariotti, M. Spolidoro, T. Pizzorusso, L. Maffei, G. M. Ratto, Extracellular matrix inhibits structural and functional plasticity of dendritic spines in the adult visual cortex. *Nat Commun* **4**, 1484 (2013).
74. P. T. Nguyen, L. C. Dorman, S. Pan, I. D. Vainchtein, R. T. Han, H. Nakao-Inoue, S. E. Taloma, J. J. Barron, A. B. Molofsky, M. A. Kheirbek, A. V. Molofsky, Microglial Remodeling of the Extracellular Matrix Promotes Synapse Plasticity. *Cell*, (2020).
75. J. D. Crapser, J. Ochaba, N. Soni, J. C. Reidling, L. M. Thompson, K. N. Green, Microglial depletion prevents extracellular matrix changes and striatal volume reduction in a model of Huntington's disease. *Brain* **143**, 266-288 (2020).
76. J. D. Crapser, E. E. Spangenberg, R. A. Barahona, M. A. Arreola, L. A. Hohsfield, K. N. Green, Microglia facilitate loss of perineuronal nets in the Alzheimer's disease brain. *EBioMedicine* **58**, (2020).
77. D. P. Schafer, E. K. Lehrman, B. Stevens, The "quad-partite" synapse: microglia-synapse interactions in the developing and mature CNS. *Glia* **61**, 24-36 (2013).
78. M. E. Tremblay, R. L. Lowery, A. K. Majewska, Microglial interactions with synapses are modulated by visual experience. *PLoS Biol* **8**, e1000527 (2010).
79. H. Wake, A. J. Moorhouse, S. Jinno, S. Kohsaka, J. Nabekura, Resting microglia directly monitor the functional state of synapses in vivo and determine the fate of ischemic terminals. *J Neurosci* **29**, 3974-3980 (2009).
80. D. P. Schafer, E. K. Lehrman, A. G. Kautzman, R. Koyama, A. R. Mardinly, R. Yamasaki, R. M. Ransohoff, M. E. Greenberg, B. A. Barres, B. Stevens, Microglia sculpt postnatal neural circuits in an activity and complement-dependent manner. *Neuron* **74**, 691-705 (2012).

81. R. C. Paolicelli, G. Bolasco, F. Pagani, L. Maggi, M. Scianni, P. Panzanelli, M. Giustetto, T. A. Ferreira, E. Guiducci, L. Dumas, D. Ragozzino, C. T. Gross, Synaptic pruning by microglia is necessary for normal brain development. *Science* **333**, 1456-1458 (2011).
82. D. P. Schafer, B. Stevens, Microglia Function in Central Nervous System Development and Plasticity. *Cold Spring Harb Perspect Biol* **7**, a020545 (2015).
83. J. L. Frost, D. P. Schafer, Microglia: Architects of the Developing Nervous System. *Trends Cell Biol* **26**, 587-597 (2016).
84. B. Stevens, N. J. Allen, L. E. Vazquez, G. R. Howell, K. S. Christopherson, N. Nouri, K. D. Micheva, A. K. Mehalow, A. D. Huberman, B. Stafford, A. Sher, A. M. Litke, J. D. Lambris, S. J. Smith, S. W. John, B. A. Barres, The classical complement cascade mediates CNS synapse elimination. *Cell* **131**, 1164-1178 (2007).
85. B. Linnartz, J. Kopatz, A. J. Tenner, H. Neumann, Sialic acid on the neuronal glycocalyx prevents complement C1 binding and complement receptor-3-mediated removal by microglia. *J Neurosci* **32**, 946-952 (2012).
86. M. Hoshiko, I. Arnoux, E. Avignone, N. Yamamoto, E. Audinat, Deficiency of the microglial receptor CX3CR1 impairs postnatal functional development of thalamocortical synapses in the barrel cortex. *J Neurosci* **32**, 15106-15111 (2012).
87. B. Basilico, F. Pagani, A. Grimaldi, B. Cortese, S. Di Angelantonio, L. Weinhard, C. Gross, C. Limatola, L. Maggi, D. Ragozzino, Microglia shape presynaptic properties at developing glutamatergic synapses. *Glia* **67**, 53-67 (2019).
88. Y. Zhan, R. C. Paolicelli, F. Sforazzini, L. Weinhard, G. Bolasco, F. Pagani, A. L. Vyssotski, A. Bifone, A. Gozzi, D. Ragozzino, C. T. Gross, Deficient neuron-microglia signaling results in impaired functional brain connectivity and social behavior. *Nat Neurosci* **17**, 400-406 (2014).
89. S. H. Lim, E. Park, B. You, Y. Jung, A. R. Park, S. G. Park, J. R. Lee, Neuronal synapse formation induced by microglia and interleukin 10. *PLoS One* **8**, e81218 (2013).
90. A. Miyamoto, H. Wake, A. W. Ishikawa, K. Eto, K. Shibata, H. Murakoshi, S. Koizumi, A. J. Moorhouse, Y. Yoshimura, J. Nabekura, Microglia contact induces synapse formation in developing somatosensory cortex. *Nat Commun* **7**, 12540 (2016).
91. C. N. Parkhurst, G. Yang, I. Ninan, J. N. Savas, J. R. Yates, 3rd, J. J. Lafaille, B. L. Hempstead, D. R. Littman, W. B. Gan, Microglia promote learning-dependent synapse formation through brain-derived neurotrophic factor. *Cell* **155**, 1596-1609 (2013).
92. J. Bruttger, K. Karram, S. Wortge, T. Regen, F. Marini, N. Hoppmann, M. Klein, T. Blank, S. Yona, Y. Wolf, M. Mack, E. Pinteaux, W. Muller, F. Zipp, H. Binder, T. Bopp, M. Prinz, S. Jung, A. Waisman, Genetic Cell Ablation Reveals Clusters of Local Self-Renewing Microglia in the Mammalian Central Nervous System. *Immunity* **43**, 92-106 (2015).
93. S. J. Rubino, L. Mayo, I. Wimmer, V. Siedler, F. Brunner, S. Hametner, A. Madi, A. Lanser, T. Moreira, D. Donnelly, L. Cox, R. M. Rezende, O. Butovsky, H. Lassmann, H. L. Weiner, Acute microglia ablation induces neurodegeneration in the somatosensory system. *Nat Commun* **9**, 4578 (2018).
94. K. N. Green, J. D. Crapser, L. A. Hohsfield, To Kill a Microglia: A Case for CSF1R Inhibitors. *Trends Immunol*, (2020).
95. G. Milinkeviciute, C. M. Henningfield, M. A. Muniak, S. M. Chokr, K. N. Green, K. S. Cramer, Microglia Regulate Pruning of Specialized Synapses in the Auditory Brainstem. *Front Neural Circuits* **13**, 55 (2019).
96. G. Milinkeviciute, S. M. Chokr, K. S. Cramer, Auditory Brainstem Deficits from Early Treatment with a CSF1R Inhibitor Largely Recover with Microglial Repopulation. *eNeuro* **8**, (2021).
97. A. Pinter, Z. Hevesi, P. Zahola, A. Alpar, J. Hanics, Chondroitin sulfate proteoglycan-5 forms perisynaptic matrix assemblies in the adult rat cortex. *Cell Signal* **74**, 109710 (2020).

98. R. Juttner, D. Montag, R. B. Craveiro, A. Babich, P. Vetter, F. G. Rathjen, Impaired presynaptic function and elimination of synapses at premature stages during postnatal development of the cerebellum in the absence of CALEB (CSPG5/neuroglycan C). *Eur J Neurosci* **38**, 3270-3280 (2013).
99. R. D. Stowell, E. L. Wong, H. N. Batchelor, M. S. Mendes, C. E. Lamantia, B. S. Whitelaw, A. K. Majewska, Cerebellar microglia are dynamically unique and survey Purkinje neurons in vivo. *Dev Neurobiol* **78**, 627-644 (2018).
100. V. Kana, F. A. Desland, M. Casanova-Acebes, P. Ayata, A. Badimon, E. Nabel, K. Yamamuro, M. Sneeboer, I. L. Tan, M. E. Flanigan, S. A. Rose, C. Chang, A. Leader, H. Le Bourhis, E. S. Sweet, N. Tung, A. Wroblewska, Y. Lavin, P. See, A. Baccarini, F. Ginhoux, V. Chitu, E. R. Stanley, S. J. Russo, Z. Yue, B. D. Brown, A. L. Joyner, L. D. De Witte, H. Morishita, A. Schaefer, M. Merad, CSF-1 controls cerebellar microglia and is required for motor function and social interaction. *J Exp Med* **216**, 2265-2281 (2019).
101. H. Nakayama, M. Abe, C. Morimoto, T. Iida, S. Okabe, K. Sakimura, K. Hashimoto, Microglia permit climbing fiber elimination by promoting GABAergic inhibition in the developing cerebellum. *Nat Commun* **9**, 2830 (2018).
102. R. Juttner, M. I. More, D. Das, A. Babich, J. Meier, M. Henning, B. Erdmann, E. C. Mu Ller, A. Otto, R. Grantyn, F. G. Rathjen, Impaired synapse function during postnatal development in the absence of CALEB, an EGF-like protein processed by neuronal activity. *Neuron* **46**, 233-245 (2005).
103. R. A. Rice, E. E. Spangenberg, H. Yamate-Morgan, R. J. Lee, R. P. Arora, M. X. Hernandez, A. J. Tenner, B. L. West, K. N. Green, Elimination of Microglia Improves Functional Outcomes Following Extensive Neuronal Loss in the Hippocampus. *J Neurosci* **35**, 9977-9989 (2015).
104. S. C. Morgan, D. L. Taylor, J. M. Pocock, Microglia release activators of neuronal proliferation mediated by activation of mitogen-activated protein kinase, phosphatidylinositol-3-kinase/Akt and delta-Notch signalling cascades. *J Neurochem* **90**, 89-101 (2004).
105. M. Ueno, Y. Fujita, T. Tanaka, Y. Nakamura, J. Kikuta, M. Ishii, T. Yamashita, Layer V cortical neurons require microglial support for survival during postnatal development. *Nat Neurosci* **16**, 543-551 (2013).
106. J. M. Antony, A. Paquin, S. L. Nutt, D. R. Kaplan, F. D. Miller, Endogenous microglia regulate development of embryonic cortical precursor cells. *J Neurosci Res* **89**, 286-298 (2011).
107. A. Nishiyori, M. Minami, Y. Ohtani, S. Takami, J. Yamamoto, N. Kawaguchi, T. Kume, A. Akaike, M. Satoh, Localization of fractalkine and CX3CR1 mRNAs in rat brain: does fractalkine play a role in signaling from neuron to microglia? *FEBS Lett* **429**, 167-172 (1998).
108. Y. Shigemoto-Mogami, K. Hoshikawa, J. E. Goldman, Y. Sekino, K. Sato, Microglia enhance neurogenesis and oligodendrogenesis in the early postnatal subventricular zone. *J Neurosci* **34**, 2231-2243 (2014).
109. C. L. Cunningham, V. Martinez-Cerdeno, S. C. Noctor, Microglia regulate the number of neural precursor cells in the developing cerebral cortex. *J Neurosci* **33**, 4216-4233 (2013).
110. I. Dalmau, B. Finsen, J. Zimmer, B. Gonzalez, B. Castellano, Development of microglia in the postnatal rat hippocampus. *Hippocampus* **8**, 458-474 (1998).
111. W. Yeo, J. Gautier, Early neural cell death: dying to become neurons. *Dev Biol* **274**, 233-244 (2004).
112. J. L. Marin-Teva, I. Dusart, C. Colin, A. Gervais, N. van Rooijen, M. Mallat, Microglia promote the death of developing Purkinje cells. *Neuron* **41**, 535-547 (2004).
113. F. Sedel, C. Bechade, S. Vyas, A. Triller, Macrophage-derived tumor necrosis factor alpha, an early developmental signal for motoneuron death. *J Neurosci* **24**, 2236-2246 (2004).
114. B. Srinivasan, C. H. Roque, B. L. Hempstead, M. R. Al-Ubaidi, R. S. Roque, Microglia-derived pronerve growth factor promotes photoreceptor cell death via p75 neurotrophin receptor. *J Biol Chem* **279**, 41839-41845 (2004).

115. A. Nimmerjahn, F. Kirchhoff, F. Helmchen, Resting microglial cells are highly dynamic surveillants of brain parenchyma in vivo. *Science* **308**, 1314-1318 (2005).
116. Y. Li, X. F. Du, C. S. Liu, Z. L. Wen, J. L. Du, Reciprocal regulation between resting microglial dynamics and neuronal activity in vivo. *Dev Cell* **23**, 1189-1202 (2012).
117. G. Kato, H. Inada, H. Wake, R. Akiyoshi, A. Miyamoto, K. Eto, T. Ishikawa, A. J. Moorhouse, A. M. Strassman, J. Nabekura, Microglial Contact Prevents Excess Depolarization and Rescues Neurons from Excitotoxicity. *eNeuro* **3**, (2016).
118. K. L. Huang, E. Marcora, A. A. Pimenova, A. F. Di Narzo, M. Kapoor, S. C. Jin, O. Harari, S. Bertelsen, B. P. Fairfax, J. Czajkowski, V. Chouraki, B. Grenier-Boley, C. Bellenguez, Y. Deming, A. McKenzie, T. Raj, A. E. Renton, J. Budde, A. Smith, A. Fitzpatrick, J. C. Bis, A. DeStefano, H. H. H. Adams, M. A. Ikram, S. van der Lee, J. L. Del-Aguila, M. V. Fernandez, L. Ibanez, R. Sims, V. Escott-Price, R. Mayeux, J. L. Haines, L. A. Farrer, M. A. Pericak-Vance, J. C. Lambert, C. van Duijn, L. Launer, S. Seshadri, J. Williams, P. Amouyel, G. D. Schellenberg, B. Zhang, I. Borecki, J. S. K. Kauwe, C. Cruchaga, K. Hao, A. M. Goate, A common haplotype lowers PU.1 expression in myeloid cells and delays onset of Alzheimer's disease. *Nat Neurosci* **20**, 1052-1061 (2017).
119. E. Spangenberg, P. L. Severson, L. A. Hohsfield, J. Crapser, J. Zhang, E. A. Burton, Y. Zhang, W. Spevak, J. Lin, N. Y. Phan, G. Habets, A. Rymar, G. Tsang, J. Walters, M. Nespi, P. Singh, S. Broome, P. Ibrahim, C. Zhang, G. Bollag, B. L. West, K. N. Green, Sustained microglial depletion with CSF1R inhibitor impairs parenchymal plaque development in an Alzheimer's disease model. *Nat Commun* **10**, 3758 (2019).
120. E. E. Spangenberg, R. J. Lee, A. R. Najafi, R. A. Rice, M. R. Elmore, M. Blurton-Jones, B. L. West, K. N. Green, Eliminating microglia in Alzheimer's mice prevents neuronal loss without modulating amyloid-beta pathology. *Brain* **139**, 1265-1281 (2016).
121. T. Zrzavy, S. Hametner, I. Wimmer, O. Butovsky, H. L. Weiner, H. Lassmann, Loss of 'homeostatic' microglia and patterns of their activation in active multiple sclerosis. *Brain* **140**, 1900-1913 (2017).
122. J. S. Henkel, J. I. Engelhardt, L. Siklos, E. P. Simpson, S. H. Kim, T. Pan, J. C. Goodman, T. Siddique, D. R. Beers, S. H. Appel, Presence of dendritic cells, MCP-1, and activated microglia/macrophages in amyotrophic lateral sclerosis spinal cord tissue. *Ann Neurol* **55**, 221-235 (2004).
123. M. R. Turner, A. Cagnin, F. E. Turkheimer, C. C. Miller, C. E. Shaw, D. J. Brooks, P. N. Leigh, R. B. Banati, Evidence of widespread cerebral microglial activation in amyotrophic lateral sclerosis: an [11C](R)-PK11195 positron emission tomography study. *Neurobiol Dis* **15**, 601-609 (2004).
124. M. Fiala, J. Lin, J. Ringman, V. Kermani-Arab, G. Tsao, A. Patel, A. S. Lossinsky, M. C. Graves, A. Gustavson, J. Sayre, E. Sofroni, T. Suarez, F. Chiappelli, G. Bernard, Ineffective phagocytosis of amyloid-beta by macrophages of Alzheimer's disease patients. *J Alzheimers Dis* **7**, 221-232; discussion 255-262 (2005).
125. W. J. Lukiw, Gene expression profiling in fetal, aged, and Alzheimer hippocampus: a continuum of stress-related signaling. *Neurochem Res* **29**, 1287-1297 (2004).
126. P. L. McGeer, S. Itagaki, H. Tago, E. G. McGeer, Reactive microglia in patients with senile dementia of the Alzheimer type are positive for the histocompatibility glycoprotein HLA-DR. *Neurosci Lett* **79**, 195-200 (1987).
127. A. Sierra, A. C. Gottfried-Blackmore, B. S. McEwen, K. Bulloch, Microglia derived from aging mice exhibit an altered inflammatory profile. *Glia* **55**, 412-424 (2007).
128. W. J. Streit, H. Braak, Q. S. Xue, I. Bechmann, Dystrophic (senescent) rather than activated microglial cells are associated with tau pathology and likely precede neurodegeneration in Alzheimer's disease. *Acta Neuropathol* **118**, 475-485 (2009).
129. L. Gan, S. Ye, A. Chu, K. Anton, S. Yi, V. A. Vincent, D. von Schack, D. Chin, J. Murray, S. Lohr, L. Patthy, M. Gonzalez-Zulueta, K. Nikolich, R. Urfer, Identification of cathepsin B as a mediator of

neuronal death induced by Abeta-activated microglial cells using a functional genomics approach. *J Biol Chem* **279**, 5565-5572 (2004).
130. S. Kim, J. Ock, A. K. Kim, H. W. Lee, J. Y. Cho, D. R. Kim, J. Y. Park, K. Suk, Neurotoxicity of microglial cathepsin D revealed by secretome analysis. *J Neurochem* **103**, 2640-2650 (2007).
131. P. J. Kingham, J. M. Pocock, Microglial secreted cathepsin B induces neuronal apoptosis. *J Neurochem* **76**, 1475-1484 (2001).
132. H. Takeuchi, H. Mizoguchi, Y. Doi, S. Jin, M. Noda, J. Liang, H. Li, Y. Zhou, R. Mori, S. Yasuoka, E. Li, B. Parajuli, J. Kawanokuchi, Y. Sonobe, J. Sato, K. Yamanaka, G. Sobue, T. Mizuno, A. Suzumura, Blockade of gap junction hemichannel suppresses disease progression in mouse models of amyotrophic lateral sclerosis and Alzheimer's disease. *PLoS One* **6**, e21108 (2011).
133. I. M. Chiu, E. T. Morimoto, H. Goodarzi, J. T. Liao, S. O'Keeffe, H. P. Phatnani, M. Muratet, M. C. Carroll, S. Levy, S. Tavazoie, R. M. Myers, T. Maniatis, A neurodegeneration-specific gene-expression signature of acutely isolated microglia from an amyotrophic lateral sclerosis mouse model. *Cell Rep* **4**, 385-401 (2013).
134. P. L. Poliani, Y. Wang, E. Fontana, M. L. Robinette, Y. Yamanishi, S. Gilfillan, M. Colonna, TREM2 sustains microglial expansion during aging and response to demyelination. *J Clin Invest* **125**, 2161-2170 (2015).
135. B. Ajami, N. Samusik, P. Wieghofer, P. P. Ho, A. Crotti, Z. Bjornson, M. Prinz, W. J. Fantl, G. P. Nolan, L. Steinman, Single-cell mass cytometry reveals distinct populations of brain myeloid cells in mouse neuroinflammation and neurodegeneration models. *Nat Neurosci* **21**, 541-551 (2018).
136. D. Mrdjen, A. Pavlovic, F. J. Hartmann, B. Schreiner, S. G. Utz, B. P. Leung, I. Lelios, F. L. Heppner, J. Kipnis, D. Merkler, M. Greter, B. Becher, High-Dimensional Single-Cell Mapping of Central Nervous System Immune Cells Reveals Distinct Myeloid Subsets in Health, Aging, and Disease. *Immunity* **48**, 599 (2018).
137. H. Ahyayauch, M. Raab, J. V. Busto, N. Andraka, J. L. Arrondo, M. Masserini, I. Tvaroska, F. M. Goni, Binding of beta-amyloid (1-42) peptide to negatively charged phospholipid membranes in the liquid-ordered state: modeling and experimental studies. *Biophys J* **103**, 453-463 (2012).
138. A. Nagarathinam, P. Hoflinger, A. Buhler, C. Schafer, G. McGovern, M. Jeffrey, M. Staufenbiel, M. Jucker, F. Baumann, Membrane-anchored Abeta accelerates amyloid formation and exacerbates amyloid-associated toxicity in mice. *J Neurosci* **33**, 19284-19294 (2013).
139. T. Jonsson, H. Stefansson, S. Steinberg, I. Jonsdottir, P. V. Jonsson, J. Snaedal, S. Bjornsson, J. Huttenlocher, A. I. Levey, J. J. Lah, D. Rujescu, H. Hampel, I. Giegling, O. A. Andreassen, K. Engedal, I. Ulstein, S. Djurovic, C. Ibrahim-Verbaas, A. Hofman, M. A. Ikram, C. M. van Duijn, U. Thorsteinsdottir, A. Kong, K. Stefansson, Variant of TREM2 associated with the risk of Alzheimer's disease. *N Engl J Med* **368**, 107-116 (2013).
140. W. M. Song, S. Joshita, Y. Zhou, T. K. Ulland, S. Gilfillan, M. Colonna, Humanized TREM2 mice reveal microglia-intrinsic and -extrinsic effects of R47H polymorphism. *J Exp Med* **215**, 745-760 (2018).
141. S. L. Franklin, S. Love, J. R. Greene, S. Betmouni, Loss of Perineuronal Net in ME7 Prion Disease. *J Neuropathol Exp Neurol* **67**, 189-199 (2008).
142. B. K. Bitanihirwe, T. U. Woo, Perineuronal nets and schizophrenia: the importance of neuronal coatings. *Neurosci Biobehav Rev* **45**, 85-99 (2014).
143. P. V. Belichenko, J. Miklossy, M. R. Celio, HIV-I induced destruction of neocortical extracellular matrix components in AIDS victims. *Neurobiol Dis* **4**, 301-310 (1997).
144. E. Gray, T. L. Thomas, S. Betmouni, N. Scolding, S. Love, Elevated matrix metalloproteinase-9 and degradation of perineuronal nets in cerebrocortical multiple sclerosis plaques. *J Neuropathol Exp Neurol* **67**, 888-899 (2008).
145. L. Mangiarini, K. Sathasivam, M. Seller, B. Cozens, A. Harper, C. Hetherington, M. Lawton, Y. Trottier, H. Lehrach, S. W. Davies, G. P. Bates, Exon 1 of the HD gene with an expanded CAG repeat

is sufficient to cause a progressive neurological phenotype in transgenic mice. *Cell* **87**, 493-506 (1996).
146. H. Oakley, S. L. Cole, S. Logan, E. Maus, P. Shao, J. Craft, A. Guillozet-Bongaarts, M. Ohno, J. Disterhoft, L. Van Eldik, R. Berry, R. Vassar, Intraneuronal beta-amyloid aggregates, neurodegeneration, and neuron loss in transgenic mice with five familial Alzheimer's disease mutations: potential factors in amyloid plaque formation. *J Neurosci* **26**, 10129-10140 (2006).
147. A. Venturino, R. Schulz, H. De Jesus-Cortes, M. E. Maes, B. Nagy, F. Reilly-Andujar, G. Colombo, R. J. A. Cubero, F. E. Schoot Uiterkamp, M. F. Bear, S. Siegert, Microglia enable mature perineuronal nets disassembly upon anesthetic ketamine exposure or 60-Hz light entrainment in the healthy brain. *Cell Rep* **36**, 109313 (2021).
148. P. V. Belichenko, J. Miklossy, B. Belser, H. Budka, M. R. Celio, Early destruction of the extracellular matrix around parvalbumin-immunoreactive interneurons in Creutzfeldt-Jakob disease. *Neurobiol Dis* **6**, 269-279 (1999).
149. R. Borner, J. Bento-Torres, D. R. Souza, D. B. Sadala, N. Trevia, J. A. Farias, N. Lins, A. Passos, A. Quintairos, J. A. Diniz, V. H. Perry, P. F. Vasconcelos, C. Cunningham, C. W. Picanco-Diniz, Early behavioral changes and quantitative analysis of neuropathological features in murine prion disease: stereological analysis in the albino Swiss mice model. *Prion* **5**, 215-227 (2011).
150. P. L. Bozzelli, A. Caccavano, V. Avdoshina, I. Mocchetti, J. Y. Wu, K. Conant, Increased matrix metalloproteinase levels and perineuronal net proteolysis in the HIV-infected brain; relevance to altered neuronal population dynamics. *Exp Neurol* **323**, 113077 (2020).
151. R. Medina-Flores, G. Wang, S. J. Bissel, M. Murphey-Corb, C. A. Wiley, Destruction of extracellular matrix proteoglycans is pervasive in simian retroviral neuroinfection. *Neurobiol Dis* **16**, 604-616 (2004).
152. G. W. Huntley, Synaptic circuit remodelling by matrix metalloproteinases in health and disease. *Nat Rev Neurosci* **13**, 743-757 (2012).
153. P. E. Gottschall, M. D. Howell, ADAMTS expression and function in central nervous system injury and disorders. *Matrix Biol* **44-46**, 70-76 (2015).
154. S. T. DeKosky, S. W. Scheff, Synapse loss in frontal cortex biopsies in Alzheimer's disease: correlation with cognitive severity. *Ann Neurol* **27**, 457-464 (1990).
155. C. M. Henstridge, D. I. Sideris, E. Carroll, S. Rotariu, S. Salomonsson, M. Tzioras, C. A. McKenzie, C. Smith, C. A. F. von Arnim, A. C. Ludolph, D. Lule, D. Leighton, J. Warner, E. Cleary, J. Newton, R. Swingler, S. Chandran, T. H. Gillingwater, S. Abrahams, T. L. Spires-Jones, Synapse loss in the prefrontal cortex is associated with cognitive decline in amyotrophic lateral sclerosis. *Acta Neuropathol* **135**, 213-226 (2018).
156. S. W. Scheff, D. A. Price, Alzheimer's disease-related alterations in synaptic density: neocortex and hippocampus. *J Alzheimers Dis* **9**, 101-115 (2006).
157. R. D. Terry, E. Masliah, D. P. Salmon, N. Butters, R. DeTeresa, R. Hill, L. A. Hansen, R. Katzman, Physical basis of cognitive alterations in Alzheimer's disease: synapse loss is the major correlate of cognitive impairment. *Ann Neurol* **30**, 572-580 (1991).
158. S. Hong, V. F. Beja-Glasser, B. M. Nfonoyim, A. Frouin, S. Li, S. Ramakrishnan, K. M. Merry, Q. Shi, A. Rosenthal, B. A. Barres, C. A. Lemere, D. J. Selkoe, B. Stevens, Complement and microglia mediate early synapse loss in Alzheimer mouse models. *Science* **352**, 712-716 (2016).
159. E. P. Azevedo, J. H. Ledo, G. Barbosa, M. Sobrinho, L. Diniz, A. C. Fonseca, F. Gomes, L. Romao, F. R. Lima, F. L. Palhano, S. T. Ferreira, D. Foguel, Activated microglia mediate synapse loss and short-term memory deficits in a mouse model of transthyretin-related oculoleptomeningeal amyloidosis. *Cell Death Dis* **4**, e789 (2013).
160. W. Y. Wang, M. S. Tan, J. T. Yu, L. Tan, Role of pro-inflammatory cytokines released from microglia in Alzheimer's disease. *Ann Transl Med* **3**, 136 (2015).

161. R. Dantzer, J. C. O'Connor, G. G. Freund, R. W. Johnson, K. W. Kelley, From inflammation to sickness and depression: when the immune system subjugates the brain. *Nat Rev Neurosci* **9**, 46-56 (2008).
162. Y. Dowlati, N. Herrmann, W. Swardfager, H. Liu, L. Sham, E. K. Reim, K. L. Lanctot, A meta-analysis of cytokines in major depression. *Biol Psychiatry* **67**, 446-457 (2010).
163. G. G. R. Leday, P. E. Vertes, S. Richardson, J. R. Greene, T. Regan, S. Khan, R. Henderson, T. C. Freeman, C. M. Pariante, N. A. Harrison, V. H. Perry, W. C. Drevets, G. M. Wittenberg, E. T. Bullmore, Replicable and Coupled Changes in Innate and Adaptive Immune Gene Expression in Two Case-Control Studies of Blood Microarrays in Major Depressive Disorder. *Biol Psychiatry* **83**, 70-80 (2018).
164. J. Steiner, H. Bielau, R. Brisch, P. Danos, O. Ullrich, C. Mawrin, H. G. Bernstein, B. Bogerts, Immunological aspects in the neurobiology of suicide: elevated microglial density in schizophrenia and depression is associated with suicide. *J Psychiatr Res* **42**, 151-157 (2008).
165. S. G. Torres-Platas, C. Cruceanu, G. G. Chen, G. Turecki, N. Mechawar, Evidence for increased microglial priming and macrophage recruitment in the dorsal anterior cingulate white matter of depressed suicides. *Brain Behav Immun* **42**, 50-59 (2014).
166. M. G. Frank, M. V. Baratta, D. B. Sprunger, L. R. Watkins, S. F. Maier, Microglia serve as a neuroimmune substrate for stress-induced potentiation of CNS pro-inflammatory cytokine responses. *Brain Behav Immun* **21**, 47-59 (2007).
167. M. Hinwood, J. Morandini, T. A. Day, F. R. Walker, Evidence that microglia mediate the neurobiological effects of chronic psychological stress on the medial prefrontal cortex. *Cereb Cortex* **22**, 1442-1454 (2012).
168. B. L. Kopp, D. Wick, J. P. Herman, Differential effects of homotypic vs. heterotypic chronic stress regimens on microglial activation in the prefrontal cortex. *Physiol Behav* **122**, 246-252 (2013).
169. R. J. Tynan, S. Naicker, M. Hinwood, E. Nalivaiko, K. M. Buller, D. V. Pow, T. A. Day, F. R. Walker, Chronic stress alters the density and morphology of microglia in a subset of stress-responsive brain regions. *Brain Behav Immun* **24**, 1058-1068 (2010).
170. E. S. Wohleb, N. D. Powell, J. P. Godbout, J. F. Sheridan, Stress-induced recruitment of bone marrow-derived monocytes to the brain promotes anxiety-like behavior. *J Neurosci* **33**, 13820-13833 (2013).
171. Y. L. Wang, Q. Q. Han, W. Q. Gong, D. H. Pan, L. Z. Wang, W. Hu, M. Yang, B. Li, J. Yu, Q. Liu, Microglial activation mediates chronic mild stress-induced depressive- and anxiety-like behavior in adult rats. *J Neuroinflammation* **15**, 21 (2018).
172. R. Avitsur, J. L. Stark, J. F. Sheridan, Social stress induces glucocorticoid resistance in subordinate animals. *Horm Behav* **39**, 247-257 (2001).
173. P. J. Barnes, I. M. Adcock, Glucocorticoid resistance in inflammatory diseases. *Lancet* **373**, 1905-1917 (2009).
174. G. P. Chrousos, M. Castro, D. Y. Leung, E. Webster, T. Kino, C. Bamberger, S. Elliot, C. Stratakis, M. Karl, Molecular mechanisms of glucocorticoid resistance/hypersensitivity. Potential clinical implications. *Am J Respir Crit Care Med* **154**, S39-43; discussion S43-34 (1996).
175. H. A. Jurgens, R. W. Johnson, Dysregulated neuronal-microglial cross-talk during aging, stress and inflammation. *Exp Neurol* **233**, 40-48 (2012).
176. K. Kleinfeld, B. Mobley, P. Hedera, A. Wegner, S. Sriram, S. Pawate, Adult-onset leukoencephalopathy with neuroaxonal spheroids and pigmented glia: report of five cases and a new mutation. *J Neurol* **260**, 558-571 (2013).
177. C. Sundal, J. A. Van Gerpen, A. M. Nicholson, C. Wider, E. A. Shuster, J. Aasly, S. Spina, B. Ghetti, S. Roeber, J. Garbern, A. Borjesson-Hanson, A. Tselis, R. H. Swerdlow, B. B. Miller, S. Fujioka, M. G. Heckman, R. J. Uitti, K. A. Josephs, M. Baker, O. Andersen, R. Rademakers, D. W. Dickson, D.

Broderick, Z. K. Wszolek, MRI characteristics and scoring in HDLS due to CSF1R gene mutations. *Neurology* **79**, 566-574 (2012).
178. I. J. Bennett, D. J. Madden, Disconnected aging: cerebral white matter integrity and age-related differences in cognition. *Neuroscience* **276**, 187-205 (2014).
179. E. R. Sowell, B. S. Peterson, P. M. Thompson, S. E. Welcome, A. L. Henkenius, A. W. Toga, Mapping cortical change across the human life span. *Nat Neurosci* **6**, 309-315 (2003).
180. M. L. Feldman, A. Peters, Ballooning of myelin sheaths in normally aged macaques. *J Neurocytol* **27**, 605-614 (1998).
181. I. Sugiyama, K. Tanaka, M. Akita, K. Yoshida, T. Kawase, H. Asou, Ultrastructural analysis of the paranodal junction of myelinated fibers in 31-month-old-rats. *J Neurosci Res* **70**, 309-317 (2002).
182. R. A. Hill, A. M. Li, J. Grutzendler, Lifelong cortical myelin plasticity and age-related degeneration in the live mammalian brain. *Nat Neurosci* **21**, 683-695 (2018).
183. S. Safaiyan, N. Kannaiyan, N. Snaidero, S. Brioschi, K. Biber, S. Yona, A. L. Edinger, S. Jung, M. J. Rossner, M. Simons, Age-related myelin degradation burdens the clearance function of microglia during aging. *Nat Neurosci* **19**, 995-998 (2016).
184. L. Haider, M. T. Fischer, J. M. Frischer, J. Bauer, R. Hoftberger, G. Botond, H. Esterbauer, C. J. Binder, J. L. Witztum, H. Lassmann, Oxidative damage in multiple sclerosis lesions. *Brain* **134**, 1914-1924 (2011).
185. F. L. Heppner, M. Greter, D. Marino, J. Falsig, G. Raivich, N. Hovelmeyer, A. Waisman, T. Rulicke, M. Prinz, J. Priller, B. Becher, A. Aguzzi, Experimental autoimmune encephalomyelitis repressed by microglial paralysis. *Nat Med* **11**, 146-152 (2005).
186. A. Lampron, A. Larochelle, N. Laflamme, P. Prefontaine, M. M. Plante, M. G. Sanchez, V. W. Yong, P. K. Stys, M. E. Tremblay, S. Rivest, Inefficient clearance of myelin debris by microglia impairs remyelinating processes. *J Exp Med* **212**, 481-495 (2015).
187. J. Liu, D. Tian, M. Murugan, U. B. Eyo, C. F. Dreyfus, W. Wang, L. J. Wu, Microglial Hv1 proton channel promotes cuprizone-induced demyelination through oxidative damage. *J Neurochem* **135**, 347-356 (2015).
188. V. E. Miron, A. Boyd, J. W. Zhao, T. J. Yuen, J. M. Ruckh, J. L. Shadrach, P. van Wijngaarden, A. J. Wagers, A. Williams, R. J. M. Franklin, C. Ffrench-Constant, M2 microglia and macrophages drive oligodendrocyte differentiation during CNS remyelination. *Nat Neurosci* **16**, 1211-1218 (2013).
189. I. Napoli, H. Neumann, Protective effects of microglia in multiple sclerosis. *Exp Neurol* **225**, 24-28 (2010).
190. B. Ferguson, M. K. Matyszak, M. M. Esiri, V. H. Perry, Axonal damage in acute multiple sclerosis lesions. *Brain* **120 (Pt 3)**, 393-399 (1997).
191. J. W. Prineas, E. E. Kwon, E. S. Cho, L. R. Sharer, M. H. Barnett, E. L. Oleszak, B. Hoffman, B. P. Morgan, Immunopathology of secondary-progressive multiple sclerosis. *Ann Neurol* **50**, 646-657 (2001).
192. W. Bruck, Y. Bruck, R. L. Friede, TNF-alpha suppresses CR3-mediated myelin removal by macrophages. *J Neuroimmunol* **38**, 9-17 (1992).
193. W. Bruck, P. Porada, S. Poser, P. Rieckmann, F. Hanefeld, H. A. Kretzschmar, H. Lassmann, Monocyte/macrophage differentiation in early multiple sclerosis lesions. *Ann Neurol* **38**, 788-796 (1995).
194. M. T. Fischer, R. Sharma, J. L. Lim, L. Haider, J. M. Frischer, J. Drexhage, D. Mahad, M. Bradl, J. van Horssen, H. Lassmann, NADPH oxidase expression in active multiple sclerosis lesions in relation to oxidative tissue damage and mitochondrial injury. *Brain* **135**, 886-899 (2012).
195. R. Hoftberger, F. Aboul-Enein, W. Brueck, C. Lucchinetti, M. Rodriguez, M. Schmidbauer, K. Jellinger, H. Lassmann, Expression of major histocompatibility complex class I molecules on the different cell types in multiple sclerosis lesions. *Brain Pathol* **14**, 43-50 (2004).

196. B. Cannella, S. Gaupp, K. M. Omari, C. S. Raine, Multiple sclerosis: death receptor expression and oligodendrocyte apoptosis in established lesions. *J Neuroimmunol* **188**, 128-137 (2007).
197. B. Cannella, C. S. Raine, Multiple sclerosis: cytokine receptors on oligodendrocytes predict innate regulation. *Ann Neurol* **55**, 46-57 (2004).
198. C. Griot, T. Burge, M. Vandevelde, E. Peterhans, Antibody-induced generation of reactive oxygen radicals by brain macrophages in canine distemper encephalitis: a mechanism for bystander demyelination. *Acta Neuropathol* **78**, 396-403 (1989).
199. C. Griot, M. Vandevelde, A. Richard, E. Peterhans, R. Stocker, Selective degeneration of oligodendrocytes mediated by reactive oxygen species. *Free Radic Res Commun* **11**, 181-193 (1990).
200. J. Husain, B. H. Juurlink, Oligodendroglial precursor cell susceptibility to hypoxia is related to poor ability to cope with reactive oxygen species. *Brain Res* **698**, 86-94 (1995).
201. A. Oka, M. J. Belliveau, P. A. Rosenberg, J. J. Volpe, Vulnerability of oligodendroglia to glutamate: pharmacology, mechanisms, and prevention. *J Neurosci* **13**, 1441-1453 (1993).
202. M. R. Kotter, W. W. Li, C. Zhao, R. J. Franklin, Myelin impairs CNS remyelination by inhibiting oligodendrocyte precursor cell differentiation. *J Neurosci* **26**, 328-332 (2006).
203. B. Erblich, L. Zhu, A. M. Etgen, K. Dobrenis, J. W. Pollard, Absence of colony stimulation factor-1 receptor results in loss of microglia, disrupted brain development and olfactory deficits. *PLoS One* **6**, e26317 (2011).
204. F. Ginhoux, M. Greter, M. Leboeuf, S. Nandi, P. See, S. Gokhan, M. F. Mehler, S. J. Conway, L. G. Ng, E. R. Stanley, I. M. Samokhvalov, M. Merad, Fate mapping analysis reveals that adult microglia derive from primitive macrophages. *Science* **330**, 841-845 (2010).
205. N. Mossadegh-Keller, S. Sarrazin, P. K. Kandalla, L. Espinosa, E. R. Stanley, S. L. Nutt, J. Moore, M. H. Sieweke, M-CSF instructs myeloid lineage fate in single haematopoietic stem cells. *Nature* **497**, 239-243 (2013).
206. P. Laslo, C. J. Spooner, A. Warmflash, D. W. Lancki, H. J. Lee, R. Sciammas, B. N. Gantner, A. R. Dinner, H. Singh, Multilineage transcriptional priming and determination of alternate hematopoietic cell fates. *Cell* **126**, 755-766 (2006).
207. S. H. Bartelmez, T. R. Bradley, I. Bertoncello, D. Y. Mochizuki, R. J. Tushinski, E. R. Stanley, A. J. Hapel, I. G. Young, A. B. Kriegler, G. S. Hodgson, Interleukin 1 plus interleukin 3 plus colony-stimulating factor 1 are essential for clonal proliferation of primitive myeloid bone marrow cells. *Exp Hematol* **17**, 240-245 (1989).
208. N. Williams, I. Bertoncello, H. Kavnoudias, K. Zsebo, I. McNiece, Recombinant rat stem cell factor stimulates the amplification and differentiation of fractionated mouse stem cell populations. *Blood* **79**, 58-64 (1992).
209. R. J. Tushinski, E. R. Stanley, The regulation of macrophage protein turnover by a colony stimulating factor (CSF-1). *J Cell Physiol* **116**, 67-75 (1983).
210. R. J. Tushinski, E. R. Stanley, The regulation of mononuclear phagocyte entry into S phase by the colony stimulating factor CSF-1. *J Cell Physiol* **122**, 221-228 (1985).
211. S. Nataf, A. Anginot, C. Vuaillat, L. Malaval, N. Fodil, E. Chereul, J. B. Langlois, C. Dumontel, G. Cavillon, C. Confavreux, M. Mazzorana, L. Vico, M. F. Belin, E. Vivier, E. Tomasello, P. Jurdic, Brain and bone damage in KARAP/DAP12 loss-of-function mice correlate with alterations in microglia and osteoclast lineages. *Am J Pathol* **166**, 275-286 (2005).
212. M. Chang, J. A. Hamilton, G. M. Scholz, P. Masendycz, S. L. Macaulay, C. L. Elsegood, Phosphatidylinostitol-3 kinase and phospholipase C enhance CSF-1-dependent macrophage survival by controlling glucose uptake. *Cell Signal* **21**, 1361-1369 (2009).
213. M. R. Elmore, A. R. Najafi, M. A. Koike, N. N. Dagher, E. E. Spangenberg, R. A. Rice, M. Kitazawa, B. Matusow, H. Nguyen, B. L. West, K. N. Green, Colony-stimulating factor 1 receptor signaling is

necessary for microglia viability, unmasking a microglia progenitor cell in the adult brain. *Neuron* **82**, 380-397 (2014).
214. M. R. P. Elmore, L. A. Hohsfield, E. A. Kramar, L. Soreq, R. J. Lee, S. T. Pham, A. R. Najafi, E. E. Spangenberg, M. A. Wood, B. L. West, K. N. Green, Replacement of microglia in the aged brain reverses cognitive, synaptic, and neuronal deficits in mice. *Aging Cell* **17**, e12832 (2018).
215. A. R. Najafi, J. Crapser, S. Jiang, W. Ng, A. Mortazavi, B. L. West, K. N. Green, A limited capacity for microglial repopulation in the adult brain. *Glia* **66**, 2385-2396 (2018).
216. C. Leng, L. Lu, G. Wang, Y. Zhang, Y. Xu, X. Lin, N. Shen, X. Xu, S. Qun, M. Sun, W. Ge, A novel dominant-negative mutation of the CSF1R gene causes adult-onset leukoencephalopathy with axonal spheroids and pigmented glia. *Am J Transl Res* **11**, 6093-6101 (2019).
217. S. J. Adams, A. Kirk, R. N. Auer, Adult-onset leukoencephalopathy with axonal spheroids and pigmented glia (ALSP): Integrating the literature on hereditary diffuse leukoencephalopathy with spheroids (HDLS) and pigmentary orthochromatic leukodystrophy (POLD). *J Clin Neurosci* **48**, 42-49 (2018).
218. T. Konno, M. Tada, M. Tada, A. Koyama, H. Nozaki, Y. Harigaya, J. Nishimiya, A. Matsunaga, N. Yoshikura, K. Ishihara, M. Arakawa, A. Isami, K. Okazaki, H. Yokoo, K. Itoh, M. Yoneda, M. Kawamura, T. Inuzuka, H. Takahashi, M. Nishizawa, O. Onodera, A. Kakita, T. Ikeuchi, Haploinsufficiency of CSF-1R and clinicopathologic characterization in patients with HDLS. *Neurology* **82**, 139-148 (2014).
219. M. T. Heneka, M. P. Kummer, E. Latz, Innate immune activation in neurodegenerative disease. *Nat Rev Immunol* **14**, 463-477 (2014).
220. Y. J. Jung, W. S. Chung, Phagocytic Roles of Glial Cells in Healthy and Diseased Brains. *Biomol Ther (Seoul)* **26**, 350-357 (2018).
221. L. Weinhard, G. di Bartolomei, G. Bolasco, P. Machado, N. L. Schieber, U. Neniskyte, M. Exiga, A. Vadisiute, A. Raggioli, A. Schertel, Y. Schwab, C. T. Gross, Microglia remodel synapses by presynaptic trogocytosis and spine head filopodia induction. *Nat Commun* **9**, 1228 (2018).
222. N. Oosterhof, I. J. Chang, E. G. Karimiani, L. E. Kuil, D. M. Jensen, R. Daza, E. Young, L. Astle, H. C. van der Linde, G. M. Shivaram, J. Demmers, C. S. Latimer, C. D. Keene, E. Loter, R. Maroofian, T. J. van Ham, R. F. Hevner, J. T. Bennett, Homozygous Mutations in CSF1R Cause a Pediatric-Onset Leukoencephalopathy and Can Result in Congenital Absence of Microglia. *Am J Hum Genet* **104**, 936-947 (2019).
223. N. Oosterhof, L. E. Kuil, H. C. van der Linde, S. M. Burm, W. Berdowski, W. F. J. van Ijcken, J. C. van Swieten, E. M. Hol, M. H. G. Verheijen, T. J. van Ham, Colony-Stimulating Factor 1 Receptor (CSF1R) Regulates Microglia Density and Distribution, but Not Microglia Differentiation In Vivo. *Cell Rep* **24**, 1203-1217.e1206 (2018).
224. J. Li, K. Chen, L. Zhu, J. W. Pollard, Conditional deletion of the colony stimulating factor-1 receptor (c-fms proto-oncogene) in mice. *Genesis* **44**, 328-335 (2006).
225. V. Chitu, F. Biundo, G. G. L. Shlager, E. S. Park, P. Wang, M. E. Gulinello, S. Gokhan, H. C. Ketchum, K. Saha, M. A. DeTure, D. W. Dickson, Z. K. Wszolek, D. Zheng, A. L. Croxford, B. Becher, D. Sun, M. F. Mehler, E. R. Stanley, Microglial Homeostasis Requires Balanced CSF-1/CSF-2 Receptor Signaling. *Cell Rep* **30**, 3004-3019 e3005 (2020).
226. A. Dobin, C. A. Davis, F. Schlesinger, J. Drenkow, C. Zaleski, S. Jha, P. Batut, M. Chaisson, T. R. Gingeras, STAR: ultrafast universal RNA-seq aligner. *Bioinformatics* **29**, 15-21 (2013).
227. Y. Liao, G. K. Smyth, W. Shi, The Subread aligner: fast, accurate and scalable read mapping by seed-and-vote. *Nucleic Acids Res* **41**, e108 (2013).
228. R Core Team. (the R Foundation for Statistical Computing, Vienna, Austria, 2017).

229. M. D. Robinson, D. J. McCarthy, G. K. Smyth, edgeR: a Bioconductor package for differential expression analysis of digital gene expression data. *Bioinformatics (Oxford, England)* **26**, 139-140 (2010).
230. B. Zhang, S. Horvath, A general framework for weighted gene co-expression network analysis. *Stat Appl Genet Mol Biol* **4**, Article17 (2005).
231. M. V. Kuleshov, M. R. Jones, A. D. Rouillard, N. F. Fernandez, Q. Duan, Z. Wang, S. Koplev, S. L. Jenkins, K. M. Jagodnik, A. Lachmann, M. G. McDermott, C. D. Monteiro, G. W. Gundersen, A. Ma'ayan, Enrichr: a comprehensive gene set enrichment analysis web server 2016 update. *Nucleic Acids Res* **44**, W90-97 (2016).
232. H. Akiyama, T. Nishimura, H. Kondo, K. Ikeda, Y. Hayashi, P. L. McGeer, Expression of the receptor for macrophage colony stimulating factor by brain microglia and its upregulation in brains of patients with Alzheimer's disease and amyotrophic lateral sclerosis. *Brain Res* **639**, 171-174 (1994).
233. S. Nandi, S. Gokhan, X. M. Dai, S. Wei, G. Enikolopov, H. Lin, M. F. Mehler, E. R. Stanley, The CSF-1 receptor ligands IL-34 and CSF-1 exhibit distinct developmental brain expression patterns and regulate neural progenitor cell maintenance and maturation. *Dev Biol* **367**, 100-113 (2012).
234. Y. Wang, O. Berezovska, S. Fedoroff, Expression of colony stimulating factor-1 receptor (CSF-1R) by CNS neurons in mice. *J Neurosci Res* **57**, 616-632 (1999).
235. S. Krasemann, C. Madore, R. Cialic, C. Baufeld, N. Calcagno, R. El Fatimy, L. Beckers, E. O'Loughlin, Y. Xu, Z. Fanek, D. J. Greco, S. T. Smith, G. Tweet, Z. Humulock, T. Zrzavy, P. Conde-Sanroman, M. Gacias, Z. Weng, H. Chen, E. Tjon, F. Mazaheri, K. Hartmann, A. Madi, J. D. Ulrich, M. Glatzel, A. Worthmann, J. Heeren, B. Budnik, C. Lemere, T. Ikezu, F. L. Heppner, V. Litvak, D. M. Holtzman, H. Lassmann, H. L. Weiner, J. Ochando, C. Haass, O. Butovsky, The TREM2-APOE Pathway Drives the Transcriptional Phenotype of Dysfunctional Microglia in Neurodegenerative Diseases. *Immunity* **47**, 566-581.e569 (2017).
236. O. Butovsky, M. P. Jedrychowski, R. Cialic, S. Krasemann, G. Murugaiyan, Z. Fanek, D. J. Greco, P. M. Wu, C. E. Doykan, O. Kiner, R. J. Lawson, M. P. Frosch, N. Pochet, R. E. Fatimy, A. M. Krichevsky, S. P. Gygi, H. Lassmann, J. Berry, M. E. Cudkowicz, H. L. Weiner, Targeting miR-155 restores abnormal microglia and attenuates disease in SOD1 mice. *Ann Neurol* **77**, 75-99 (2015).
237. O. Butovsky, M. P. Jedrychowski, C. S. Moore, R. Cialic, A. J. Lanser, G. Gabriely, T. Koeglsperger, B. Dake, P. M. Wu, C. E. Doykan, Z. Fanek, L. Liu, Z. Chen, J. D. Rothstein, R. M. Ransohoff, S. P. Gygi, J. P. Antel, H. L. Weiner, Identification of a unique TGF-beta-dependent molecular and functional signature in microglia. *Nat Neurosci* **17**, 131-143 (2014).
238. L. Kempthorne, H. Yoon, C. Madore, S. Smith, Z. K. Wszolek, R. Rademakers, J. Kim, O. Butovsky, D. W. Dickson, Loss of homeostatic microglial phenotype in CSF1R-related Leukoencephalopathy. *Acta Neuropathol Commun* **8**, 72 (2020).
239. L. A. Glantz, J. H. Gilmore, R. M. Hamer, J. A. Lieberman, L. F. Jarskog, Synaptophysin and postsynaptic density protein 95 in the human prefrontal cortex from mid-gestation into early adulthood. *Neuroscience* **149**, 582-591 (2007).
240. E. C. Onwordi, E. F. Halff, T. Whitehurst, A. Mansur, M. C. Cotel, L. Wells, H. Creeney, D. Bonsall, M. Rogdaki, E. Shatalina, T. Reis Marques, E. A. Rabiner, R. N. Gunn, S. Natesan, A. C. Vernon, O. D. Howes, Synaptic density marker SV2A is reduced in schizophrenia patients and unaffected by antipsychotics in rats. *Nat Commun* **11**, 246 (2020).
241. C. L. Waites, S. A. Leal-Ortiz, N. Okerlund, H. Dalke, A. Fejtova, W. D. Altrock, E. D. Gundelfinger, C. C. Garner, Bassoon and Piccolo maintain synapse integrity by regulating protein ubiquitination and degradation. *Embo j* **32**, 954-969 (2013).
242. A. Dityatev, D. A. Rusakov, Molecular signals of plasticity at the tetrapartite synapse. *Curr Opin Neurobiol* **21**, 353-359 (2011).

243. R. Frischknecht, M. Heine, D. Perrais, C. I. Seidenbecher, D. Choquet, E. D. Gundelfinger, Brain extracellular matrix affects AMPA receptor lateral mobility and short-term synaptic plasticity. *Nat Neurosci* **12**, 897-904 (2009).
244. H. Tanaka, W. Shan, G. R. Phillips, K. Arndt, O. Bozdagi, L. Shapiro, G. W. Huntley, D. L. Benson, D. R. Colman, Molecular modification of N-cadherin in response to synaptic activity. *Neuron* **25**, 93-107 (2000).
245. K. A. Giamanco, M. Morawski, R. T. Matthews, Perineuronal net formation and structure in aggrecan knockout mice. *Neuroscience* **170**, 1314-1327 (2010).
246. H. Pantazopoulos, M. Markota, F. Jaquet, D. Ghosh, A. Wallin, A. Santos, B. Caterson, S. Berretta, Aggrecan and chondroitin-6-sulfate abnormalities in schizophrenia and bipolar disorder: a postmortem study on the amygdala. *Transl Psychiatry* **5**, e496 (2015).
247. N. Hayashi, K. Tatsumi, H. Okuda, M. Yoshikawa, S. Ishizaka, S. Miyata, T. Manabe, A. Wanaka, DACS, novel matrix structure composed of chondroitin sulfate proteoglycan in the brain. *Biochem Biophys Res Commun* **364**, 410-415 (2007).
248. G. Matuszko, S. Curreli, R. Kaushik, A. Becker, A. Dityatev, Extracellular matrix alterations in the ketamine model of schizophrenia. *Neuroscience* **350**, 13-22 (2017).
249. H. Okuda, K. Tatsumi, S. Morita, Y. Shibukawa, H. Korekane, N. Horii-Hayashi, Y. Wada, N. Taniguchi, A. Wanaka, Chondroitin sulfate proteoglycan tenascin-R regulates glutamate uptake by adult brain astrocytes. *J Biol Chem* **289**, 2620-2631 (2014).
250. M. T. Fitch, J. Silver, Activated macrophages and the blood-brain barrier: inflammation after CNS injury leads to increases in putative inhibitory molecules. *Exp Neurol* **148**, 587-603 (1997).
251. N. N. Dagher, A. R. Najafi, K. M. Kayala, M. R. Elmore, T. E. White, R. Medeiros, B. L. West, K. N. Green, Colony-stimulating factor 1 receptor inhibition prevents microglial plaque association and improves cognition in 3xTg-AD mice. *J Neuroinflammation* **12**, 139 (2015).
252. A. Olmos-Alonso, S. T. Schetters, S. Sri, K. Askew, R. Mancuso, M. Vargas-Caballero, C. Holscher, V. H. Perry, D. Gomez-Nicola, Pharmacological targeting of CSF1R inhibits microglial proliferation and prevents the progression of Alzheimer's-like pathology. *Brain* **139**, 891-907 (2016).
253. D. Gomez-Nicola, N. L. Fransen, S. Suzzi, V. H. Perry, Regulation of microglial proliferation during chronic neurodegeneration. *J Neurosci* **33**, 2481-2493 (2013).
254. R. Mancuso, G. Fryatt, M. Cleal, J. Obst, E. Pipi, J. Monzon-Sandoval, E. Ribe, L. Winchester, C. Webber, A. Nevado, T. Jacobs, N. Austin, C. Theunis, K. Grauwen, E. Daniela Ruiz, A. Mudher, M. Vicente-Rodriguez, C. A. Parker, C. Simmons, D. Cash, J. Richardson, N. Consortium, D. N. C. Jones, S. Lovestone, D. Gomez-Nicola, V. H. Perry, CSF1R inhibitor JNJ-40346527 attenuates microglial proliferation and neurodegeneration in P301S mice. *Brain* **142**, 3243-3264 (2019).
255. B. M. Davis, M. Salinas-Navarro, M. F. Cordeiro, L. Moons, L. De Groef, Characterizing microglia activation: a spatial statistics approach to maximize information extraction. *Sci Rep* **7**, 1576 (2017).
256. M. Nikodemova, R. S. Kimyon, I. De, A. L. Small, L. S. Collier, J. J. Watters, Microglial numbers attain adult levels after undergoing a rapid decrease in cell number in the third postnatal week. *J Neuroimmunol* **278**, 280-288 (2015).
257. F. Biundo, V. Chitu, G. G. L. Shlager, E. S. Park, M. E. Gulinello, K. Saha, H. C. Ketchum, C. Fernandes, S. Gokhan, M. F. Mehler, E. R. Stanley, Microglial reduction of colony stimulating factor-1 receptor expression is sufficient to confer adult onset leukodystrophy. *Glia*, (2020).
258. E. M. Andrews, R. J. Richards, F. Q. Yin, M. S. Viapiano, L. B. Jakeman, Alterations in chondroitin sulfate proteoglycan expression occur both at and far from the site of spinal contusion injury. *Exp Neurol* **235**, 174-187 (2012).
259. Z. W. Li, J. J. Li, L. Wang, J. P. Zhang, J. J. Wu, X. Q. Mao, G. F. Shi, Q. Wang, F. Wang, J. Zou, Epidermal growth factor receptor inhibitor ameliorates excessive astrogliosis and improves the

regeneration microenvironment and functional recovery in adult rats following spinal cord injury. *J Neuroinflammation* **11**, 71 (2014).
260. D. Schulz, Y. Severin, V. R. T. Zanotelli, B. Bodenmiller, In-Depth Characterization of Monocyte-Derived Macrophages using a Mass Cytometry-Based Phagocytosis Assay. *Sci Rep* **9**, 1925 (2019).
261. M. Tada, T. Konno, M. Tada, T. Tezuka, T. Miura, N. Mezaki, K. Okazaki, M. Arakawa, K. Itoh, T. Yamamoto, H. Yokoo, N. Yoshikura, K. Ishihara, M. Horie, H. Takebayashi, Y. Toyoshima, M. Naito, O. Onodera, M. Nishizawa, H. Takahashi, T. Ikeuchi, A. Kakita, Characteristic microglial features in patients with hereditary diffuse leukoencephalopathy with spheroids. *Ann Neurol* **80**, 554-565 (2016).
262. T. Konno, K. Yoshida, T. Mizuno, T. Kawarai, M. Tada, H. Nozaki, S. I. Ikeda, M. Nishizawa, O. Onodera, Z. K. Wszolek, T. Ikeuchi, Clinical and genetic characterization of adult-onset leukoencephalopathy with axonal spheroids and pigmented glia associated with CSF1R mutation. *Eur J Neurol* **24**, 37-45 (2017).
263. H. S. Keirstead, J. M. Levine, W. F. Blakemore, Response of the oligodendrocyte progenitor cell population (defined by NG2 labelling) to demyelination of the adult spinal cord. *Glia* **22**, 161-170 (1998).
264. J. D. Crapser, M. A. Arreola, K. I. Tsourmas, K. N. Green, Microglia as hackers of the matrix: sculpting synapses and the extracellular space. *Cell Mol Immunol* **18**, 2472-2488 (2021).
265. Y. Wu, W. Shao, T. W. Todd, J. Tong, M. Yue, S. Koga, M. Castanedes-Casey, A. L. Librero, C. W. Lee, I. R. Mackenzie, D. W. Dickson, Y. J. Zhang, L. Petrucelli, M. Prudencio, Microglial lysosome dysfunction contributes to white matter pathology and TDP-43 proteinopathy in GRN-associated FTD. *Cell Rep* **36**, 109581 (2021).
266. F. Cignarella, F. Filipello, B. Bollman, C. Cantoni, A. Locca, R. Mikesell, M. Manis, A. Ibrahim, L. Deng, B. A. Benitez, C. Cruchaga, D. Licastro, K. Mihindukulasuriya, O. Harari, M. Buckland, D. M. Holtzman, A. Rosenthal, T. Schwabe, I. Tassi, L. Piccio, TREM2 activation on microglia promotes myelin debris clearance and remyelination in a model of multiple sclerosis. *Acta Neuropathol* **140**, 513-534 (2020).
267. C. Perego, S. Fumagalli, M. G. De Simoni, Temporal pattern of expression and colocalization of microglia/macrophage phenotype markers following brain ischemic injury in mice. *J Neuroinflammation* **8**, 174 (2011).
268. L. Marinova-Mutafchieva, M. Sadeghian, L. Broom, J. B. Davis, A. D. Medhurst, D. T. Dexter, Relationship between microglial activation and dopaminergic neuronal loss in the substantia nigra: a time course study in a 6-hydroxydopamine model of Parkinson's disease. *J Neurochem* **110**, 966-975 (2009).
269. D. C. Backstrom, M. Eriksson Domellof, J. Linder, B. Olsson, A. Ohrfelt, M. Trupp, H. Zetterberg, K. Blennow, L. Forsgren, Cerebrospinal Fluid Patterns and the Risk of Future Dementia in Early, Incident Parkinson Disease. *JAMA Neurol* **72**, 1175-1182 (2015).
270. S. Harris, G. Comi, B. A. C. Cree, D. L. Arnold, L. Steinman, J. K. Sheffield, H. Southworth, L. Kappos, J. A. Cohen, I. Ozanimod Study, Plasma neurofilament light chain concentrations as a biomarker of clinical and radiologic outcomes in relapsing multiple sclerosis: Post hoc analysis of Phase 3 ozanimod trials. *Eur J Neurol* **28**, 3722-3730 (2021).
271. M. Benatar, J. Wuu, V. Lombardi, A. Jeromin, R. Bowser, P. M. Andersen, A. Malaspina, Neurofilaments in pre-symptomatic ALS and the impact of genotype. *Amyotroph Lateral Scler Frontotemporal Degener* **20**, 538-548 (2019).
272. A. L. Benedet, A. Leuzy, T. A. Pascoal, N. J. Ashton, S. Mathotaarachchi, M. Savard, J. Therriault, M. S. Kang, M. Chamoun, M. Scholl, E. R. Zimmer, S. Gauthier, A. Labbe, H. Zetterberg, P. Rosa-Neto, K. Blennow, I. Alzheimer's Disease Neuroimaging, Stage-specific links between plasma neurofilament light and imaging biomarkers of Alzheimer's disease. *Brain* **143**, 3793-3804 (2020).

273. S. N. Hayer, I. Krey, C. Barro, F. Rossler, P. Kortvelyessy, J. R. Lemke, J. Kuhle, L. Schols, NfL is a biomarker for adult-onset leukoencephalopathy with axonal spheroids and pigmented glia. *Neurology* **91**, 755-757 (2018).
274. A. von Streitberg, S. Jakel, J. Eugenin von Bernhardi, C. Straube, F. Buggenthin, C. Marr, L. Dimou, NG2-Glia Transiently Overcome Their Homeostatic Network and Contribute to Wound Closure After Brain Injury. *Front Cell Dev Biol* **9**, 662056 (2021).
275. S. H. Kang, Y. Li, M. Fukaya, I. Lorenzini, D. W. Cleveland, L. W. Ostrow, J. D. Rothstein, D. E. Bergles, Degeneration and impaired regeneration of gray matter oligodendrocytes in amyotrophic lateral sclerosis. *Nat Neurosci* **16**, 571-579 (2013).
276. G. Behrendt, K. Baer, A. Buffo, M. A. Curtis, R. L. Faull, M. I. Rees, M. Gotz, L. Dimou, Dynamic changes in myelin aberrations and oligodendrocyte generation in chronic amyloidosis in mice and men. *Glia* **61**, 273-286 (2013).
277. Y. J. Wu, Y. F. Tang, Z. C. Xiao, Z. M. Bao, B. P. He, NG2 cells response to axonal alteration in the spinal cord white matter in mice with genetic disruption of neurofilament light subunit expression. *Mol Neurodegener* **3**, 18 (2008).
278. P. W. Tipton, E. R. Stanley, V. Chitu, Z. K. Wszolek, Is Pre-Symptomatic Immunosuppression Protective in CSF1R-Related Leukoencephalopathy? *Mov Disord* **36**, 852-856 (2021).
279. J. M. Gelfand, A. L. Greenfield, M. Barkovich, B. A. Mendelsohn, K. Van Haren, C. P. Hess, G. N. Mannis, Allogeneic HSCT for adult-onset leukoencephalopathy with spheroids and pigmented glia. *Brain* **143**, 503-511 (2020).
280. F. S. Eichler, J. Li, Y. Guo, P. A. Caruso, A. C. Bjonnes, J. Pan, J. K. Booker, J. M. Lane, A. Tare, I. Vlasac, H. Hakonarson, J. F. Gusella, J. Zhang, B. J. Keating, R. Saxena, CSF1R mosaicism in a family with hereditary diffuse leukoencephalopathy with spheroids. *Brain* **139**, 1666-1672 (2016).